รหัสโครงการ SUT7-706-44-36-19

รายงานการวิจัย

การศึกษาผลของมิวตาโรเตชั่นในการเติบโตของผลึกคาร์โบไฮเดรต (A Study into the Effect of Mutarotation on Crystal Growth of Carbohydrates)

ได้รับทุนอุดหนุนการวิจัยจาก

มหาวิทยาลัยเทคโนโลยีสุรนารี

ผลงานวิจัยเป็นความรับผิดชอบของหัวหน้าโครงการวิจัยแต่เพียงผู้เดียว

รหัสโครงการ SUT7-706-44-36-19

รายงานการวิจัย

การศึกษาผลของมิวตาโรเตชั่นในการเติบโตของผลึกคาร์โบไฮเดรต (A Study into the Effect of Mutarotation on Crystal Growth of Carbohydrates)

คณะผู้วิจัย

หัวหน้าโครงการ

รองศาสตราจารย์ ดร.เอเดรียน ฟลัด

สาขาวิชาวิศวกรรมเคมี

สำนักวิชาวิศวกรรมศาสตร์

มหาวิทยาลัยเทคโนโลยีสุรนารี

ผู้ร่วมวิจัย

นางสาวสุกัญญา ศรีสง่า

ได้รับทุนอุดหนุนการวิจัยจากมหาวิทยาลัยเทคโนโลยีสุรนารี ปีงบประมาณ พ.ศ. 2544

ผลงานวิจัยเป็นความรับผิดชอบของหัวหน้าโครงการวิจัยแต่เพียงผู้เดียว

กุมภาพันธ์ 2551

Acknowledgements

The research presented in this report was funded by the Suranaree University of Technology Research Fund, and this support is gratefully acknowledged. Dr. Sukanya Srisa-nga should also be acknowledged for much of the experimental work described here, as should be Professor E. T. White, who assisted us in crystal growth rate measurements. Ms. Yanling Hua is responsible for setting the conditions on, and performing much of the nuclear magnetic resonance work described herein.

บทคัดย่อ

น้ำตาลจัดเป็นสารที่มีความสำคัญในอุตสาหกรรมอาหารและอุตสาหกรรมอื่น ๆ ที่เกี่ยวข้อง ปกติในสารละลายน้ำตาลเกือบทั้งหมดจะอยู่ในรูปโมเลกุล anomers และ tautomers โมเลกุลของน้ำตาลสองรูปนี้จะเปลี่ยนกลับไปกลับมาได้ตามสมดุลปฏิกริยาที่เรียกว่า mutarotation แต่ในการตกผลึกจะมีเพียงโมเลกุลแบบเดียวเท่านั้นที่สามารถตกผลึกได้ภายใต้สภาวะจำเพาะ ตัวอย่างเช่น น้ำตาล glucose monohydrate และ glucose anhydrous จะตกผลึกในรูปโมเลกุลชนิด α – D – glucopyranose ในขณะที่น้ำตาล fructose จะตกผลึกในรูปของ β - D fructopyranose จากการที่โมเลกุลน้ำตาลเพียงรูปเดียวสามารถตกผลึกได้ ดังนั้น เพื่อไม่ให้อัตราการตกผลึกลดลงอย่างรวดเร็ว ในสารละลายน้ำตาลจึงจำเป็นต้องมีโมเลกุลรูปนั้นอยู่ในปริมาณความเข้มข้นที่สูงตลอดเวลา ดังนั้น ปฏิกิริยา mutarotation จึงเป็นสิ่งสำคัญในการควบคุมการตกผลึกทั้งหมดของน้ำตาล

ในการศึกษาผลของปฏิกริยา mutarotation ต่อการตกผลึกน้ำตาลจึงต้องทราบอัตราการเกิดปฏิกริยา mutarotation และสภาวะที่เข้าสู่สมดุลว่าขึ้นอยู่กับความเข้มข้นของน้ำตาลในสารละลาย ตลอดจนอุณหภูมิอย่างไร นอกจากนี้จะต้องทราบว่าอุณหภูมิและการอิ่มตัวยิ่งยวด (supersaturation) มีผลอย่างไรต่ออัตราการตกผลึก ในการศึกษานี้ได้สร้างแบบจำลองทางคณิตศาสตร์ (model) ขึ้นมาและสามารถใช้ได้กับการตกผลึกน้ำตาลในรูปโมเลกุลใดก็ได้ที่อยู่ในสารละลาย ได้ทำการศึกษาอัตราการเกิดปฏิกริยา mutatotation และการเข้าสู่สมดุลของน้ำตาลที่ยังไม่เคยศึกษาวิเคราะห์มาก่อน น้ำตาลที่ทำการศึกษาคือ น้ำตาลโมเลกุลเดี่ยว (monosaccharides) และน้ำตาลโมเลกุลคู่ (disaccharides) น้ำตาล aldose และ น้ำตาล ketose ในการศึกษาอัตราการตกผลึกได้ทดลองกับน้ำตาล glucose monohydrate และทดสอบกับแบบจำลองทางคณิตศาสตร์ 2 แบบเพื่อศึกษาผลของปฏิกริยา mutarotation ต่ออัตราการตกผลึกของน้ำตาล แบบจำลองแรกมีลักษณะง่ายกว่าโดยสมมุติให้อัตราการเติบโตของผลึกมีค่าเดียว ส่วนแบบจำลองที่สองได้ใช้อัตราการเติบโตของผลึกทุกค่า ได้ทำการทดลองหาค่าความเข้มข้นของ anomers กับเวลา ความหนาแน่นของผลึกทั้งหมดกับเวลา ขนาดของผลึกและอัตราการเกิดผลึก

จากการทดลองพบว่าค่าคงที่ของอัตราการเกิดปฏิกริยา mutarotation สำหรับน้ำตาล aldose มีค่าต่ำมากเมื่อเปรียบเทียบกับน้ำตาล ketose ดังนั้นจึงทำให้ปฏิกิริยา mutarotation สำหรับน้ำตาล aldose มีความสำคัญ นอกจากนั้น

ยังพบว่าการที่ปฏิกริยา mutatorotation จะมีผลต่อการตกผลึกมากน้อยแค่ไหนนั้นขึ้นอยู่กับสภาวะการตกผลึก ได้แก่ อัตราการ seeding อุณหภูมิ และค่าเริ่มต้นของการอิ่มตัวยิ่งยวดของถังตกผลึกอีกด้วย

Abstract

Sugars are very important industrial and food chemicals. Nearly all sugars have multiple forms in solution (anomers and tautomers), and these forms interconvert in solution via an equilibrium reaction called mutarotation. Only one of the forms crystallizes under a particular condition, for instance glucose monohydrate and anhydrous glucose both crystallize in the α-D-glucopyranose form, while fructose crystallizes in the β-D-fructopyranose form. Since only one form crystallizes from the solution, this form must be replenished by reaction from the remaining forms, otherwise the driving force for the crystallization will be rapidly reduced as the concentration of the crystallizing form quickly decreases. Thus, the mutarotation reaction in the solution may be a rate controlling step in the crystallization of the significant sugars (with the exception of sucrose, which has no anomers).

To determine how much effect the mutarotation reaction has on the overall crystallization rate of sugars it is necessary to know the rates and equilibriums of the mutarotation reactions as functions of sugar content in solution and temperature, and the crystallization kinetics as functions of temperature, supersaturation, and crystallization conditions. This study has investigated the effect of the mutarotation reaction on the crystallization of sugars, and has produced a model that can be used for the crystallization of any sugar having different forms in solution. The rates and equilibriums in the mutarotation reaction of sugars not previous discussed in the literature have been measured, and these measurements have included both monosaccharides (single ring sugars) as well as disaccharides (two ring sugars), aldose sugars, and ketose sugars. For the crystallization kinetics, glucose monohydrate was used as a test case (full determination of nucleation limits and crystallization kinetics of a single sugar requires a year's work). The crystallization kinetics of other common sugars (such as fructose, anhydrous glucose, and xylose) are already known from the literature. Two models have been produced to determine the effect of the mutarotation reaction on the overall crystallization rates of sugars, and both models are suitable for all sugars, however require basic measurements of crystal growth rates and nucleation rates. The first model is a simpler model and assumes a point value of the crystal growth rate distribution: it can give qualitative results indicating whether the mutarotation reaction is significant to the overall crystallization rate. The second model requires the full crystal growth rate distribution, but then gives an exact

result for the anomer concentrations as a function of time, crystal population densities as a function of time and crystal size, and the overall rate of crystal formation.

It has been found that the mutarotation rate constants for aldose sugars (monosaccharides and disaccharides) are significantly lower than those of the ketose sugar, so that the reaction is more significant for the aldose sugars. The degree with which the reaction determines the overall crystallization rate also depends on key crystallization conditions, including the rate of seeding, the crystallization temperature, and initial level of supersaturation in the crystallizer.

Contents

Tables

Figures

Chapter I
Introduction

Sugars are one of the most abundant and most significant classes of organic compounds found in nature, and have particular significance to human nutrition and the global economy. Glucose is one of the most common and also one of the most important sugars: it is the primary six-carbon sugar (hexose: the most common size of monosaccharide sugar) having the chemical formula $C_6H_{12}O_6$ with a molecular weight of 180.59: it is an aldose sugar, since the molecule contains an aldehyde group. Glucose is also called blood sugar, because it is present in human blood, and grape sugar, since pure glucose was first obtained from grape juice[1]. Currently, most glucose is produced from the hydrolysis of starch, and the production is one of the largest of any chemicals produced industrially.

Fructose is also an industrially significant sugar, having been marketed as a low calorie sweetener since it is almost twice as sweet as table sugar, and is also commonly used as a sweetener for diabetics. Fructose is an isomer of glucose, and thus has the same elemental analysis and molecular weight, but is a ketose sugar since it contains a ketose group rather than an aldehyde group. Fructose is also common in natural materials, however for economic reasons it is produced industrially from enzymatic conversion of starch to glucose, and further conversion with glucose isomerase enzymes to a mixture of fructose and glucose. Potentially it can also be produced from hydrolyzing sucrose (table sugar) however this process is not as cost effective as the processing starting with starch.

Other sugars such as mannose, xylose, sorbose, and others, also have significant economic potential. What all of these sugars has in common (along with almost all others in the same class of compounds) is that they exist as stereoisomers called tautomers (or anomers depending on their relationship to each other). This means that an individual sugar occurs as up to six (or even more in rare cases) different molecules in solution, with these molecules freely inter-converting between each other. In the six carbon sugars such as glucose and fructose, the forms typically comprise of a straight chain form of the sugar, a hydrated straight chain, two six-membered ring forms (pyranoses), and two five-membered ring forms (furanoses). The forms inter-convert freely between each other through the straight chain form in solution, as shown in Figure 1.1 for glucose, and Figure 1.2 for fructose. Despite having multiple forms in solution, only one form of the sugar can be

stable in the crystal phase under a particular condition, and typically the same form is stable under all conditions of temperature and pressure relevant to the industrial processing of the sugar.

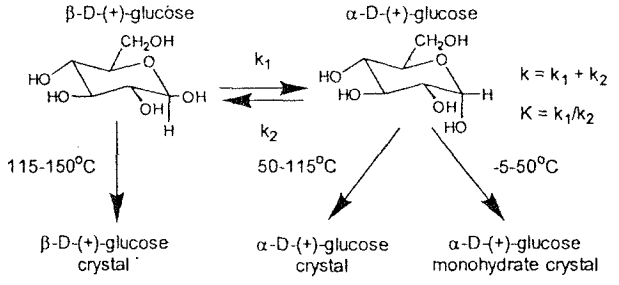

Fig. 1.1 Mutarotation of glucose (with a straight chain form as an intermediate), showing forms potentially crystallizable and their stable range of temperature.

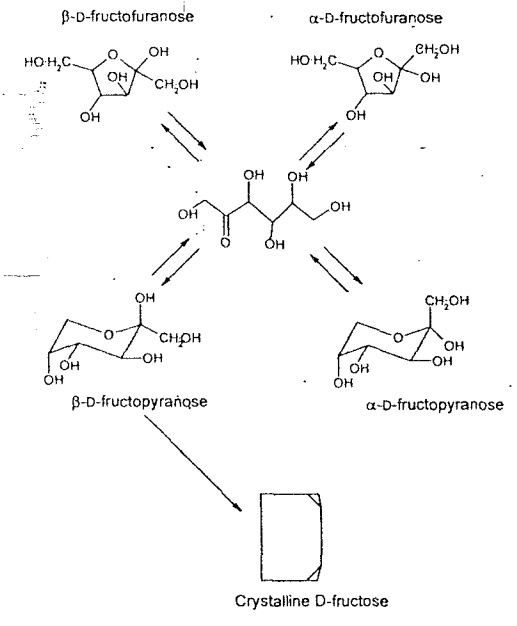

Fig. 1.2 Mutarotation of fructose, showing the stable crystalline form.

The only common commercial sugar which does not form anomers or tautomers is sucrose (table sugar). Sucrose is made up of one glucose moiety and one fructose moiety with a glycosidic bonds between the two anomeric carbons, meaning that these two carbons are not available for producing stereoisomers. The other sugars crystallize into only one form of the sugar (for instance fructose crystallizes as β-D-fructopyranose, a six-membered ring in the beta-form), while all forms exist in solution in equilibrium. This

means that as the preferred crystalline form crystallizes from solution it needs to be replaced from the equilibrium reaction between it and the other forms of the sugar. Potentially these equilibrium mutarotation reactions are slower than the crystallization rate, and therefore are the rate determining step. In this case the crystallizer designer must take into account the rate of the mutarotation step in order to produce a correct crystallizer volume and residence or batch time.

The research here aims to prepare the experimental data and models necessary to predict for which sugars, and under what conditions, the mutarotation reaction is likely to be a rate determining step in crystallization of sugars. The rates and equilibriums for the mutarotation reaction have been measured for the sugars for which it was not already characterized, and a larger data set than currently available has been measured for glucose as a typical case. For glucose the rate and equilibrium has been determined as a function of sugar concentration in aqueous solution, and solution temperature, which are the main two variables in the crystallization system. Crystal growth rates under a range of conditions have been measured for glucose monohydrate: these experiments are very time consuming and difficult, so only this sugar was used as a test case. Crystal growth rates for anhydrous glucose, fructose, mannose, and xylose are known from the literature already, and these rates can be used in the general models derived in this research. A simple model (a series of 5 ordinary differential equations describing the main state variables in the crystallizer) using only the mean growth rate has been derived to give an approximate dependence of the mutarotation reaction on the overall crystallization rate. Finally a more exact model, using the entire crystal growth rate distribution to predict the entire crystal population density as a function of time, and the concentration of the total sugar, and crystallizing form of the sugar as a function of time in a batch crystallizer has been derived. The model is general for any sugar, however it requires measured values of the mutarotation rate and equilibrium, and crystal growth rates, as well as properties of the sugar. If the sugar crystallizes in a hydrate form then the model requires a correction factor that is the ratio of the molecular weights of the anhydrous and hydrated form of the sugar in order to correctly close the mass balance between the crystal and the solution phase.

Chapter II

Mutarotation Reactions of Simple Carbohydrates

2.1 Introduction

Recently it has been shown that the mutarotation reaction of reducing sugars plays a significant role in determining the crystallization rate of these sugars[2,3], and thus it is necessary to be able to model and predict mutarotation rates for common sugars in order to properly design industrial crystallization units for their purification. The mutarotation rate and equilibrium of simple carbohydrates: D-glucose, D-galactose, D-cellobiose, D-maltose, and D-turanose, in aqueous solutions were measured between 7 and 35°C, using ^{13}C-NMR. Glucose was chosen since it was the sugar that will be used as an example for crystal growth rate and crystallizer design modeling topics later in the research. The other sugars were chosen because they are representative of both monosaccharide and disaccharide sugars, and both aldose and ketose sugars. The data for these sugars was also compared to preexisting data for the other common monosaccharides and disaccharides. The effects of sugar concentration and temperature on the rate of mutarotation and mutarotation equilibrium were observed. It has been found that the rate of mutarotation slightly decreases as the sugar concentration increases. This suggests that the reaction is not a true first order reaction, which would not display concentration dependence in the rate constant. The rate constant of the studied sugars follows an Arrhenius relationship with respect to temperature. There are no clear correlations between the equilibrium constant and the sugar concentration or the temperature but neither parameter affects the equilibrium constant strongly. The equilibrium composition is difficult to correlate in terms of the sugar type (i.e. ketose and aldose) because the steric and solvent effects vary strongly even among the individual aldose and ketoses sugars. Finally, it is quite clear that the mutarotation rate of ketose sugars is higher than the mutarotation rate of aldose sugars, and the number of rings in the structure (i.e. monosaccharide or disaccharide) does not have a significant effect on the rate of mutarotation.

The general formula of the monosaccharide sugars is $(CH_2O)_n$ or $C_n(H_2O)_n$ with n commonly ranging from 3 to 7: this is why these compounds are called carbohydrates (hydrates of carbon). For $n = 2$ the molecule is not a carbohydrate, while linear or cyclic monosaccharides with $n \geq 8$ are very unstable, and therefore unlikely to exist in any significant amount. Monosaccharides are also divided into aldoses or ketoses according to

whether their acyclic form possesses an aldehyde (aldoses) or ketone group (ketoses). 2-Ketoses (with the ketone group on the second carbon) are easily the most common ketose sugars. Examples of monosaccharide aldoses and 2-ketoses in the open chain form appear in Table 2.1 and Table 2.2, respectively. In these tables, monosaccharides are also classified according to the number of carbon atoms present. Carbohydrates are referred to as trioses, tetroses, pentoses, and hexoses when they contain 3, 4, 5, and 6 carbon atoms, respectively. There are only two trioses, glyceraldehyde and dihydroxyacetone, that are the simplest aldose and ketose, respectively. Other aldoses and ketoses can be derived from these two forms by adding carbon atoms, each with a hydroxyl group[4]. Monosaccharides can combine with each other to form more complex carbohydrates. Oligosaccharides are compounds in which monosaccharides are joined by glycosidic linkages. They are also named disaccharides (having two monosaccharide moieties), trisaccharides (three monosaccharide moieties), and so on, after the saccharidic lengths. The most abundant oligosaccharides are disaccharides, examples of which in the ring form are shown in Table 2.3.

Table 2.1 Examples of common aldose monosaccharides.

Number of Carbons	**Monosaccharide**	**Acyclic Form**
3 (Aldotriose)	**D**-Glyceraldehye	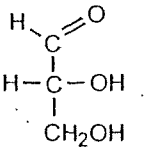
4 (Aldotetrose)	**D**-Erythrose	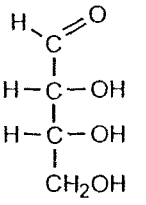
	D-Threose	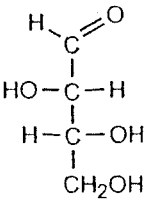

5 (Aldopentose)	**D**-Ribose	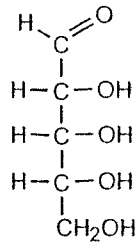
	D-Arabinose	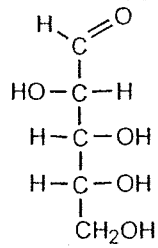
	D-Xylose	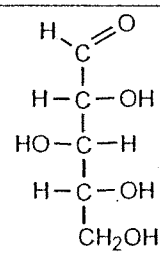
	D-Lyxose	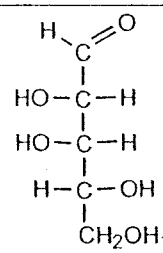
6 (Aldohexose)	**D**-Allose	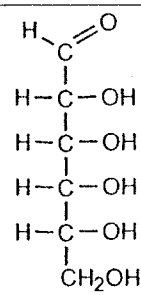
	D-Altrose	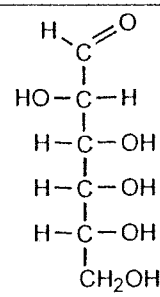

D-Glucose	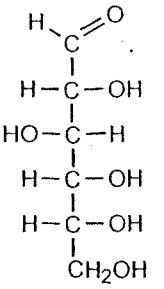
D-Mannose	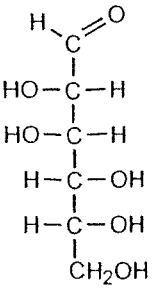
D-Gulose	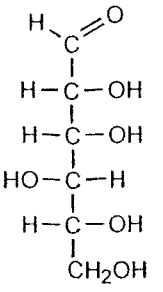
D-Idose	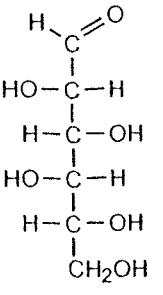
D-Galactose	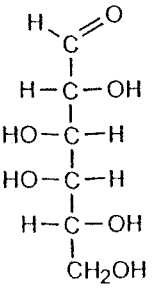

	D-Talose	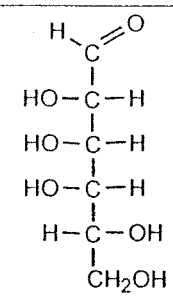

Table 2.2 Examples of 2-ketose monosaccharides.

Number of Carbon	**Monosaccharide**	**Acyclic Form**
3 (Ketotriose)	Dihydroacetone	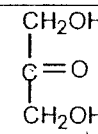
4 (Ketotetrose)	**D**-Erythrulose	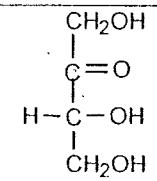
5 (Ketopentose)	**D**-Ribulose	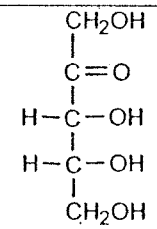
	D-Xylulose	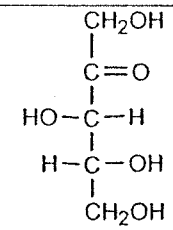
6 (Ketohexose)	**D**-Psicose	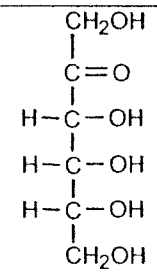

	D-Fructose	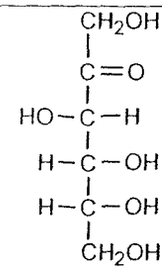
6 (Ketohexose)	**L**-Sorbose	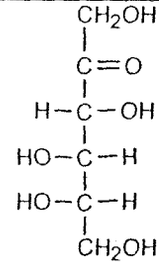
	D-Tagatose	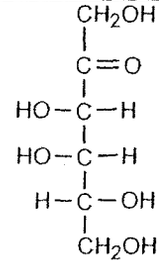

Table 2.3 Examples of disaccharides.

Disaccharide	**Description**	**Full name** [a]	**Cyclic Form (main)**
Sucrose [b]	common table sugar	α-**D**-glucopyranosyl- β-**D**-fructofuranoside	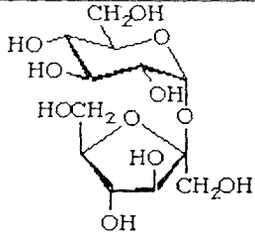
Lactose	main sugar in milk	4-*O*-β-**D**-galactopyranosyl- **D**-glucose	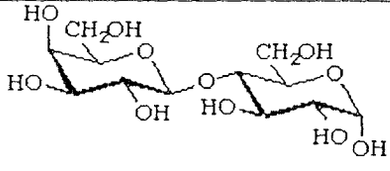
Maltose	product of starch hydrolysis	4-*O*-α-**D**-glucopyranosyl -**D**-glucose	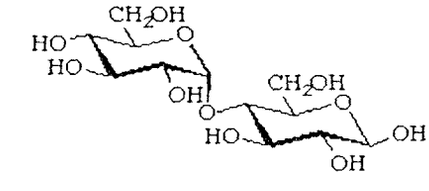

Cellobiose	product of cellulose hydrolysis	4-*O*-β-**D**-glucopyranosyl-**D**-glucose	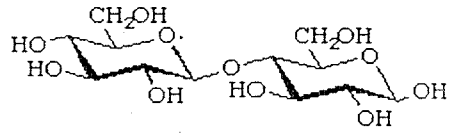
Turanose	rare sugar	3-*O*-α-**D**-glucopyranosyl-**D**-fructose	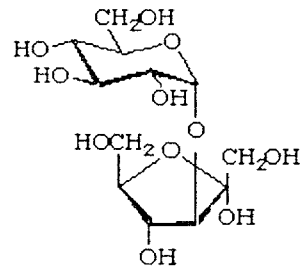
Trehalose [b]	found in fungi	α-**D**-glucopyranosyl-α-**D**-glucopyranoside	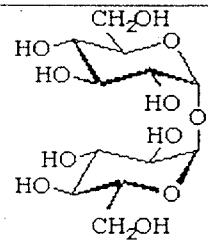

[a] The last name (i.e. D-glucose, D-fructose) suggests the reducing ring, it can be α- or β-forms and can be furanose (a five-membered ring) or pyranose (a six-membered ring). The definition of these terms is described in Section 2.2.1.

[b] Non-reducing sugars

2.2 The Mutarotation Reaction

The linear form of sugars (i.e. glucose) is normally energetically unfavorable relative to a cyclic hemiacetal form[5], so in various medias (i.e. aqueous solution) sugars with four or more carbons tend to be cyclized to form ring structures. A six-membered cyclic form of most hexoses is the preferred structure for this type of sugar[4]. This structure is called a pyranose form and it is created by reaction of the hydroxyl group at C-5 with the carbonyl group. In some sugars, the hydroxyl group at C-4 reacts instead, and in this case the cyclic that is formed has a five-membered ring; this type of cyclic monosaccharide is called a furanose. The ring formation can occur because of the "intramolecular" bonds between the carbonyl (C=O) and hydroxyl (OH) group in the same sugar molecule[4,6]. This force bends a straight form of the sugar and allows the ring to be formed. The ring closing mechanism is not described in detail here, however it starts with the carbonyl oxygen being protonated by an acid catalyst, then the alcohol oxygen attacks the carbonyl carbon, and finally a proton is lost from the resulting positively charged oxygen[4]. Each step is

reversible. During these processes, bonds between carbon atoms are rotated and cause the different ring structures that can be formed (pyranose, furanose, α, and β). If the bond between C-4 and C-5 rotates, the pyranose form is expected, and the furanose form is obtained if the bond between C-3 and C-4 is rotated. The rotation around the C-1 and C-2 bond causes two different forms, the α- and β-forms. In the α-anomer, the hydroxyl group of the anomeric carbon is pointing almost perpendicular to the plane of the molecule, also called the axial orientation. The hydroxyl group of the anomeric carbon of the β-anomer is pointing out along the plane of the molecule, and this is called equatorial orientation. The example of this is shown in Figure 2.1, which are α-glucopyranose and β-glucopyranose in the chair structure, and also shows the mutarotation mechanism that is described below. However, these forms are in equilibrium with each other in solution.

Sugars undergo interconversion between the anomeric (or tautomeric) forms (pyranose, furanose, and open-chain form) in solution. The interconversion is particularly important in aqueous solution, because the sugars appear in aqueous solutions in biological systems, and most processing of the sugar is also performed in aqueous solution. (Although aqueous ethanolic crystallizations are also performed for some sugars due to far lower values of the solubility in aqueous ethanolic solutions, which can result in higher yields if the sugar is temperature sensitive, and also lower viscosity of mother liquours[2,3]. The models prepared in the current research will be equally valid for aqueous ethanol crystallizations, however new parameters would need to be determined for the crystallization and reaction rates). This interconversion causes changes in the optical rotation of the solutions, and thus it is called the mutarotation reaction (muta = change). The interconversion between the different ring forms of the sugars must pass through the straight chain (aldehyde or keto) form of the sugar via ring opening and ring closing reactions, and this is shown using D-glucose as an example in Figure 2.1. These reactions are acid/base catalyzed, and at approximately pH 4 the reaction rate is minimized; the reactions are faster at extremes of pH[7,8]. This apparent first order reaction is catalyzed by substances which can act simultaneously as proton donors and acceptors e.g. polar solvents, and also follows an Arrhenius relationship with respect to temperature[2,9].

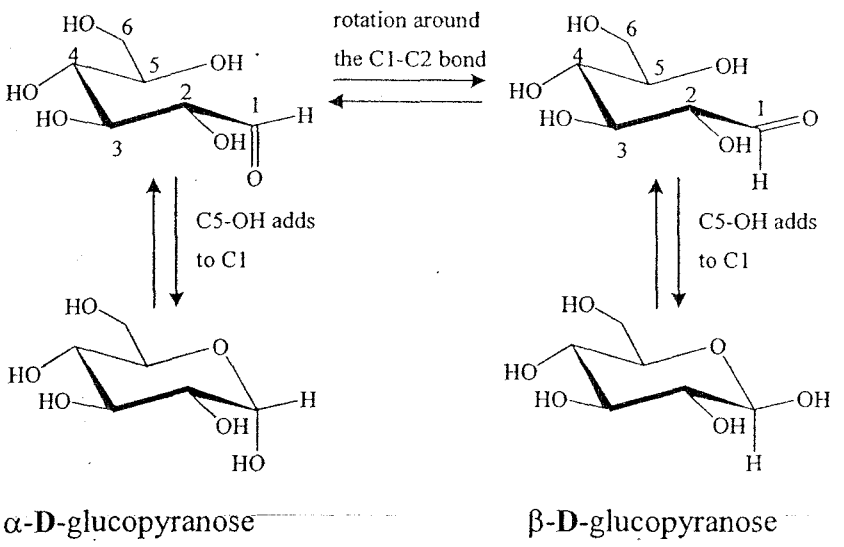

Fig. 2.1 Mutarotation reaction schemes of D-glucose.

Many studies have investigated the mutarotation rate and mutarotation equilibrium of simple carbohydrates in aqueous solutions. In the first period of research in this field (circa 1900-1940), the observation of the optical rotation change was a popular technique. More recently GLC, FTIR, and NMR have been used since they are more powerful techniques.

2.3 Materials and Methods

2.3.1 Materials

Sugar solutions used in the mutarotation experiments were prepared from AR grade sugars, HPLC grade water, and deuterium oxide (D_2O). The supplying details of all sugars are as follows: α-**D**-Glucose anhydrous, Carlo Elba; β-**D**-Glucose, Sigma; **D**-Galactose, Sigma; **D**-Maltose monohydrate, Sigma; **D**-Cellobiose, Sigma; and **D**-Turanose, Acros. All chemicals were used without further purification. The D_2O was used in this experiment as a reference for the chemical shift assignment. However, previous work[7] (Isbell and Pigman, 1969) has shown it had an effect on the mutarotation rates. In this work, % D_2O (v/v) in solute-free solvent was varied to also observe this effect. The prepared solution volume should not be more than 700 μL due to the requirement of NMR.

2.3.2 Experimental Procedure

The solution was prepared by introducing known amounts of sugar and solvent into a 2 ml vial. The solution was vigorously shaken until the solids dissolved completely. The solution was transferred to a 5 mm NMR tube using a pipette, and the experiment was immediately started. The delay times between the initial dissolution and the start of the experiment were controlled within 2-3 minutes, except in high concentration experiments where delay times were found to be within 4-5 minutes. Typically these time delays were not a serious impediment to accurate results because the time constants for the mutarotation reaction are usually around one to two orders of magnitude larger than this.

^{13}C-NMR was performed on a Varian Unity Inova 300 spectrometer at 75.42 MHz. A switchable broadband (SW/BB) and Fourier transform technique was used. Chemical shift (expressed as parts per million downfield from TMS) were calculated by using the deuterium signal of D_2O as a reference. A 90° pulse (9.2 μs, at a power of 52 dB) was applied to acquire maximum peak intensity. A 5.0 s time delay before every pulse was chosen based to obtain quantitative results having a peak as long as possible, while minimizing the time delay between data points in the kinetic experiments. Kinetic experiments were performed using 16 scans per data point in order to obtain suitable peak heights, while minimizing data collection time to obtain the maximum number of data points. Each experiment was stopped when the mutarotation mechanisms reached their equilibrium (1.5-7.0 hr).

NMR spectroscopy is based on the property of the nuclear spin. When a molecule is placed in a magnetic field, the nuclear spin can align and leads to different energy levels. The NMR spectrum obtained from such a measurement contains information on the chemical environment of atoms (chemical shift), the molecular geometry (spin-spin coupling), and the number of atoms giving rise to the signal (integral).

2.4 Results and Discussion

Typical ^{13}C-NMR spectrums obtained almost immediately after dissolution and at the equilibrium of monosaccharide sugars are shown in Figure 2.2 and 2.3 respectively while Figure 2.4 and 2.5 are the spectrums for disaccharide sugars. For the first spectra after the dissolution (Figure 2.2 and 2.4), only the carbon chemical shifts of dissolved form and very small peaks of the other forms are present. At equilibrium (Figure 2.2 and 2.5) almost all carbon peaks of anomers were present, excepting where some peaks coincided

with others. The coincident chemical shifts were not used in the composition calculations. Peaks were assigned based on the literature data[10,11]. The anomeric compositions were calculated from the chemical peak height.

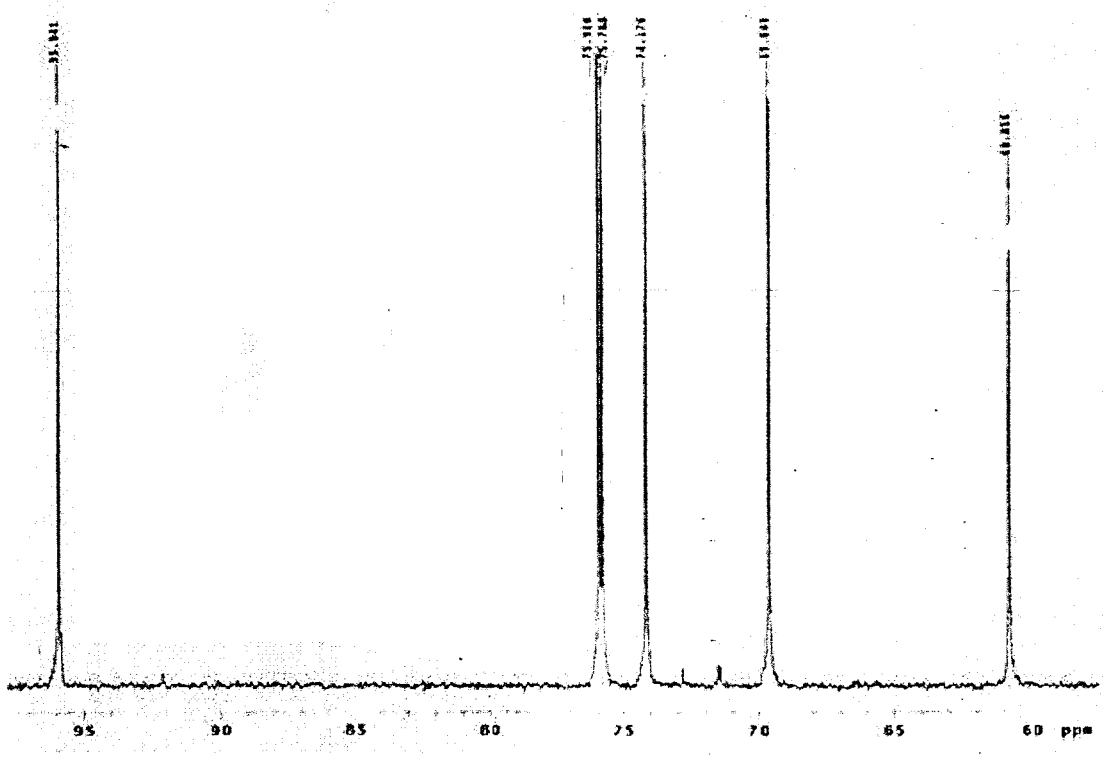

Fig. 2.2 Typical ^{13}C-NMR spectrums after dissolution of 33% β-glucopyranose in aqueous solution at 24°C.

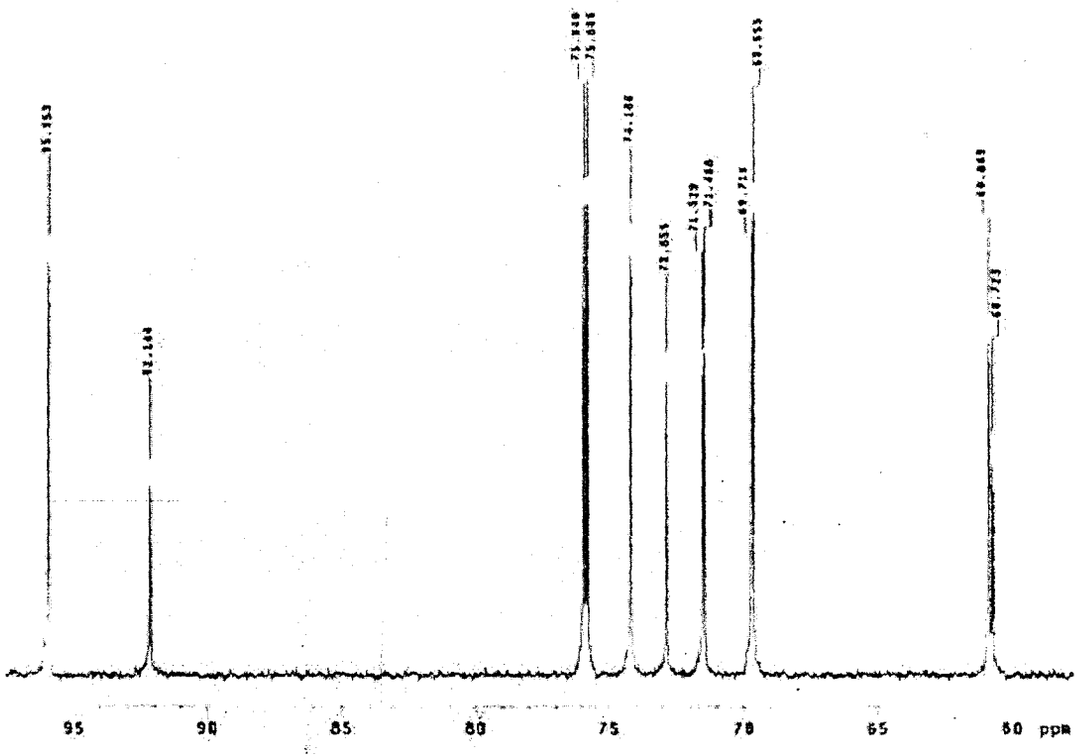

Fig. 2.3 Typical ^{13}C-NMR spectrums at equilibrium of 33% β-glucopyranose in aqueous solution at 24°C.

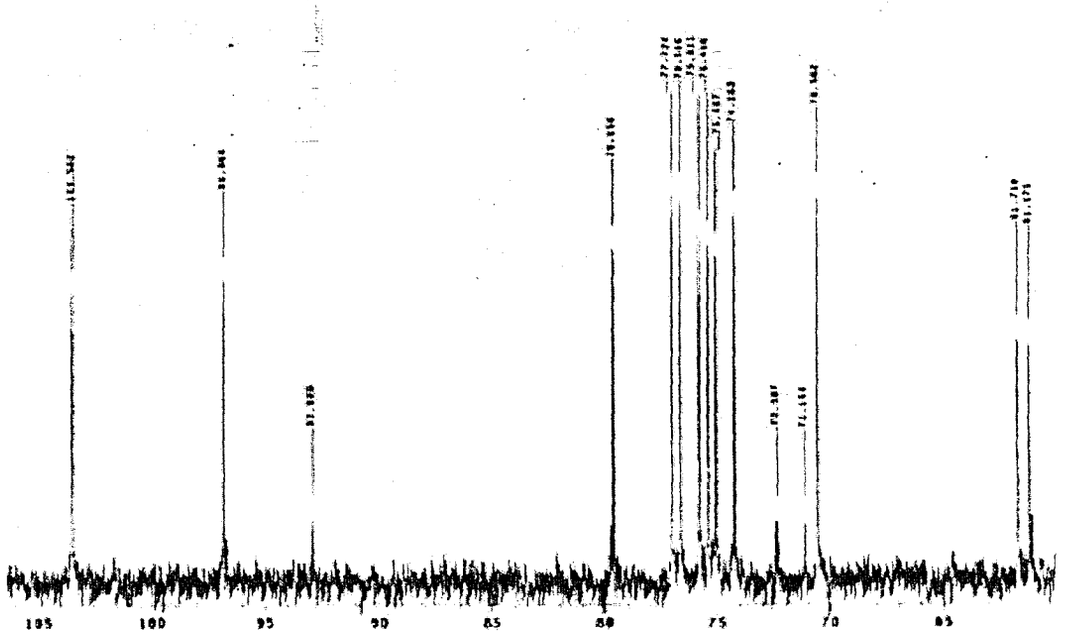

Fig. 2.4 Typical ^{13}C-NMR spectrums after dissolution of 8% cellobiose in aqueous solutic at 25°C.

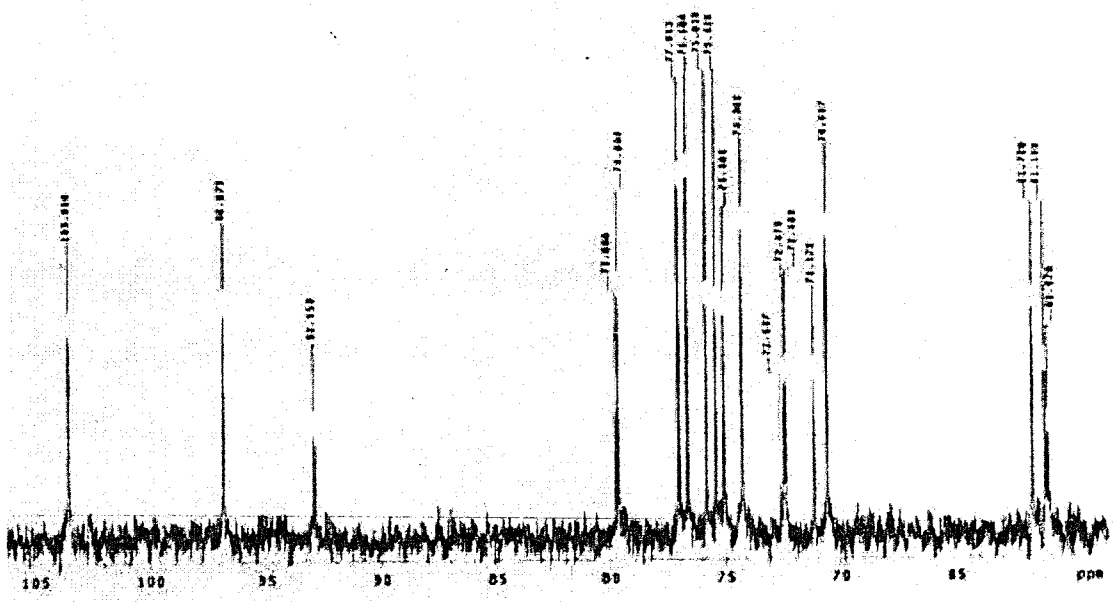

Fig. 2.5 Typical ^{13}C-NMR spectrums at equilibrium of 8% cellobiose in aqueous solution at 25°C.

In the time dependent experiments, only the α-aldopyranose and β-aldopyranose forms of the aldose sugars, and β-ketopyranose, α-ketofuranose, and β-ketofuranose of the ketose sugars, are evident because of the low number of scans per data point in these experiments, and the other forms are present at very low concentrations. A small number of scans per data point were necessary in order to follow the time dependence of the mutarotation accurately. From this information, the composition fraction of each form can be easily calculated. The plot between the fractions (or percent compositions) based on all existing carbons with time showed the mutarotation behavior (time course) of that sugar as shown in Figure 2.6 (as an example). It shows that while the content of the dissolved form is decreased, the other form replaces it, and the total composition is constant over the time course of reaction.

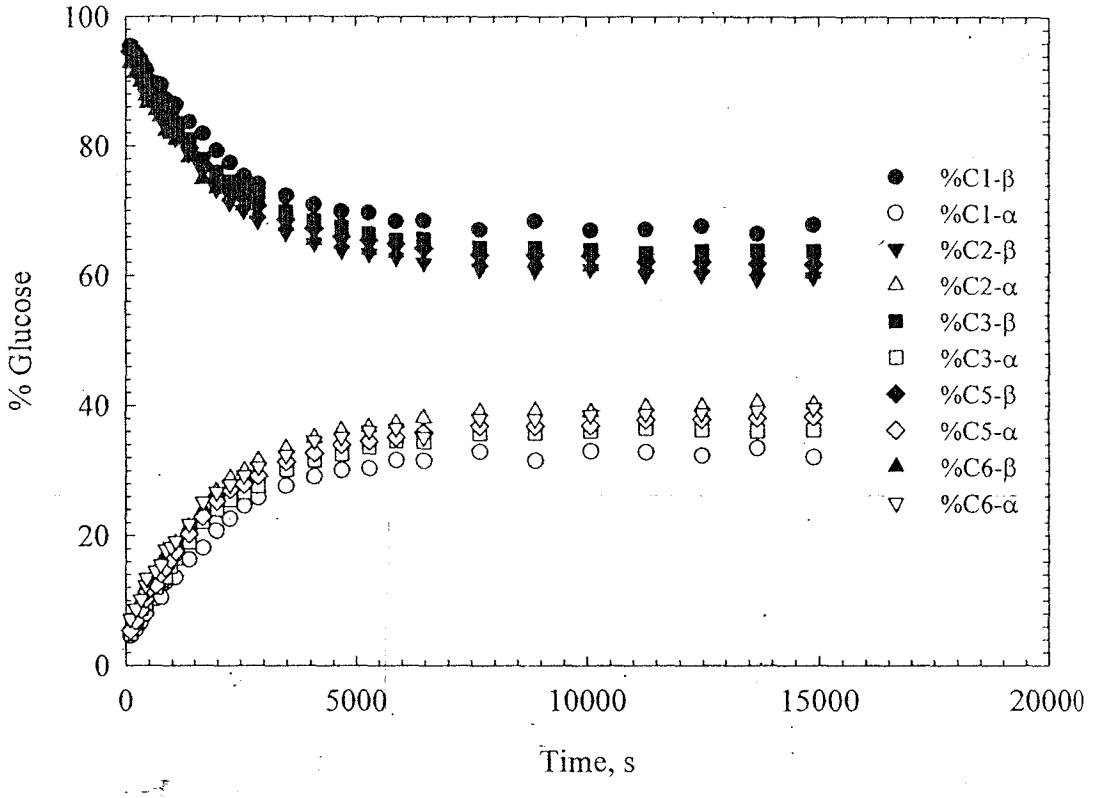

Fig. 2.6 The mutarotation behavior of glucose in aqueous solution at 24°C. Note that zero time corresponds to the starting of the NMR measurement, not to the initial mixing time.

Figure 2.7 shows the mutarotation behavior of glucose in aqueous solution, where only C-2 is used in the plot, to investigate the effect of temperature on its behavior. This graph shows the qualitative point of view of the mutarotation rates and mutarotational equilibrium. This figure shows that the rate is higher at higher temperature, which shows the steeper slope of the fraction changes, and the final values (the equilibrium values) are similar. The quantitative analysis of the temperature effect is discussed in section 2.4.1.

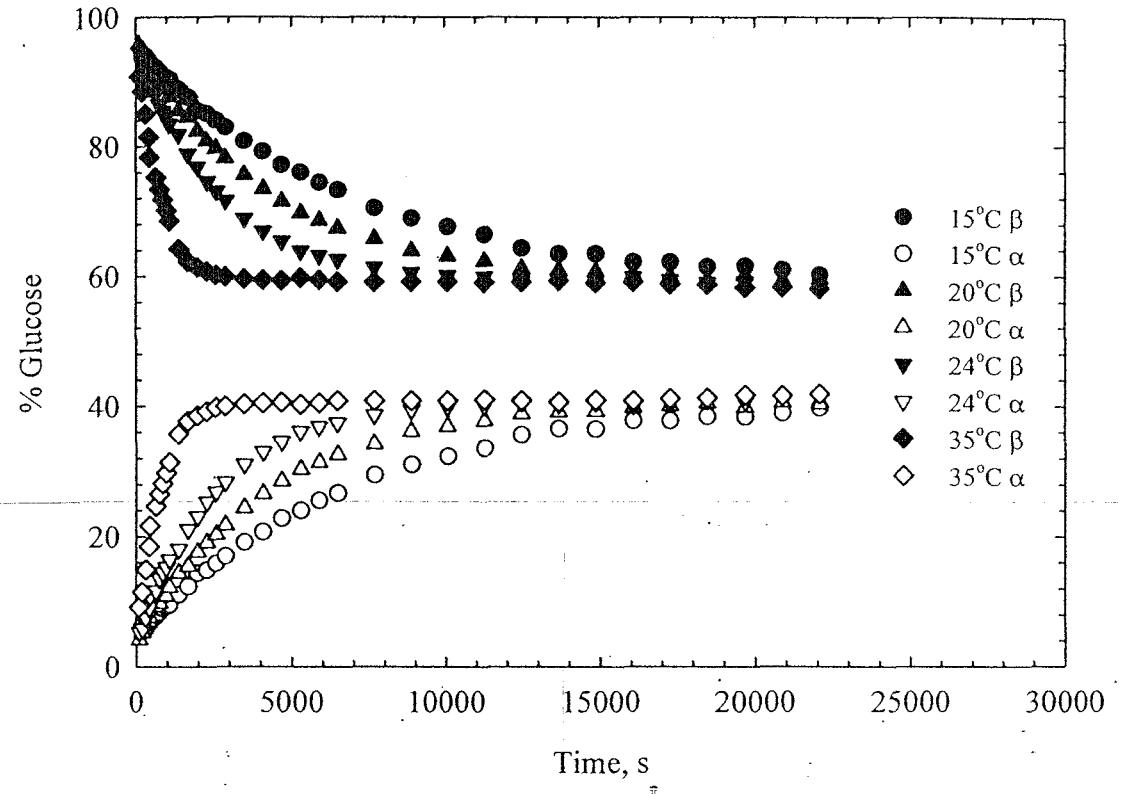

Fig. 2.7 The mutarotation behavior of glucose in aqueous solution over the experimental temperatures. Note that zero time corresponds to the starting of the NMR measurement, not to the initial mixing time.

The mutarotation kinetics and equilibrium of monosaccharide aldose sugars were determined based on the relative fractions of α-pyranose and β-pyranose calculated from C-2 carbon atom only, as it was found well separated downfield from the other resonances[12]. The mutarotation parameters of disaccharide aldose were determined based on relative fractions calculated using C-2 carbons of the anomer-determining ring (the ring which determines whether the sugar is in the α- or β- form) only. The anomeric carbon (C-1) was not used because it always gives much smaller peaks than the others. The C-3 and C-5 were not used due to the β-anomer peaks of these carbons were not well separated, especially where high sugar concentrations were used. The α-C-4 and β-C-4 peaks were not used since they were not separated in the initial period of the experiment. The relative fractions of pyranose and furanose (α-furanose + β-furanose) forms of ketose calculated using C-2, C-3, and C-5 of the anomer-determining ring were used in the mutarotation kinetic and equilibrium calculation; C-1, C-4, and C-6 were not used due to these peaks not

being well separated in some cases. The mutarotation rates and equilibrium compositions were determined by fitting the relative fractions and time with a first order equation (Equation 2.1 and 2.2). The delay time, overall reaction rate, and equilibrium composition were used as the fitting parameters. A time delay was used since slow dissolution made the exact time the mutarotation reaction began uncertain.

First order exponential decay for the dissolved form:

$$f_{or} = b - a(1-\exp[-k(t-t_d)]) \quad (2.1)$$

First order exponential growth for the other form:

$$f_{ot} = a(1-\exp[-k(t-t_d)]) \quad (2.2)$$

where f_{or} and f_{ot} are the composition fractions of dissolved form and other form, a and b are the constant, k is the overall mutarotation rate, and t and t_d are the experimental time and delay time, respectively.

2.4.1 Temperature effect on the mutarotation rate and mutarotation equilibrium

Figure 2.8 shows an Arrhenius plot of glucose in aqueous solution with varying glucose content. In this figure, two main remarkable conclusions can be pointed out; first the mutarotation of glucose follows an Arrhenius relationship with respect to temperature very well, and second the mutarotation rate is not a function of sugar content since only one line can be significantly modeled. However, the effect of concentration on the mutarotation kinetics is considered in Section 2.4.2. An Arrhenius plot of mutarotation rates with respect to the reaction temperature of all sugars investigated in the current study is shown in Figure 2.9. Data at any particular temperature is the averaged value from different concentrations since the concentration does not have a significant effect on the rates (see the detail in Section 2.4.2). It is quite clear that the rates of all studied sugars are temperature dependent, with higher rates at higher temperatures, and also follow an Arrhenius relationship. A true first order reaction must follow an Arrhenius relationship. Although the current system is only pseudo-first order (the reaction scheme involves intermediates and other products), it closely follows first order kinetics. Most other reactions also approximately follow Arrhenius relationship with respect to temperature. The activation energy of each sugar is calculated from the slope of this plot and is shown in Table 2.4. The equilibrium composition of the most abundant form of each sugar is also

shown in Table 2.4. The aldose sugars only contain large quantities of the pyranose tautomers, whilst the ketose sugars often contain significant amounts of the furanose tautomers also. This suggests that the pyranose anomers are significantly more stable than the furanose anomers for aldose sugars, while the relative free energies of the pyranose and furanose forms are more similar for ketose sugars. It is more difficult to make firm conclusions about the effect of sugar type on the anomeric equilibrium of the pyranose forms, however it is very likely that steric effects will have a significant effect on the stability of each anomer. Therefore the positions of the hydroxyl groups near the anomeric carbon may have a very significant effect.

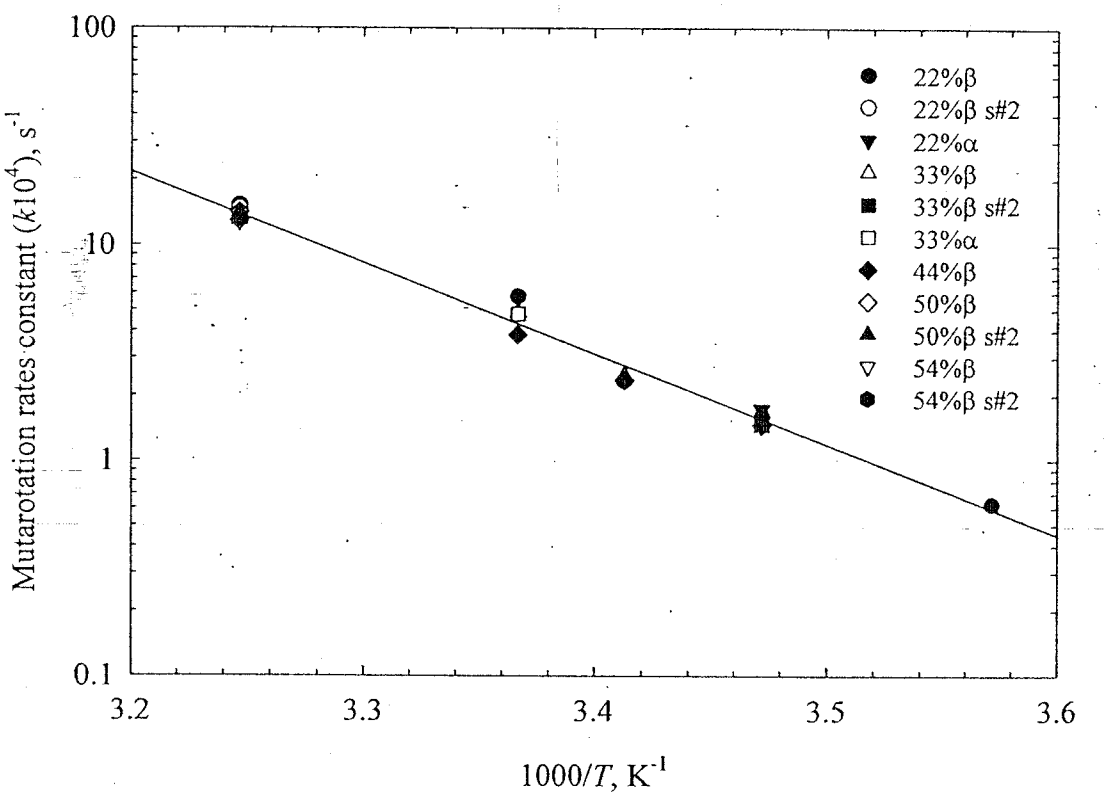

Fig. 2.8 Arrhenius plot of glucose shows the temperature dependence mutarotation rates. Line is the Arrhenius regression.

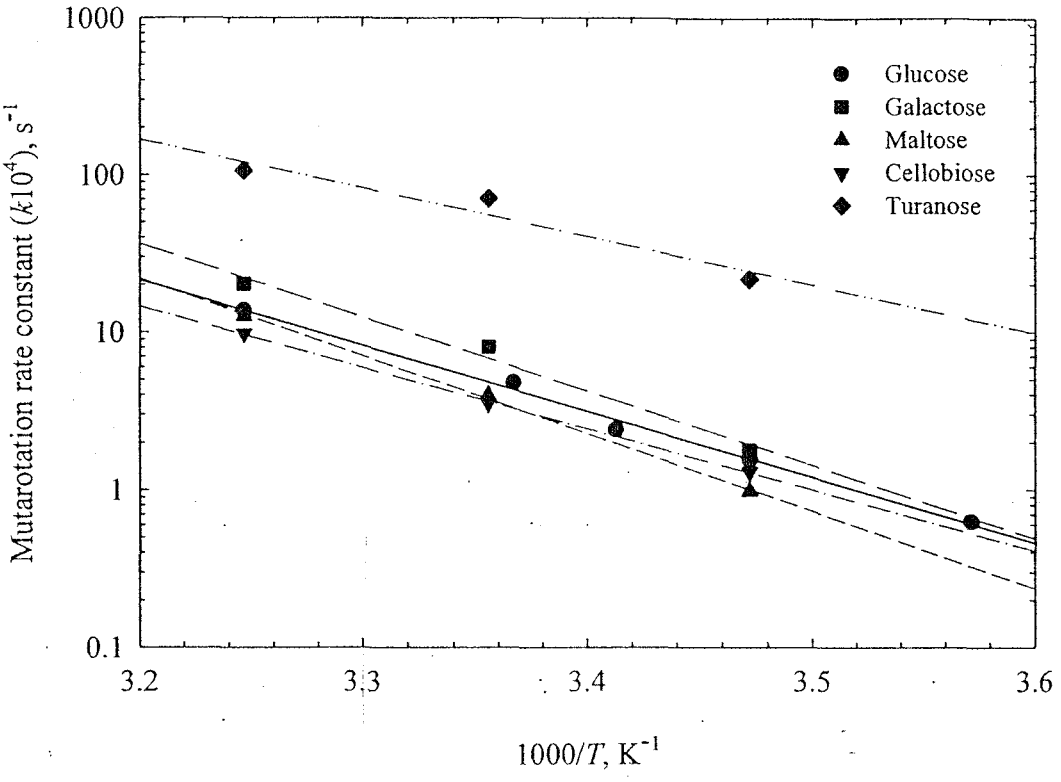

Fig. 2.9 Arrhenius plot of studied sugars shows the temperature dependence mutarotation rates. Lines are the Arrhenius regressions for each sugar.

2.4.2 Concentration effect on the mutarotation rate and mutarotation equilibrium

Currently there is no clear conclusion to whether there is a concentration effect on the mutarotation rate or equilibrium of sugars[13-16]. This is an important point in a study of the mutarotation reaction because if the mutarotation rate or equilibrium depends on the sugar content, the reaction can not be a true first order reaction (but may be able to be approximated with a first order reaction). To study this effect, the concentration of glucose was varied from 22% by weight to close to the solubility value at a particular temperature. The study in supersaturated solutions is difficult due to the difficulty of dissolution into supersaturated solutions. The experimental results are shown in Figure 2.10. This figure shows that the rate is not affected by the sugar content at low temperature (i.e. up to 20°C), but at higher temperature the rates seem to be slightly dependent on the glucose concentration. The dependence shows that at higher glucose concentration the mutarotation rate is lower. This significance of this dependency is still undetermined, with several contradictory studies having been published. Due to the very weak dependence of

concentration on the mutarotation rate, the averaged value of the rates at each temperature was used.

Figure 2.11 shows a slightly increase in α-glucose content at equilibrium when glucose concentration is increased. This result is consistent with the previous result of Barc'H, Grossel, Looten, and Mathlouthi[13]. The equilibrium α-glucose point at 7°C appears to be an outlier. This inconsistency may be due to the nature of the NMR equipment; at low temperature the chemical peaks are not well separated, or may be due to the experimental data is not enough to fit it with an accurate time course made an uncertainty in the equilibrium composition. However, the α-glucose at equilibrium can be concluded to be 40.0 ± 3.0 % (neglecting the value at 7°C) which is also shown the same range as the previous work. This value suggests the equilibrium constant K (the ratio of the β-glucose and α-glucose at equilibrium) of 1.50 ± 0.2. Kraus and Nývlt[9] (1994) also used 1.72 for the equilibrium constant with no dependence on temperature.

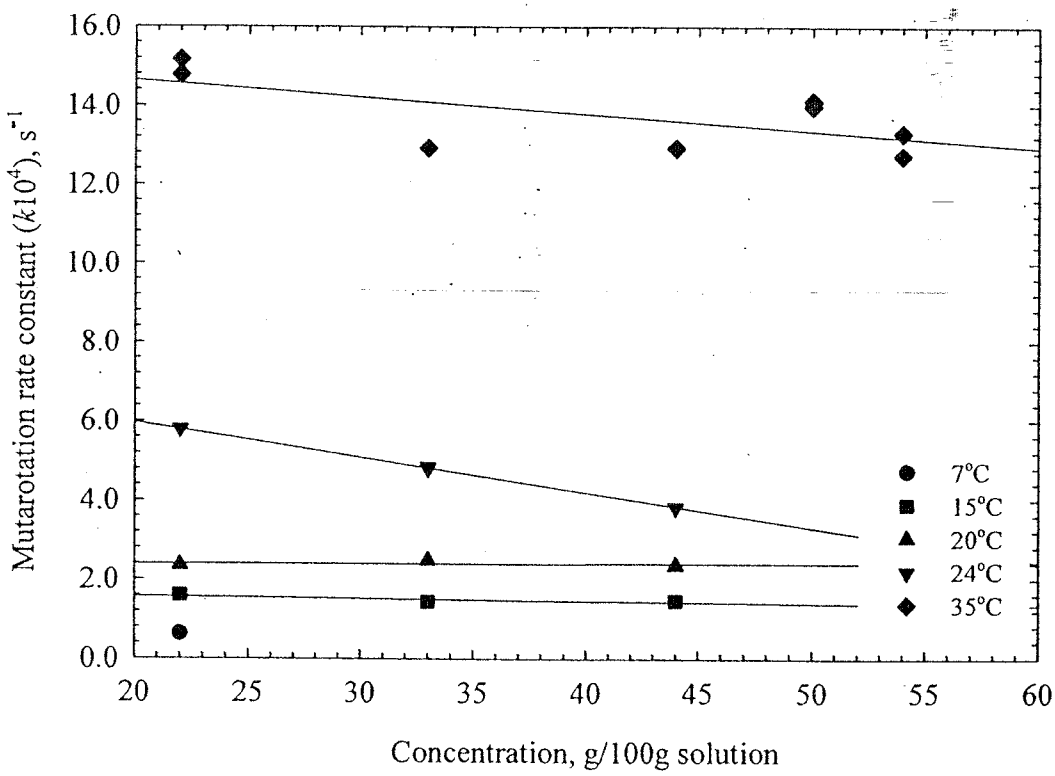

Fig. 2.10 Glucose mutarotation rate as a function of concentration in solution.

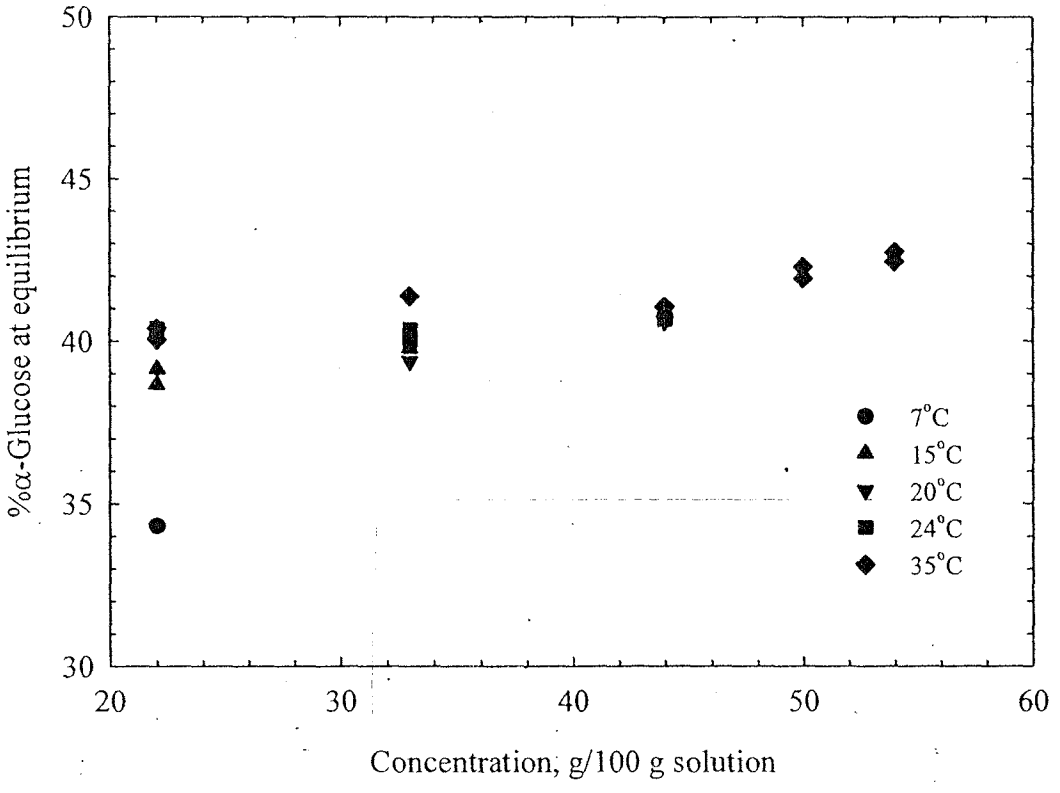

Fig. 2.11 The effect of glucose concentration on the α-glucose at equilibrium.

2.4.3 Solvent effect on the mutarotation rate and mutarotation equilibrium

Deuterium oxide (D_2O) was chosen to observe this effect since it was necessary to use this solvent as a reference for the chemical peak assignment in the NMR equipment. A preliminary study on the effect of D_2O on the mutarotation rate and equilibrium of D-glucose was performed. The 7 experiments were carried out at 24°C and concentration of glucose was fixed at 33% by weight. The amount of D_2O used (in solute-free basis) was varied from 0% to 100%. The overall mutarotation rate with respect to $\%D_2O$ is shown in Figure 2.12, while the equilibrium composition of α-glucose with respect to $\%D_2O$ is demonstrated in Figure 2.13.

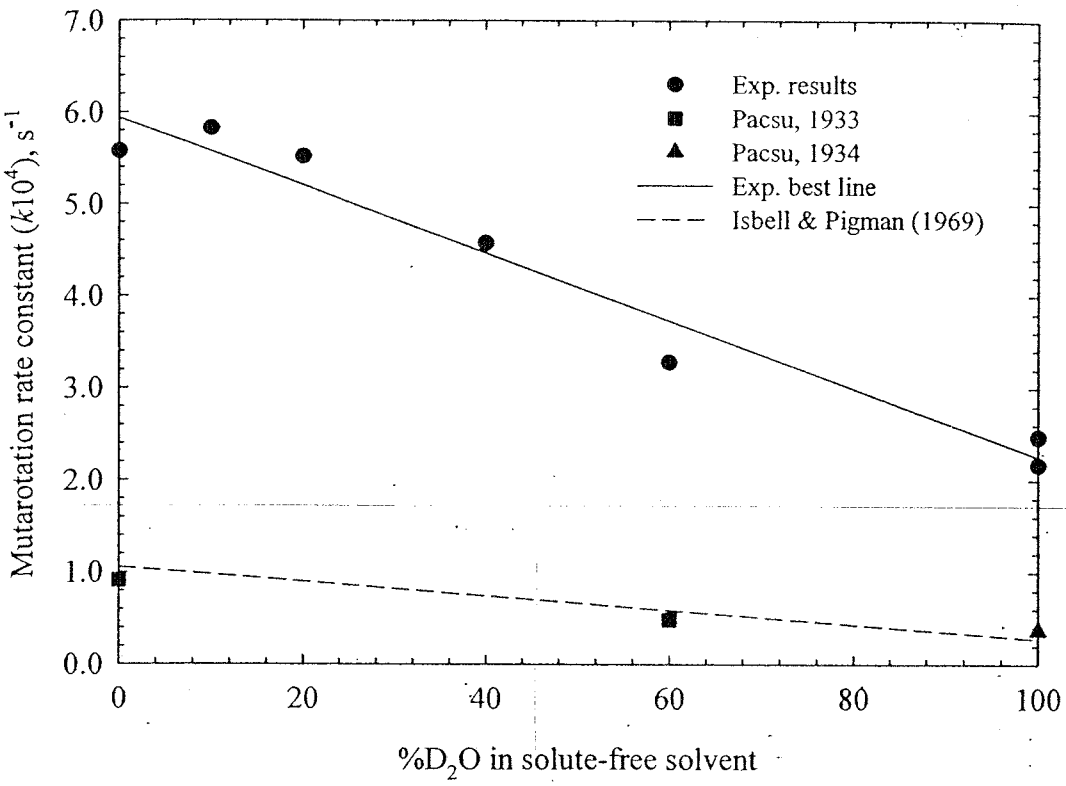

Fig. 2.12 The overall mutarotation rate of glucose as a function of an amount of D_2O. Experimental temperature, this work: 24°C, Pacsu (1933): 18°C, Pacsu (1934): 20°C, and Isbell and Pigman (1969): 20°C.

Figure 2.12 shows the mutarotation rate is a slight function of D_2O composition in the solvent, as a relationship: $k\times10^4 = 5.9376 - 0.037\times\%D_2O$, where k is an overall mutarotation rate (in s^{-1}). This relationship suggests that the rate decreases 0.037×10^{-4} s^{-1} for every 1% increases in D_2O. The result expresses the isotope effect as a k_H/k_D ratio, the ratio of the rate in normal water over the rate in heavy water, of 2.65, while Isbell and Pigman show this ratio of 3.87 and 3.80 for the mutarotation of α-glucopyranose at 20°C and 25°C, respectively. The results from Pacsu's work at 18°C and 20°C seem to show the same range of the isotope effect as Isbell and Pigman's. The results from the current work demonstrate that the isotope effect is less significant than previously thought, and show that adding a small amount of D_2O to achieve improved NMR resolution will not change the mutarotation rate and equilibrium data significantly.

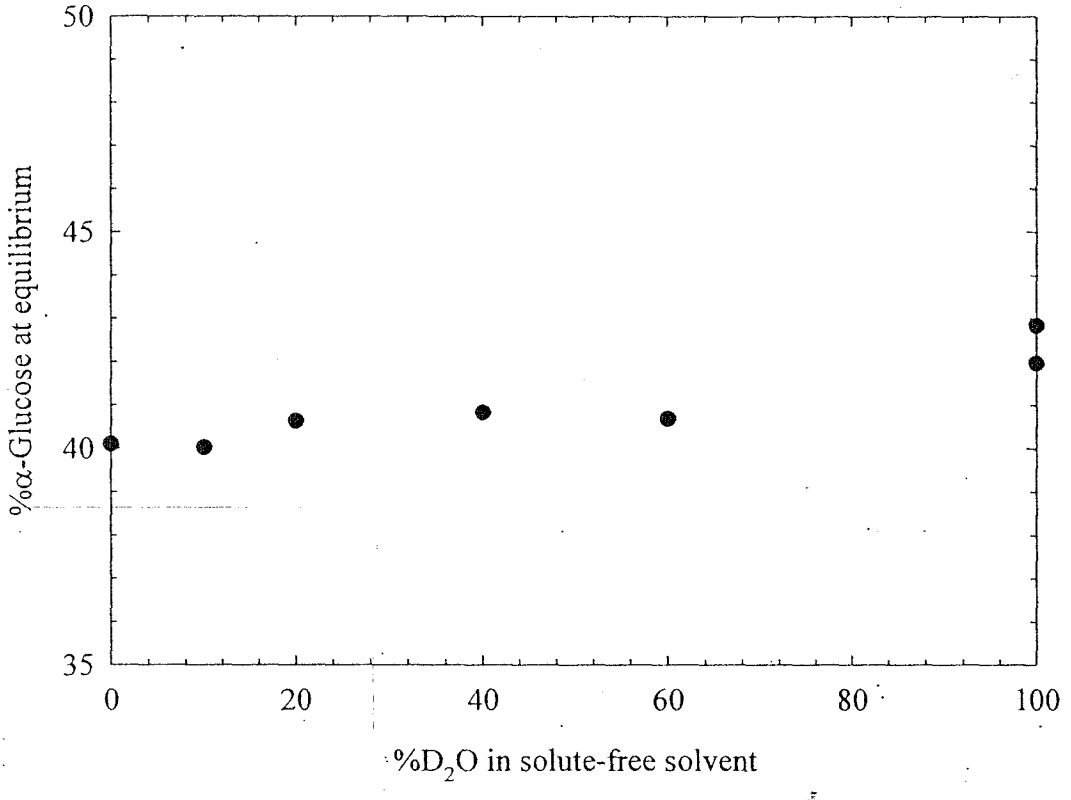

Fig. 2.13 Percent α-glucose as a function of an amount of D_2O in the system.

Figure 2.13 shows the effect of $\%D_2O$ on the equilibrium compositions of α glucopyranose. This figure suggests a very weak correlation between these tw parameters. The D_2O shifts the mutarotation equilibrium of glucose up, but in very smal amount, say 1-2% α-glucose. This effect can be neglected when the accuracy of th equipment is considered.

2.4.4 The effect of ring structure on the mutarotation rate and mutarotatio equilibrium (aldoses versus ketoses)

The mutarotation rates of the sugars in the current study are compared to th mutarotation rate of the monosaccharide ketoses D-fructose[8] and L-sorbose[17], and th monosaccharide D-mannose[17,18] in Figure 2.14. Extra data for D-glucose was taken fro many previous studies[8,9,13,14,17-19], and all these results were used in the calculation. Th galactose rates of mutarotation were also taken from various studies[17,19,] and were treate in the same way as for glucose. This plot shows whether there is a relationship betwee the type of sugar (aldose and ketose), and the size of the sugar (monosaccharide

disaccharide) and the mutarotation rate. The overall mutarotation rates of the ketose sugars (turanose, fructose, and sorbose) fall in a band that is significantly higher than that of all the aldose sugars. The aldose sugars (glucose, mannose, galactose, maltose, and cellobiose) have mutarotation rates in a narrow range; with the fastest rate (that of mannose) being only approximately double that of the slowest rate (that of glucose).

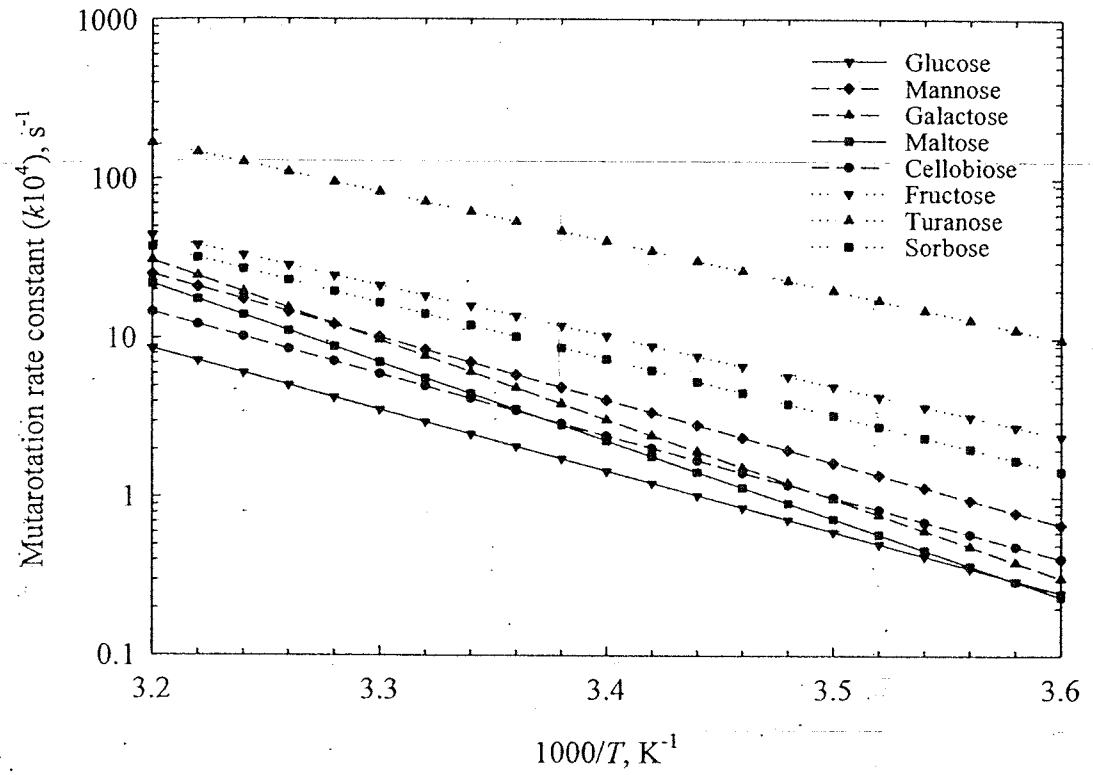

Fig. 2.14 Arrhenius plots for the overall mutarotation rates of common sugars. Symbols are from the Arrhenius model, and used to distinguish curves for different sugars only.

2.4.5 The effect of the number of rings on the mutarotation rate and mutarotation equilibrium (monosaccharides versus disaccharides)

Figure 2.15 is the Arrhenius plot of aldose sugars studied in this work. There appears to be no strong correlation between the number of rings of the sugar and the mutarotation rate; disaccharides appear to have a rate very similar to that of the mutarotating monosaccharide in their structure. This result suggests that the chemistry of the non-mutarotating ring of a disaccharide does not have a significant effect on the reaction at the anomeric carbon of the mutarotating ring. Thus the mutarotation rate of a

disaccharide may be reasonably well predicted as the rate of the monosaccharide in the anomer-determining ring.

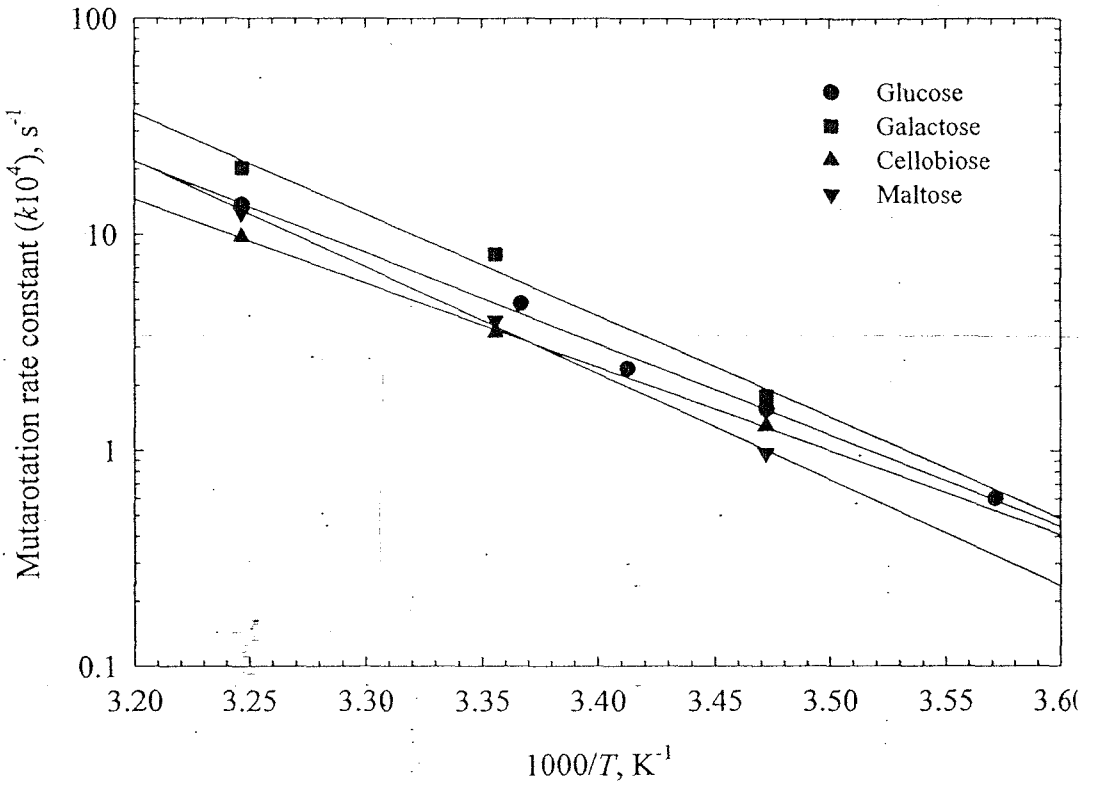

Fig. 2.15 Arrhenius plots for the overall mutarotation rates of aldoses.

Table 2.4 The equilibrium compositions of the mutarotation reaction of common sugars in aqueous solutions.

Sugar	Temp. [°C]	Conc. [%][a]	Form[b]	%Equilibrium composition
D-glucose	7	22.0	β-pyr.	65.68±4.191
	15	22.0-44.0		60.06±0.680
	20	22.0-44.0		59.92±0.466
	24	22.0-44.0		59.67±0.367
	35	22.0-54.0		58.47±0.410
D-glucose	30	40.0-52.2	β-pyr.	60.15±0.499
	35	43.8-56.0		59.49±0.511
	40	50.0-60.0		59.28±0.462
	45	52.1-62.4		58.50±0.463
D-glucose	N/A	N/A	β-pyr.	60.2
D-galactose	15	10.0	β-pyr.	67.33±1.657
	25	5.0-15.0		66.49±1.119
	35	10.0		66.68±1.695
D-galactose	N/A	N/A	β-pyr.	62.6[c]
D-galactose	15	40[d]	β-pyr.	63.8±2.0
	25	40[d]		62.4±2.4
D-mannose	36	N/A	α-pyr.	63.03

Table 2.4 Continued

Sugar	Temp. [°C]	Conc. [%][a]	Form[b]	%Equilibrium composition
D-cellobiose	15	8.0	β-pyr.	59.60±4.466
	25	8.0		57.71±1.543
	35	8.0		56.16±1.664
D-maltose	N/A	N/A	β-pyr.	55.1
D-maltose monohydrate	15	10.0-20.0	β-pyr.	56.03±10.093
	25	10.0-30.0		59.21±1.407
	35	10.0-30.0		58.91±1.345
D-maltose	N/A	N/A	β-pyr.	55.1
D-turanose	15	20.0	β-pyr.	56.06±1.693
	25	20.0		55.96±0.969
	35	20.0		57.08±0.741
D-fructose	30	N/A	β-pyr.	72.0±2.0[e]
L-sorbose	30	N/A	α-pyr.	95.0±2.0[f]

[a] % by weight, except where specified, [b] the other principle form is calculated by subtract from 100, [c] 31.9% α-pyranose and 5.4% open chain form, [d] 40% w/v, [e] 5% α-furanose and 23% β-furanose, [f] 5% α-furanose

Mutarotation data for other sugars (particularly the monosaccharide sugars can be found in the literature already cited in this chapter).

Chapter III

Secondary Nucleation Thresholds of Sugars in Aqueous Solutions

3.1 Introduction

Although the mutarotation rates and equilibrium was determined for a large number of sugars, essentially completing the knowledge of these reactions in common sugars, it is not possible to do this for the parameters relating to crystallization (particularly solubility, nucleation limits and rates, and crystal growth rates) within the time of this study. It takes approximately one year to acquire sufficient data to fully characterize a single sugar. For this reason it was decided to characterize the crystallization parameters of only one sugar, glucose monohydrate. This data has already be characterized previously for several other mutarotating sugars, notably fructose, anhydrous glucose, mannose, and xylose. The data from the other studies is sufficient to be able to use in the models of the crystallization processes with mutarotation described in Chapter V. This chapter describes secondary nucleation thresholds in the system of glucose monohydrate. These limits are necessary so as to know maximum concentrations that may be used in an industrial crystallizer to avoid unwanted spontaneous nucleation. If these limits are ignored, uncontrolled spontaneous nucleation will occur, and this will result in very small product crystal size, and an undesirable product.

Secondary nucleation is the main source of the nucleation occurring in the majority of industrial crystallizers. Nucleation is typically avoided or minimized in crystallization processes since it is difficult to control and introduces undesired variability in the product size distribution. For this reason, the secondary nucleation thresholds of glucose monohydrate in aqueous solutions were determined in an agitated batch system prior the crystal growth experiment to ensure no nucleation will take place in the crystallizer. Over the experimental temperature range the widths of the secondary nucleation thresholds decreased as the induction time increased and were found to be temperature independent when supersaturation was based on the absolute concentration driving force. This data was used to determine time dependent concentration limits in the batch crystallization experiments discussed in Chapter V.

As the previous chapter mentions, crystallization is considered to be a two-step process, namely nucleation followed by crystal growth. Nucleation is the formation of new crystals suspended in the solution. Crystal growth is the growth of these crystals to

larger sizes through deposition of solute from the solution. Both nucleation and crystal growth require a supersaturated environment in order to occur. This can be explained in terms of thermodynamics; the supersaturated solution is not at equilibrium and the system moves toward the equilibrium state (in this case the solubility) by crystallizing out. When the crystallization starts, the supersaturation can be reduced by a combination of nucleation and crystal growth processes. Controlling the degree of nucleation and crystal growth during the operation can control the product crystal size and size distribution.

Supersaturated solutions exhibit a metastable zone, where crystals can grow without significant birth of new crystals (nuclei). Further increases in the supersaturation will cause the solution to reach a value where secondary nucleation in the presence of prior crystals occurs; this limit is known as the metastable limit for secondary nucleation. Nucleation is necessarily avoided or minimized in crystallization processes since it is difficult to control and gives a bad product size distribution. In batch processes,. if possible, operation is usually undertaken in the metastable zone, and crystallization is initiated through the addition of seed crystals, thus avoiding large amounts of nucleation. Fortunately, the secondary nucleation thresholds (SNT) of sugars is usually quite large[21-23].

3.1.1 Phase Diagrams

In order to study the crystallization of glucose in aqueous solution, the phase diagram of this system is required. Figure 4.1 is the phase diagram of glucose[24] and establishes the solubility curve of each of the crystalline forms of glucose in aqueous solution. This figure represents the four solids formed, i.e. ice, α-glucose monohydrate crystal, α-glucose anhydrous crystal, and β-glucose anhydrous crystal, present in the system in the temperature range of –22 to 120°C. For the glucose-water system, three forms of glucose may be deposited from aqueous solution depending upon the temperature: α-monohydrate from approximately –5 up to 55°C, α-anhydrous from 55 up to 91°C, and β-anhydrous above approximately 91°C. If the crystallization is below 0°C, ice is formed with some formations of glucose crystalline (depends on solution concentration).

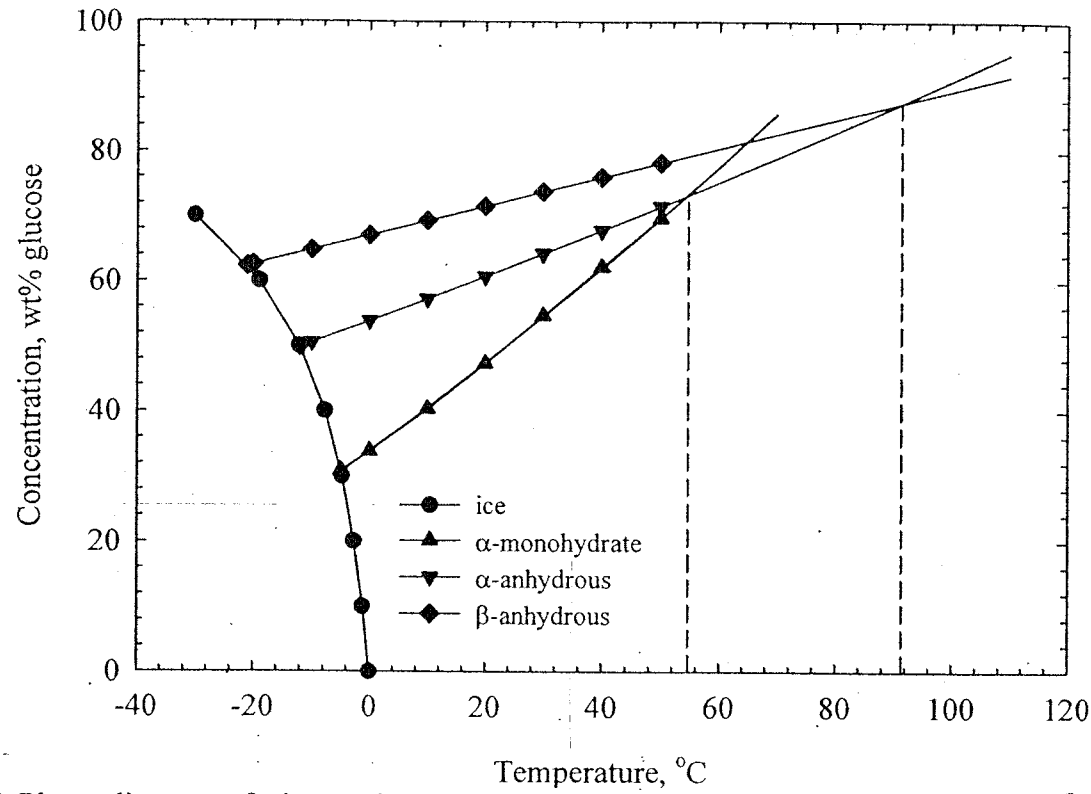

Fig. 3.1 Phase diagram of glucose in water, showing the temperature dependence of the glucose solubility in aqueous solution[24]. Dashed lines show the transition points of α-monohydrate to α-anhydrous (at approximately 55°C) and α-anhydrous to β-anhydrous (at approximately 91°C).

The phase diagram for fructose has also been measured[25] and is shown in Figure 3.2. There are several phases existing in this system, with the stable phase depending on the temperature and fructose content in the syrup, which include anhydrous fructose, fructose dehydrate, fructose hemihydrate, and gel. The phase diagrams of other mutarotating sugars have also been studied, including galactose, xylose, and mannose, but the phase diagrams are not as complete as for fructose and glucose.

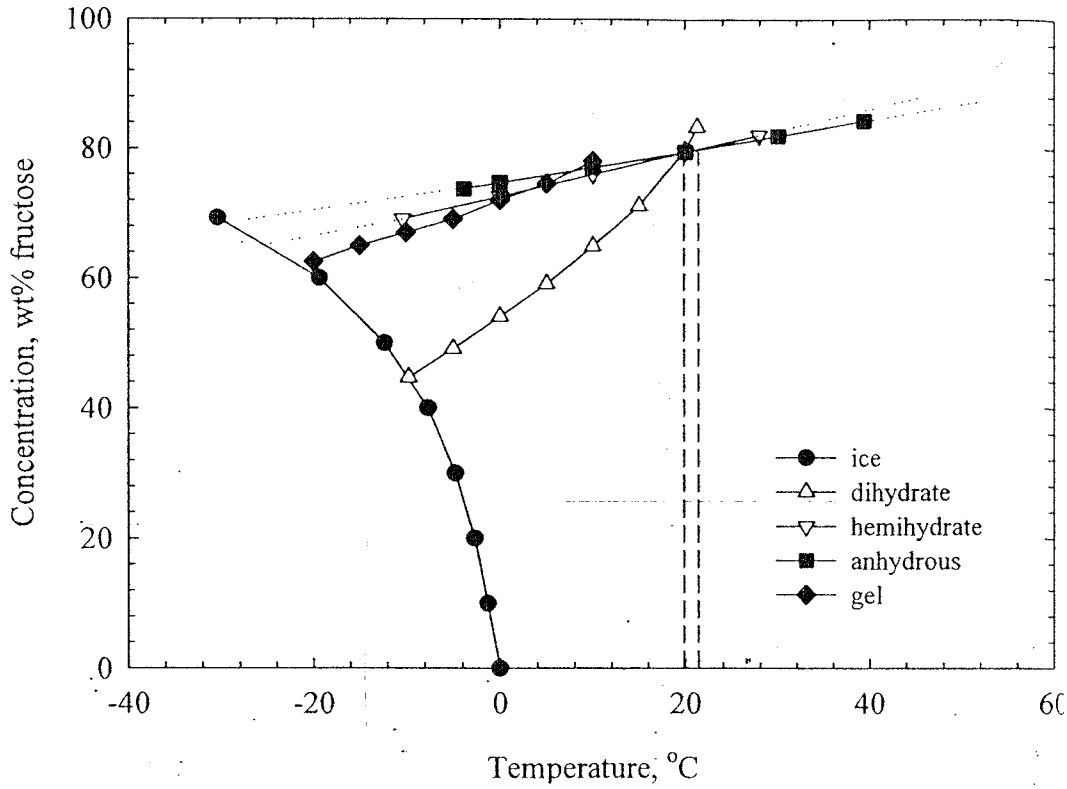

Fig. 3.2 Phase diagram of fructose in water, which shows the temperature dependence o the fructose solubility in aqueous solution[25]. Dotted lines were extrapolated from th experimental data. The two dashed lines represent two transition points.

3.1.2 Theory in Nucleation

Nucleation from solution can occur by either primary or secondary mechanisms Figure 3.3 shows primary nuclei can appear spontaneously in homogeneous systems or b enhanced by the presence of suspended dust particles or apparatus surfaces: the later cas is called heterogeneous nucleation. Secondary nucleation describes a range of mechanism relating to the presence of suspended solute crystals. Secondary nucleation can b separated into several mechanisms as presented in Figure 3.4. In this figure the secondar nucleation can be divided into nucleation by contact, shear, fracture, attrition, and needl breeding. Randolph and Larson[26] also propose an initial breeding nucleation mechanism which is the important nucleation source of nuclei in seeded system. Myerson and Ginde[2] explain that the initial breeding or dust breeding nuclei are formed by the tiny crystals o dust on the surface of dry particles that are directly introduced into the solution in the start up of the batch operation. This dust is swept off and acts as nucleation sites.

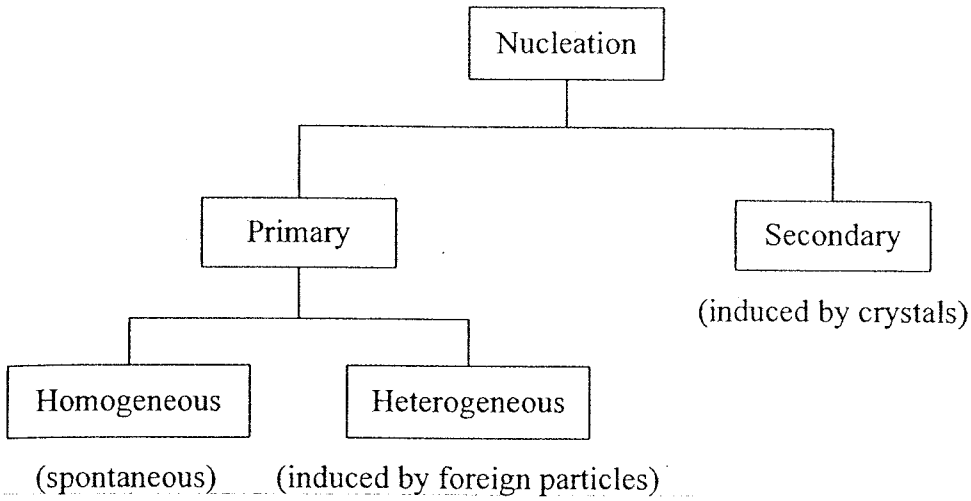

Fig. 3.3 Categorization of nucleation mechanisms[28].

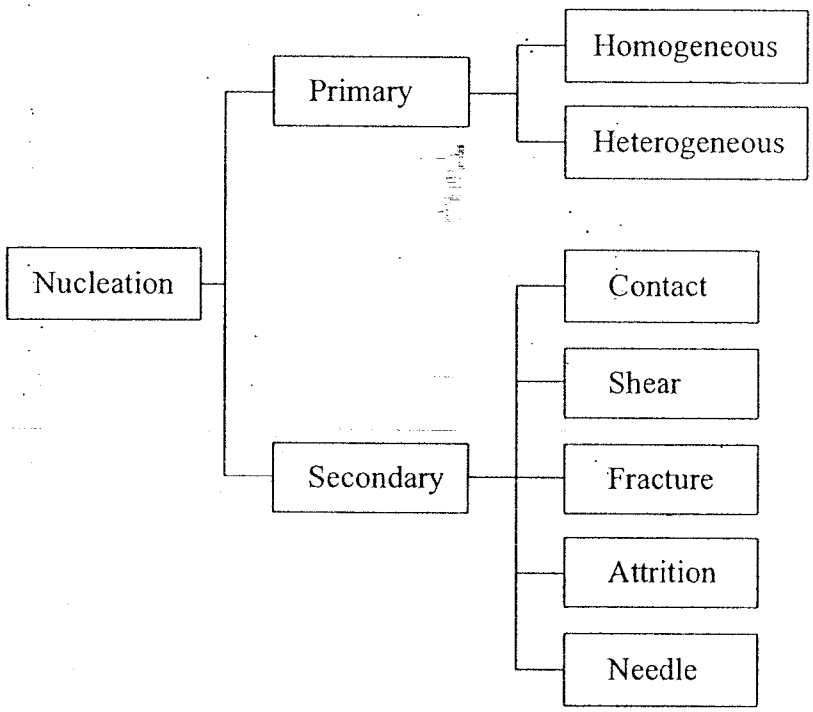

Fig. 3.4 Nucleation mechanisms[26].

The secondary nucleation mechanisms can be clearly explained using the diagram of a growing crystal in Figure 3.5. This diagram can be separated into three parts, the parent crystal, the absorbed layer containing solute molecules, and the solute molecules in the supersaturated bulk solution. Fracture and attrition concern the breakage of the parent crystal, while the other mechanisms concern the absorbed layer. When the fragile particles

suspended in a dense suspension are subjected to violent agitation or high velocit pumping, the damage is usually done by crystal-crystal interaction or crystal-apparatu contact. Attrition is merely fracture but the fragments are very much smaller than th parent and the visible damage is usually less than for fracture. Needle breeding occu because of dendritic growth of the absorbed layer on the parent crystal. This piece is ver easy to break especially under violent conditions. Nucleation by fluid shear results whe the fluid velocity relative to the crystal velocity is large and some of the absorbed layer removed. If there is enough energy these absorbed molecules may agglomerate togeth and form nuclei; else they will disappear. The most important source of nuclei in industri crystallization is contact nuclei that result from the contact between the particles an stirrer, pump, flow-lines or other crystals. The products of the contact may be attritio fracture, or contact nuclei, but the last differs from the others because it is concerned wit the absorbed layer, not the parent crystal.

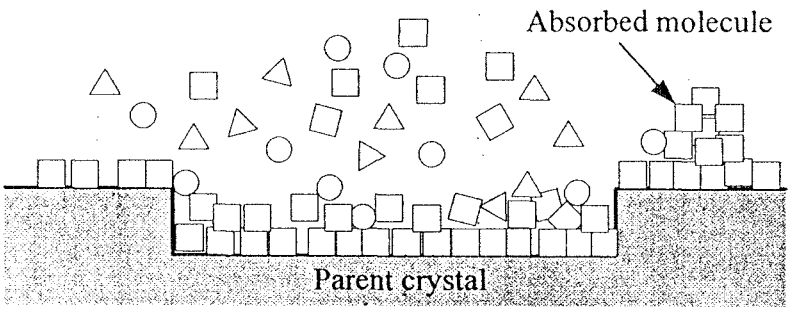

Fig. 3.5 Absorbed layer of solutes on the surface of growing crystal. Different symbo (square, triangle, and circle) represent the different types of molecular species. Adapte from Randolph and Larson[26].

It is obvious that heterogeneous primary nucleation and secondary nucleation a the most important sources of new crystals formation in industrial crystallization[2] Homogeneous nucleation is considered to be an insignificant phenomenon in crystallize since it is nearly impossible to produce a system with an absence of dust and dirt in th original solution. The best method for inducing crystallization is to seed a supersaturate solution with small particles of the material to be crystallized[28], which is also the reaso that homogeneous nucleation can be neglected in industrial crystallizers.

3.1.3 Metastable Zone and Secondary Nucleation Threshold

The phase diagram is a necessary tool for solution crystallization. The crystallization diagram allows us to determine whether a solution will crystallize at a given condition, i.e. at a particular temperature and pressure, and if so, what species will crystallize: it is a map for the crystallization operation. The condition of supersaturation with respect to temperature alone is not sufficient for a system to begin to crystallize[26,28]. Knowledge of the zones of the metastable region is necessary for the operation. Since this study concerns secondary nucleation only, the time dependent secondary nucleation threshold (SNT) is specified. This section shows details on the metastable zone for different nucleation mechanisms and the SNT time dependent, while the details concerning the kinetics of crystal growth will be discussed in Chapter 4.

Supersaturated solutions exhibit a metastable zone as shown in Figure 3.6 where the widths of this zone for different nucleation mechanisms are drawn. The lowest solid line is the solubility curve where solid and liquid are in equilibrium with each other. In this state, the solute deposition rate and the solute removal from the crystal occur at the same magnitude. Thus, the induction time (t_{ind}, defined as the time where the nuclei appear) for nucleation (both primary and secondary) is infinite at this condition. Further increases in the supersaturation from the solubility will cause the solution to reach a value where secondary nucleation, heterogeneous primary, and homogeneous primary nucleation, occurs progressively. The limit of each mechanism is known as the metastable limit or nucleation threshold for the particular mechanism.

The secondary nucleation zone in Figure 3.6 is expanding in Figure 3.7. The upper dashed line in this figure is the instantaneous secondary nucleation threshold (metastable limit, $t_{SNT} = 0$). Between this line and the solubility curve, which is called secondary nucleation zone, the time dependent secondary nucleation thresholds are drawn. It is noted that the time that necessary to use to induce the secondary nuclei is varied from zero (at the metastable limit for secondary nucleation) to infinite (at solubility curve). This can be explained through the fact that the smaller the supersaturation the greater the time required to induce the nucleation with the presence of the solute crystals in system.

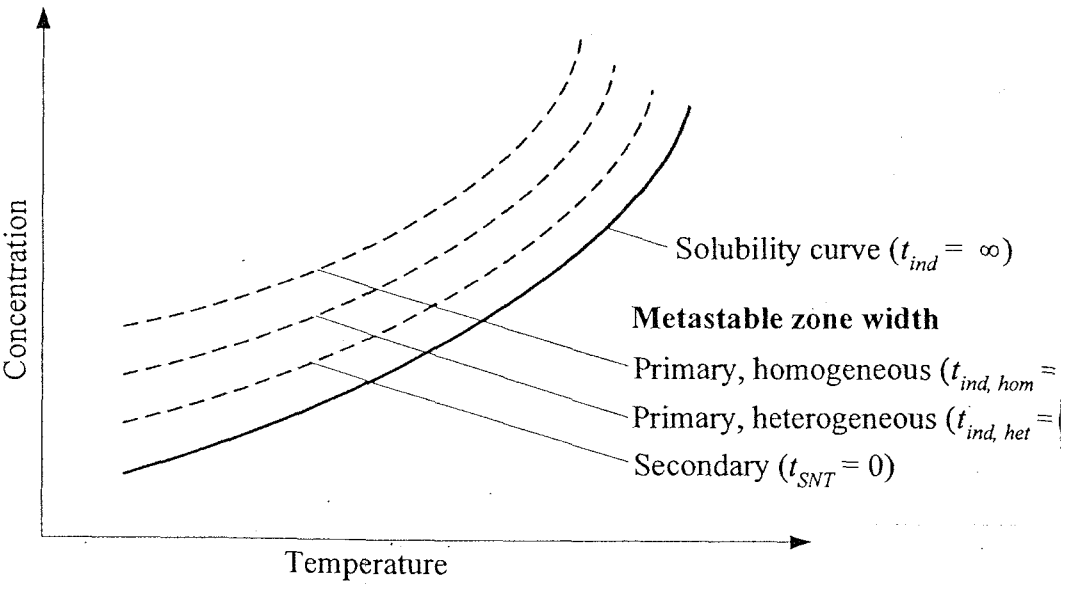

Fig. 3.6 Metastable zone widths for different nucleation mechanisms[29] (Mersmann, 1995) The t_{SNT}, $t_{ind, het}$, and $t_{ind, hom}$, are the induction time for secondary nucleation heterogeneous, and homogeneous nucleation, respectively.

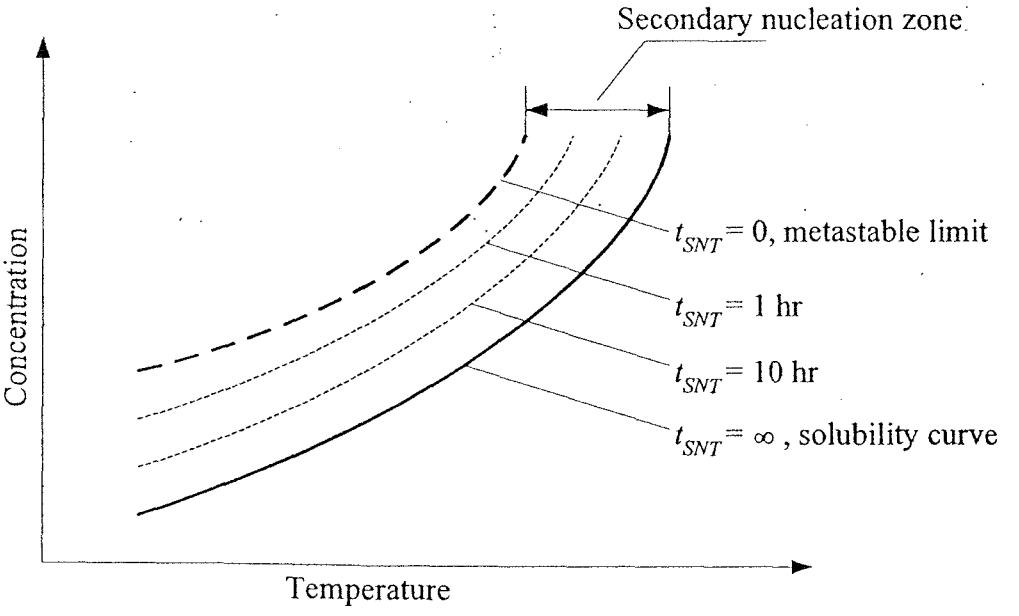

Fig. 3.7 A diagrammatic representation of the secondary nucleation thresholds of solution crystallization

3.2 Materials and Methods

3.2.1 Materials

All glucose solutions used in the secondary nucleation experiments were prepared from analytical reagent (AR) grade anhydrous D-glucose supplied by Chem-Supply Pty. Ltd., Australia, and water treated by reverse osmosis (RO). The anhydrous D-glucose was confirmed less than 2% moisture using a vacuum evaporation (dry substance method) explained in Section 4.3.4. The solution was made from known amounts of glucose and water dissolved in a microwave oven, for which the power was set at the medium level to avoid chemical degradation. Seed crystals were prepared from D-glucose monohydrate supplied by Asia Pacific Specially Chemical Limited (APS), Australia. A seed size larger than 180 μm (dry-sieved) was used since it is easy to distinguish between the seed added and the nuclei formed.

3.2.2 Apparatus

A schematic diagram of the 50 ml stirred bottles are shown in Figure 3.8. These were used as agitated batch crystallizers for the secondary nucleation experiments. The research group of Prof. White of the Particle and System Design Centre (PSDC), Department of Chemical Engineering, the University of Queensland, Australia, designed this bottle. The attrition and breakage of the particles caused by contact with the stirrer and the bottom of vessel is minimized by used of a stirrer bar supported some distance above the base of the bottle using an axle mounted on a hub in the bottom of the bottle. A multi-point submerged stirring plate set at 200 rpm drove the stirrer bars. This stirrer speed was chosen since it was the stirring speed where the particles were just suspended, and the stirrer caused no significant breakage of the particles.

The stirred bottles and the submerged stirrer plate were placed in a constant temperature water bath, where the experimental temperature was controlled within ± 0.5°C. A cooling unit is required at low experimental temperatures (i.e. at 10°C).

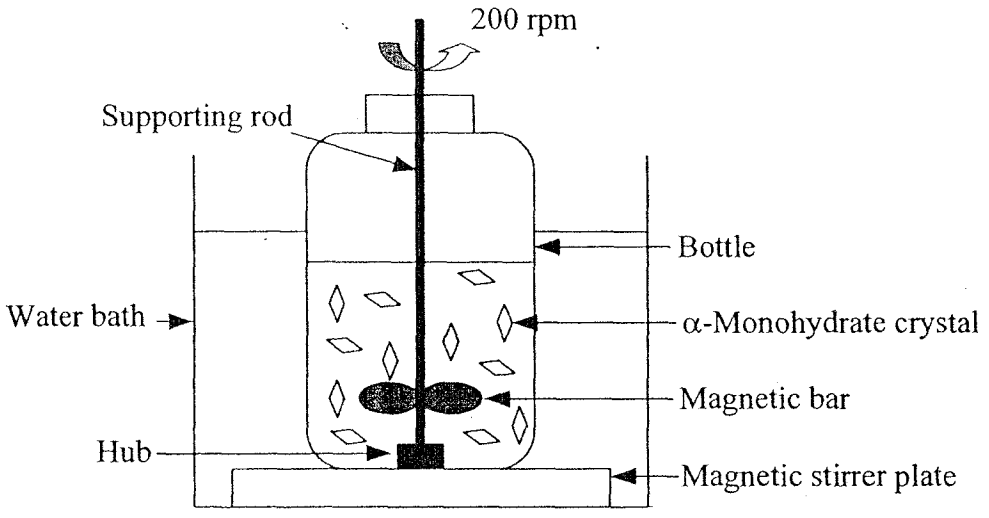

Fig. 3.8 Secondary nucleation experimental setup drawing (not to scale).

3.2.3 Experimental Procedure

Secondary nucleation experiments were performed at 10, 25, and 40°C. Each secondary nucleation run involved observation of the nucleation of a number o supersaturated solutions containing α-glucose monohydrate crystals. A series o supersaturated solution was prepared and heated to 20°C above the experimenta temperature for 20 minutes to ensure that no ghost nuclei remained in the solution. These nuclei may appear during the storage of the solution overnight, especially in cases of high supersaturation. Approximately 1 mg of α-glucose monohydrate crystals was added t each solution to induce secondary nucleation. Nucleation was determined visually at many time intervals, with nucleation being indicated by precipitation or clouding by amounts o very fine nuclei. Concentrations of the highest concentrated solution that had no nucleated and the lowest that had were recorded; concentrations being those of the initia concentration prior to nucleation. The experiments were duplicated (at 25°C) or replicate (at 10 and 40°C) to check reproducibility.

3.2.4 Dry Substance Method

The dry substance method is a very accurate technique to measure the suga concentration in solution. However, this technique is time consuming, so it was not use for concentration measurement in this research. The method was used to monitoring chec the amount of water (percent moisture) in the glucose anhydrous crystals to ensure that th

storage of the crystals is sufficiently good to keep the crystals dry without water absorption from their surrounding.

Special apparatus

1. Glass weighing bottles approximately 10 ml in volume with ground glass stoppers.

2. Strips of filter paper 60 × 4.5 cm, rolled in loose coils and placed inside the bottles.

Procedure

1. Pre-dry the bottle and filter paper in a vacuum oven at 63°C overnight.

2. Stopper immediately after removal from the oven and cool in a desiccator for 30 minutes.

3. Weigh the sealed bottle plus paper; this is assigned to be equal to W_1.

4. Remove the paper and then weigh (W_2).

5. Introduce approximately 2 g of glucose (crystal or solution) and weigh (W_3).

6. Add approximately 2 ml of distilled water, mixed by swirling.

7. Insert the paper coil and allowed to stand for 30 minutes before drying process.

8. Dry the sample at 63°C for 16 hours under a vacuum of 26 to 29 in. Hg.

9. Close the stopper and cool for 30 minutes before weighing (W_4).

The dry substance is calculated from the relationship:

$$\text{Dry Substance} = \frac{W_4 - W_1}{W_3 - W_2} \qquad (3.1)$$

Percent moisture is calculated from (1.00-Dry substance)×100%.

3.3 Results and Discussion

3.3.1 Effect of observation time and temperature on SNT

The effect of observation time on the measured SNT at three different temperatures is shown in Figure 3.9. The raw data for all experiments performed can be found in the Ph.D. Thesis of Sukanya Srisa-nga[30]. In this figure, each data value consists of two data points joined by a vertical line: the upper point represents the lowest absolute supersaturation that nucleated, and the lower point represents the highest absolute supersaturation that did not nucleate. The true value of the SNT must lie between these two points. The figure shows that the SNT decreases as the observation time (or induction time) increases. An instantaneous (or initial) secondary nucleation zone width (SNZW) in

absolute supersaturation is about 16g/100g solution. At large induction time (i.e. 50 hours) SNZW is about 5g/100g solution. Even after two days some of the low supersaturated solutions had not nucleated.

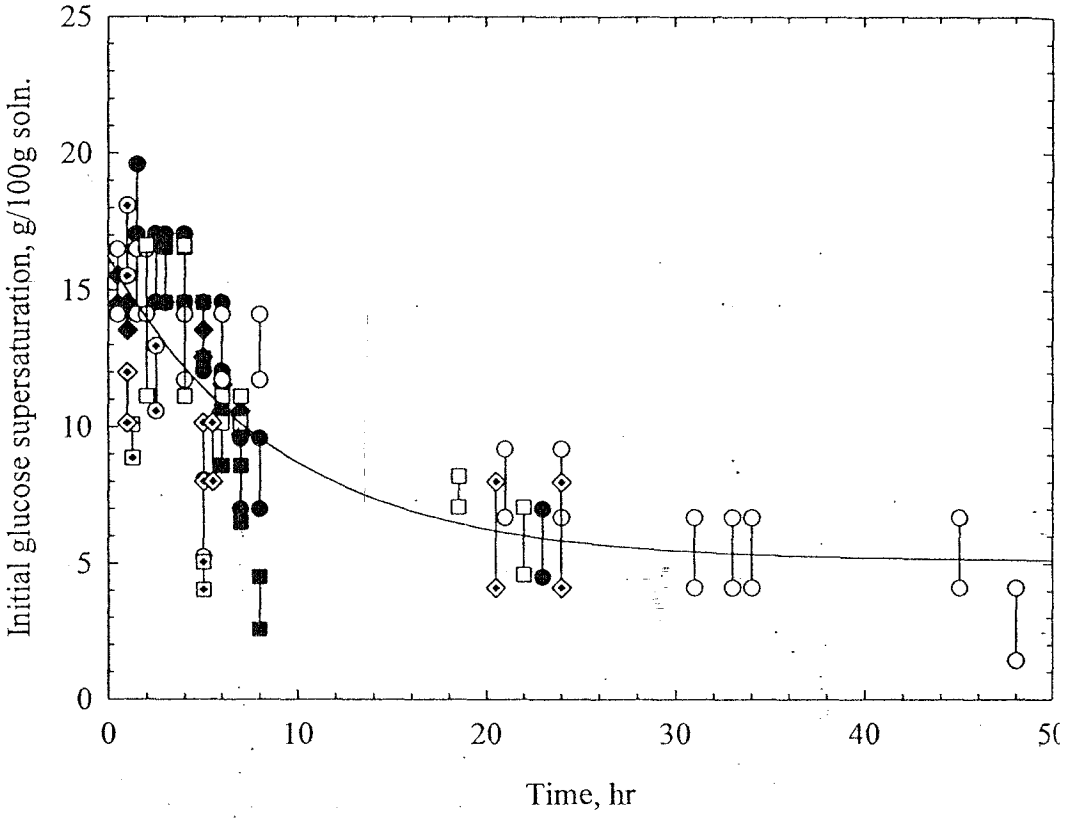

Fig. 3.9 The time dependence of the secondary nucleation zone width. Filled symbols ar for the triplicate experiments at 10°C, open symbols are for the duplicate experiments a 25°C, and open symbols containing a character are for the triplicate experiments at 40°C A solid line is a best-fitted line for all experimental temperatures.

The SNT at 10, 25, and 40°C overlap when plotted in terms of the absolute value c the supersaturation, as in Figure 3.9. This allows a single line to represent the zone widt for the three temperatures studied. This implies that temperature does not have significant effect on SNT over the range of temperatures where glucose monohydrate likely to be crystallized. Because the solubility of glucose is a strong function c temperature this same result does not result if the data is plotted with respect to relativ supersaturation, which is the more common measure of the driving force for cryst growth. In a limited number of the SNT experiments, both points are below, or both poin

are above the line of best fit. This is thought to be due to the stochastic nature of the nucleation process. While a large number of experiments could have been done to locate the mean of the stochastic distribution with high accuracy, this was not considered worthwhile as the secondary nucleation experiments are very time consuming and the results are of acceptable accuracy for further use.

The line of best fit to the data is an exponential decay with three parameters (equation 3.2), where C represents the total glucose concentration in g glucose/100g solution, C^* is the solubility, and t is the observation time in hour.

$$SNZW: C - C^* = 5.093 + 11.11\exp(-0.1129t) \qquad (3.2)$$

Accurate solubility data for glucose monohydrate in water has already been published (Young, 1957). The solubility data in the temperature range of 0 to 50°C was fitted using a quadratic polynomial equation, with the result shown in equation 3.3 where T represents the experimental temperature in degree Celsius.

$$Solubility: C^* = 33.82 + 0.6484\,T + 0.00135\,T^2 \text{ (for } 0°C < T < 50°C) \qquad (3.3)$$

Substitution of equation 3.3 into equation 3.2 gives the SNT concentration as a function of time, as shown in equation 3.4. Because the SNT is not a significant function of temperature, and glucose monohydrate is stable between –5 to 50°C it is likely that this equation is reasonably accurate representation of the SNT concentration over the entire range of conditions where glucose monohydrate crystallizes.

$$SNT: C = 38.91 + 0.6484\,T + 0.00135\,T^2 + 11.11\exp(-0.1129t) \qquad (3.4)$$

3.3.2 Use of SNT in the non-nucleating batch bulk crystallization

Figure 3.10 displays the induction time dependent secondary nucleation thresholds of glucose monohydrate in aqueous solutions. This graph is very important in non-nucleating batch crystallizations because it shows limitations on either the operation concentration or the batch time to ensure that nuclei are not formed, so the system can be easily controlled. For instance, when crystallization occurs at 30°C and the operating time

is within 24 hour, the initial concentration that can operate without a significant birth o new crystals is up to approximately 60 g glucose/100 g solution. This initial concentratio may be higher if the concentration decrease is rapid enough to ensure that the combinatio of concentration and time always puts the mother liquor at a point below the SNT.

Figure 3.11 is the phase diagram of glucose-water system where the metastabl zone for secondary nucleation of α-glucose monohydrate is specified. The dashed line i the plot is the SNT at 48 hours, which is assumed to be equal to the SNT at infinite tim (as indicated from Figure 3.10 and equation 3.4). This region is assumed to valid over th crystallizing temperature range of α-glucose monohydrate (-5.5 to 55°C), however, th operation near the transition points (-5.5°C and 55°C) needs to be minimized to avoid th formation of metastable phase. For instance, seeded batch operation over approximatel 42°C and solution concentration higher than approximately 68.5%, nucleation of α-glucos monohydrate may occur together with the formation of α-glucose anhydrous crystal Several researchers have found this phenomenon, either with glucose or other commo sugars such as galactose[24,25,31-33].

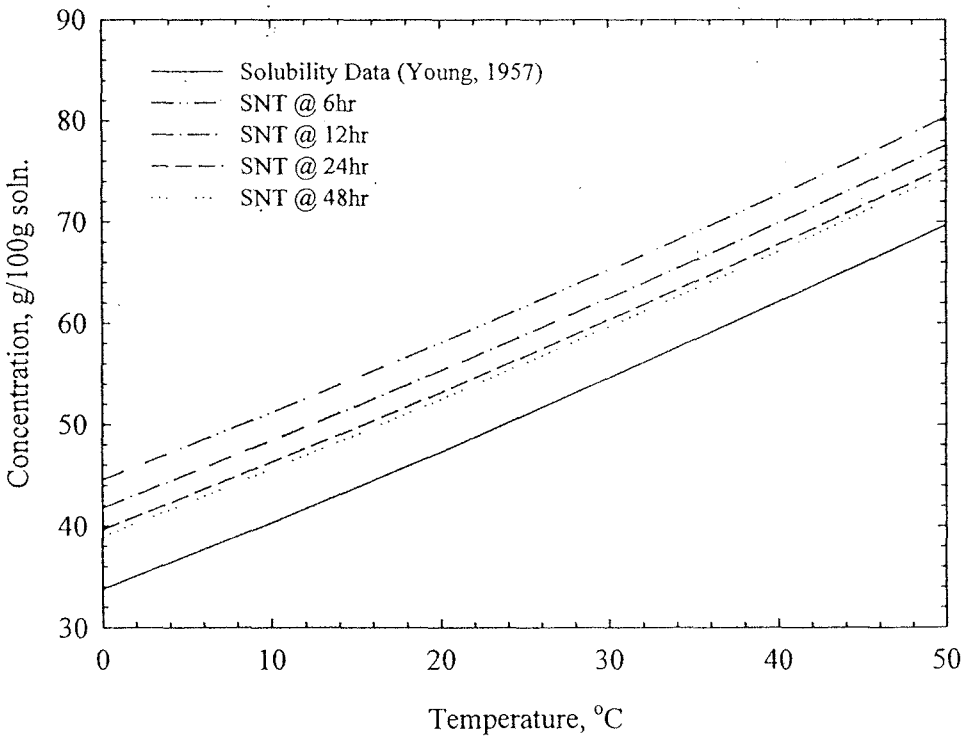

Fig. 3.10 Secondary nucleation thresholds for α-glucose monohydrate at the operating tir of 6, 12, 24, and 48 hr.

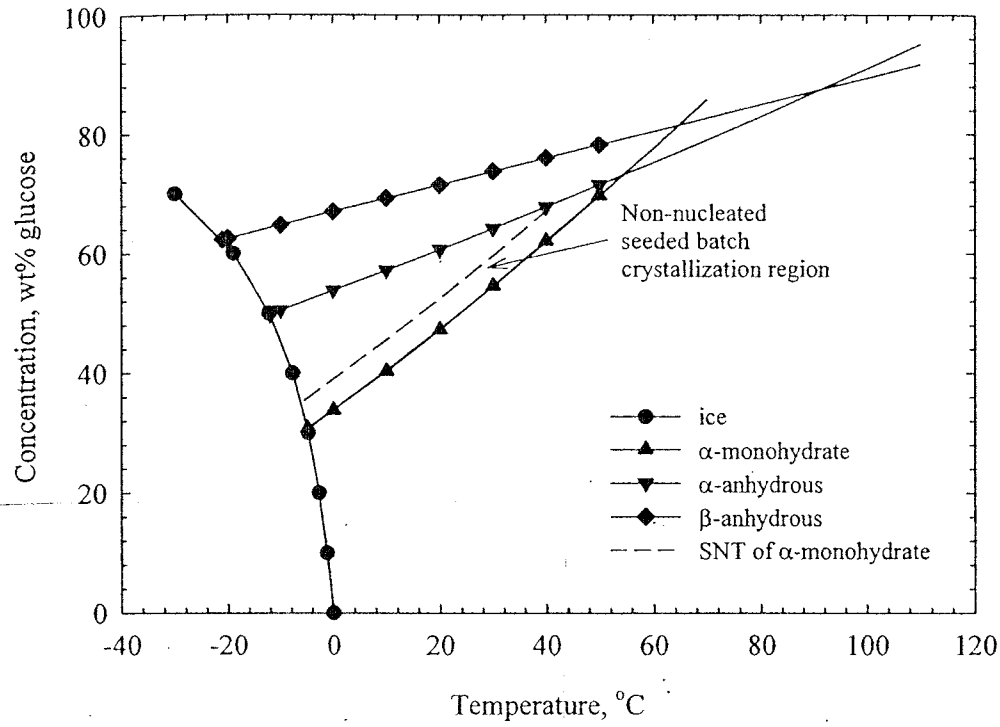

Fig. 3.11 Phase diagram of glucose-water system with the large time metastable region for secondary nucleation of α-glucose monohydrate specified.

Unlike glucose monohydrate, nucleation limits of fructose have been measured previously, and although the data is not as complete as that measured for glucose in the current study, it is sufficient for design purposes. The data has been measured in aqueous ethanol solutions, as this is the most likely solvent for industrial crystallization of fructose: in aqueous solutions the solubility of fructose is extremely high so that yields are extremely low, and solution viscosity is too high for convenient crystallization. It is likely that the metastable limit is similar in aqueous solutions, since the ethanol content of the solvent has no effect on the metastable limit in the range tested, which was quite wide. Crystal growth rate data and other data necessary for modeling and design have also been measured in aqueous ethanol solutions, and will be discussed in future chapters. The instantaneous (short-term) nucleation thresholds for fructose from aqueous ethanol solutions are shown in Figure 3.12[22]. The data is plotted on the phase diagram in Figure 3.13.

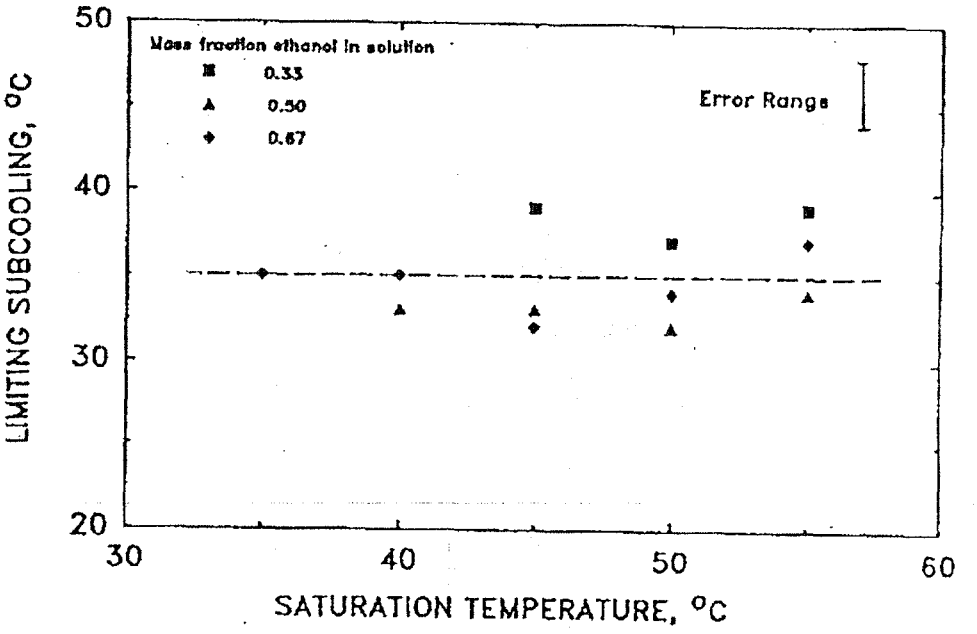

Fig. 3.12 Nucleation thresholds (based on subcooling from the saturation point) fo fructose[22]. The data is represented by differences in temperature between equilibrium an actual conditions. This may be converted to a concentration difference using the slope o the equilibrium line vs temperature.

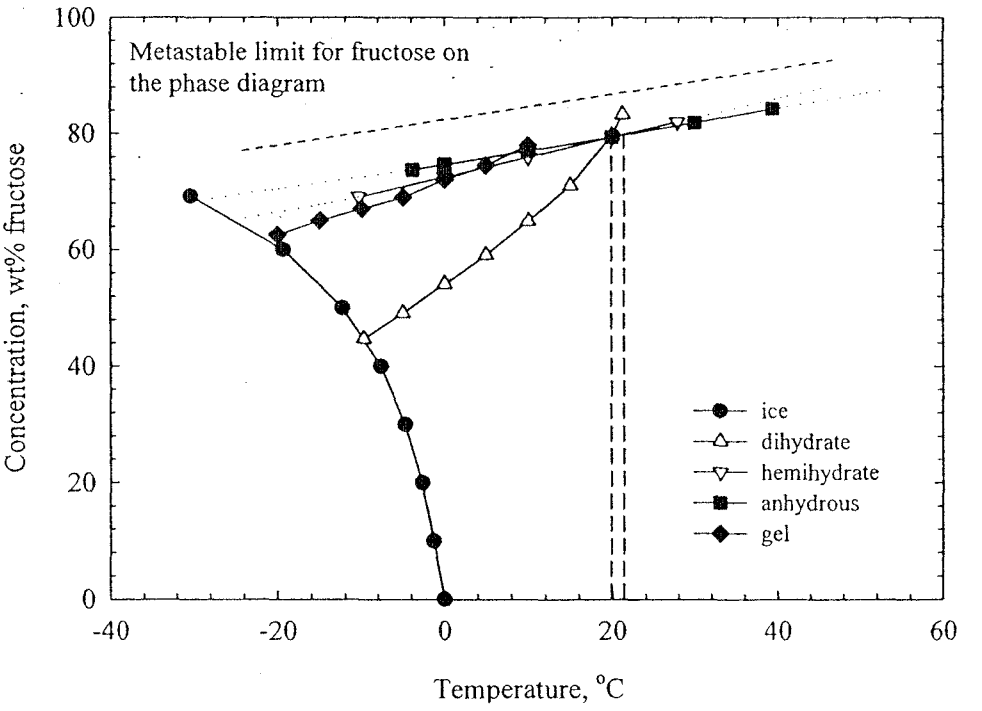

Fig. 3.13 Phase diagram of the fructose-water system with the large time metastable regio for secondary nucleation of α-fructose specified.

Chapter IV

Crystal Growth Kinetics of Sugars from Aqueous Solutions

4.1 Introduction

As with the previous chapter, there was insufficient time to measure crystal growth kinetics for a large number of materials in the present study, but this fact is not very important since growth kinetics for a large number of sugars have already been measured and published in the literature, including fructose from aqueous solutions[34], fructose from aqueous ethanol solutions[2], anhydrous glucose[21]), xylose[35], galactose[31,32], and others. These data on growth rates are all sufficient to use in the simplified model of the system described in the next chapter (and also using mutarotation data from chapter II), and therefore sufficient for obtaining a reasonable estimate of the effect of mutarotation in the crystallization in the particular sugar being studied.

There is no significant literature data for the crystallization of α-glucose monohydrate from any solvent, even for aqueous systems. This part of the research aims to determine the crystal growth kinetics of this sugar in aqueous solution in the region where the nucleation does not play any role on the system (i.e. at very low seeding rates meaning that the crystallization rate is very low in comparison to the mutarotation rate). The bulk crystallization experiments were performed in an isothermal and agitated batch crystallizer. The crystal growth of particles was initiated by adding pre-treated α-glucose monohydrate crystals into prepared glucose solutions. Mother liquor and crystal samples were taken at various time intervals to measure the solution concentration and the particle size distribution. The results showed that glucose monohydrate crystals had an abnormally fast growth rate during the first period of the experiment (i.e. 1 hour) and then the growth rate remained constant at constant supersaturation. The growth rate constant followed an Arrhenius relationship with respect to temperature, and the activation energy of surface integration controlled crystal growth of glucose monohydrate was calculated from this dependence. The results from this study can be used together with mutarotation kinetics and equilibrium data to model the industrial crystallization of this sugar considering the effect of mutarotation.

Crystallization is one of the main separation and purification processes used in the production of a wide range of materials. It is used in many industries to remove a valuable substance from an impure mixture, glucose monohydrate from hydrolyzed starch, for

example. Industrial crystallization processes in the chemical, pharmaceutical, and food industries mostly involve crystallization from solution. The crystallizing form can be anhydrous or hydrated depending on the operating conditions; however, usually only one crystal form is stable at a particular condition. D-glucose, for example, can be crystallized from aqueous solution in three different forms: α-D-glucose monohydrate, anhydrous α-D-glucose, and anhydrous β-D-glucose. The first two forms are produced commercially while the last one is available as a specialty chemical. In aqueous solutions, from the eutectic point at approximately -5°C up to approximately 55°C, the solution is in equilibrium with α-D-glucose monohydrate. Between 55°C and approximately 91°C, anhydrous α-D-glucose is the solid phase in equilibrium, whereas at temperatures above 91°C the stable phase is anhydrous β-D-glucose[1,9,24,36,37]. At conditions near the transformation points (approximately 55°C and 91°C), the two most stable forms can exist simultaneously. Away from these points, the less stable phase is transformed to the more stable one. At just below approximately 55°C, the hydrate-to-anhydrous transformation point, both hydrate and α-D-glucose anhydrous can be crystallized out[33]. This phenomenon occurs when the crystallizer is operated at a high supersaturation, well above the solubility of the anhydrous α-D-glucose form. However the unstable anhydrous crystals dissolve later in the crystallization process to form the hydrate form, as the solubility concentration of the anhydrous form is above the solubility of the hydrate. In the same way, the phase transition of the anhydrous β form may occur near 91°C, which is the α-anhydrous-to-β-anhydrous transformation point. Note the transition points quoted are a bit different from different sources but mainly ranging from 50 to 55°C for the α-monohydrate-to-α-anhydrous transition point, and 90 to 115°C for the α-anhydrous-to-β-anhydrous transition point. The words transformation and transition are used with the same meaning here.

The crystallization of D-glucose also involves mutarotation[21]. In solution, both α-D-glucose and β-D-glucose anomers exist simultaneously and undergo reversible mutarotation along with crystallization by the scheme shown in Figure 4.1 (a). If a part of the α-anomer is crystallized out, part of the β-anomer slowly converts into the α-anomer and, if necessary, vice versa. If the rates of the mutarotation reactions are slower than the rates of crystallization, the crystallizing anomer will be depleted such that it is below the anomeric equilibrium in solution, leading to a decrease in the driving force for

crystallization. Thus mutarotation could have an important effect on the kinetics of crystallization of D-glucose in aqueous solution, by affecting the supersaturation[21]. This behavior has also been reported for fructose crystallized from aqueous ethanol solutions, where the mutarotation kinetics is particularly slow due to less polar nature of the solvent[2]. Consequently, the authors reported the crystal growth rate with respect to the concentration of the crystallizing form (β-fructopyranose, in this case) instead of the total fructose in the system. The group of Arlt and Beckmann noted similar behavior for galactose, including initial nucleation of the unstable crystalline form, followed by a solution mediated (mutarotation controlled) phase transition to the stable crystalline phase[31,32]. They also defined the crystallization driving force with respect to the α-anomer, which is the stable crystalline form. The crystallization scheme including the mutarotation and an unstable phase transformation of galactose is shown in Figure 4.1 (b).

Mutarotation may be the rate-limiting step, depending on the relative rate constants of the mutarotation and crystallization kinetics. The crystallization kinetics also depends on nucleation, but the secondary nucleation thresholds of industrial sugar crystallizations are large, so operation is mostly seeded and non-nucleating. In seeded batch crystallizations, the kinetics depends on the initial suspension density, which in industrial crystallization of glucose monohydrate is about 3 to 15% by volume[38]. However, in order to study the crystallization kinetics, where the mutarotation effect is to be neglected, the depletion of the crystallizing anomer due to the crystal growth needs to be significantly slower than the generation via mutarotation. This can be achieved using batches containing small numbers of seed crystals operating within the metastable zone (operation with no nucleation).

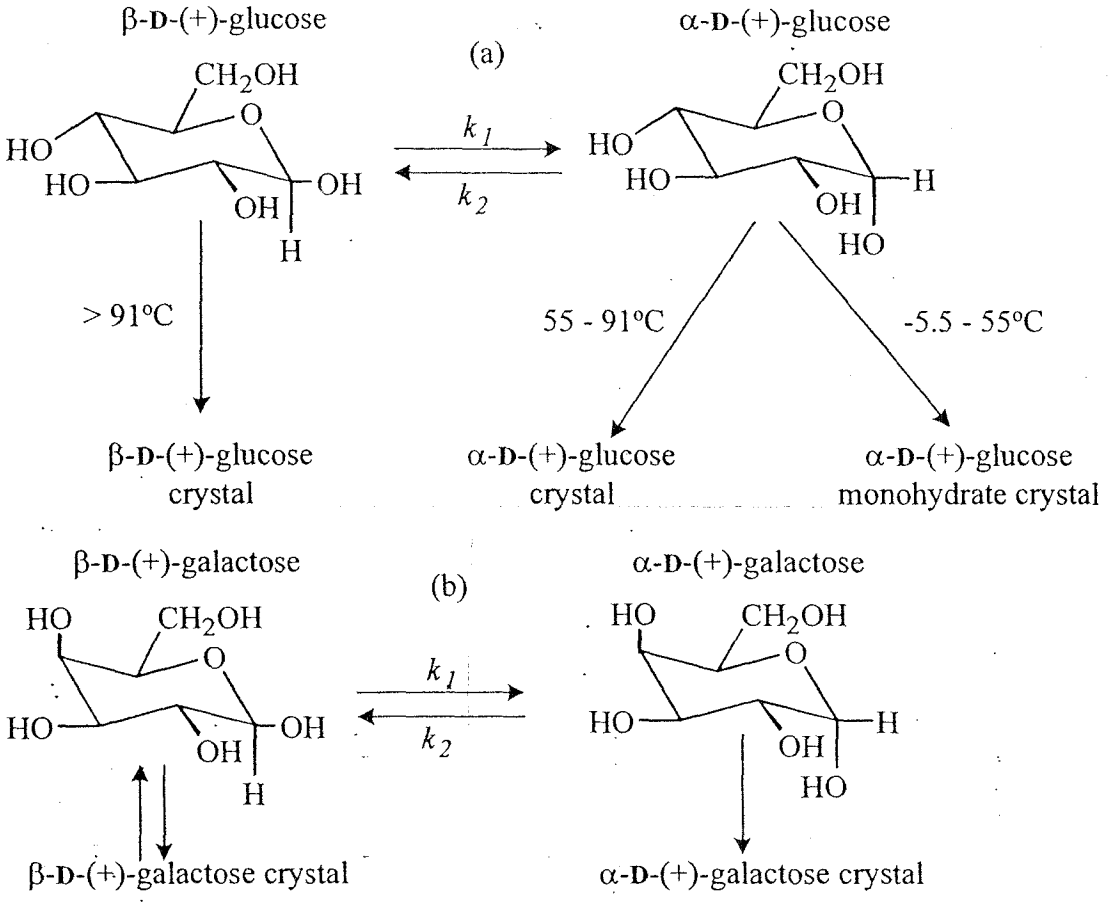

Fig. 4.1. Reaction schemes for the crystallization including the mutarotation reaction of (a D-glucose and (b) D-galactose.

Here, the effects of temperature and supersaturation on the crystal growth wer investigated. Pure aqueous solutions were crystallized in isothermal batch crystallizers i order to simplify the system studied. Due to the very slow crystal growth of this sugar, an the small amount of seed added, the supersaturation in the crystallizer was essentiall constant during the crystallization.

4.2 Materials and Methods

4.2.1 Materials

The glucose solutions used in both the secondary nucleation and crystal grow experiments were prepared similarly and shown previously in Section 3.3.1. The prepar solution was kept overnight at 10°C above the experimental temperature to ensure t establishment of the mutarotation equilibrium and that no nuclei were formed. Se

crystals were prepared from α-glucose monohydrate supplied by Asia Pacific Specially Chemical Limited (APS), Australia, and a pretreatment stage was found to be necessary to minimize nucleation due to the presence of surface nuclei and particle dust. The procedure is presented in the following section.

4.2.2 Seed Slurry Preparation

Due to the possible formation of tiny crystals on the surface of the α-glucose monohydrate crystals, and also dust on the surface of the particles, a pre-treatment process was performed before the seeds were introduced into the crystallizer. The pre-treatment minimized dust-breeding secondary nucleation, which is a serious problem in industrial batch operation[27]. Seed crystals were prepared using the technique that initially sieved the commercial glucose monohydrate crystals through a set of sieves ranging from 45 to 250 μm. Sieving was performed to produce seed crystals with a narrow size distribution to reduce difficulties in sizing wide particle size distributions, and to avoid the larger crystals growing out of size range measurable using Malvern MasterSizer/E. The 63 to 90 μm dry-sieved fraction of commercial α-glucose monohydrate crystals was wet sieved in denatured ethanol using a 63-μm sieve in order to remove fine crystals and dust from the particles. The wet-sieved product was then washed in 50% (by weight) aqueous glucose solution in water, which is undersaturated by a small amount at room temperature (approximately 25°C), to remove the dust or surface nuclei from the surface of the particles. Observation of the crystals under a microscope showed that the appearance of the crystals was good and no significant amount of nuclei in the seed particles or on the crystal surface was seen. Two samples of this slurry were taken to measure the particle size distribution (PSD) using the Malvern MasterSizer/E before each experiment, and these results noted as the seed size. Two batches of seed crystals were produced, as the initial batch prepared, used for the 25°C experiments, was insufficient to complete the experiments at 10 and 40°C. The particle size distributions of the two batches of seed crystals prepared were slightly different, with the seed prepared for the 25°C experiments having the same volume mean size (approximately), but a slightly larger coefficient of variation. Examples of the seed PSDs for the experiments at 10, 25, and 40°C are shown in Figure 4.2. It was also confirmed that there was no difference between the seed size measured before, and immediately after, addition to the crystallizer.

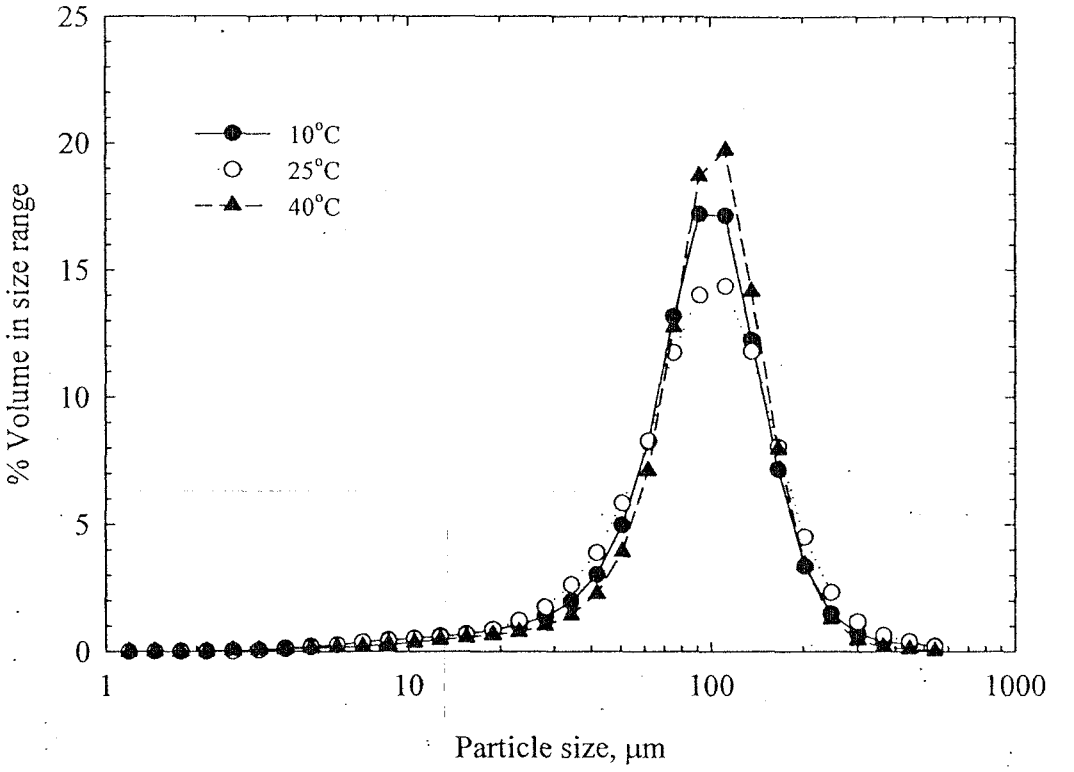

Fig. 4.2 Averaged volume based particle size distributions for seed crystals used experiments at 10, 25, and 40°C.

4.2.3 Dispersant Preparation

A supporting medium, which is also called the dispersant, is required to disper the sugar crystals inside the sample cell during the particle size distribution (PSI measurements using the Malvern MasterSizer/E. The rules for choosing this dispersant a that the medium must be transparent to the laser wavelength, and have a differe refractive index than the crystals. The particles must not dissolve, flocculate, or rea chemically with the supporting media. The suspension medium used for the PS measurement in this work was prepared from anhydrous ethanol (CSR Ltd., Sydney) a water treated by reverse osmosis (RO). Ethanol was chosen since there is no signific dissolution of glucose crystals in it, and water was added to prevent the dehydration water from the hydrate crystals. An amount of α-glucose anhydrous in excess of t solubility, i.e. more than 2.8% by weight[39], was added to the 10% of water in ethanol a the solution was agitated using magnetic stirrer at 40°C overnight. A tight capping of t bottle is necessary to prevent the evaporation of ethanol from the bottle. This solution w then kept under stagnant conditions until the solution temperature decreased to ro

temperature and the remaining glucose crystals settled down. Only clear solutions were pipetted for use in the size measurement. There was no point to filter this solution since the filtrate was still suspended with the large amount of fine particles (even in case of using the 0.22 μm membrane filter). α-Glucose monohydrate crystals did not dissolve in this solution since there was no significant change in the PSD of α-glucose monohydrate crystals resulting from Malvern MasterSizer/E over time, indicating no growth or dissolution.

4.2.4 Experimental Apparatus

The apparatus comprises of 1-litre glass crystallizers, 4-blade agitators, and overhead stirrers. These experimental setups were placed inside a constant temperature water bath, where the temperature was controlled within ± 0.5°C, the schematic drawing of the experimental setup is illustrated in Figure 4.3. Two batch crystallizations were performed simultaneously to check reproducibility.

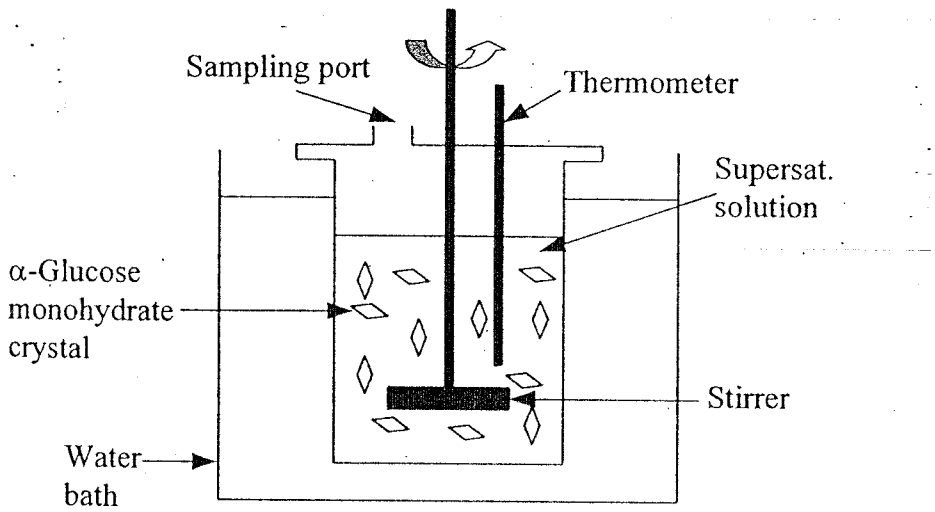

Fig. 4.3 Experimental setup schematic (not to scale).

4.2.5 Experimental Procedure

Preliminary work was performed to check what agitation rate is required for the crystal growth mechanism to be controlled by the surface integration step. The experiments were carried out isothermally at 25°C with stirring speeds of 400, 500, and

550 rpm. The experimental conditions, such as solution concentration, seeding amount, experimental time, were controlled at the same values for all experiments.

The crystallization of α-glucose monohydrate was performed isothermally at 10, 25, and 40°C. Initial crystallization experiments at varying agitation rates demonstrated that the crystallization was surface integration controlled at least at, and above, 450 rpm. It was important to achieve negligible attrition and/or breakage of seed crystals, so 500 rpm was chosen as the agitation speed for the crystallization experiments. A certain amount of prepared solution was introduced to each crystallizer before addition of seed. The experiment was duplicated in a parallel crystallizer.

Batches were initiated by the addition of 10 ml of seed slurry. Before the addition of the seed to the crystallizer, and during the batch run, duplicate samples were taken at various time intervals to measure the PSD. The total experimental time depended on how quickly the crystals grew under the given conditions, but was chosen to be less than that for the secondary nucleation limit at the initial supersaturation to avoid undesired nucleation. Observation of samples under a microscope indicated that nucleation did not occur. The refractive index of the clear liquor was periodically monitored during the experimental run to ensure the concentration was essentially constant during crystallization. A digital refractometer (RFM 340, Bellingham & Stanley Limited, UK) was used and the discrimination of the refractive index (RI) value for this instrument is within ± 0.00001 RI units. A calibration curve of known concentration solutions was used to determine total glucose concentrations from the RI measurements. The low amount of seed added to the batch, and slow growth kinetics should ensure that the batches were at constant composition within the accuracy of the measurements.

4.2.6 Particle Size Measurement

The PSD and volume concentrations were measured using the Malvern MasterSizer/E. The Malvern details and the measuring procedure are described here.

4.2.6.1 The Malvern MasterSizer/E

The Malvern MasterSizer/E, shown in Figure 4.4, is a laser light scattering sizing technique. In general, it is used to measure the size of any one material phase in another measures the particle size of α-glucose monohydrate crystals in 90% saturated ethanol solution, which is shown the prepared method in Section 4.3.3, in this case. All particl

size analysis used a 300 mm focal length lens with the small sample cell having a beam length of 14.3 mm. This focal length measures the crystal sizes between 1.2 and 600 μm. Crystals are suspended in the path of a helium-neon laser beam (wavelength 633 nm) and scatter the laser beam as it passes through the sample. The scattered laser pattern passes through a focus lens and the laser light is focus onto a detector. A PC that is attached to the Malvern records the scattering pattern and the size distribution of the sample is calculated. The basic principle of the Malvern is shown as Figure 4.5. The example of the data re-plotted from the raw data of the Malvern output is shown in Figure 4.6. The relative error in the volume median size obtained from Malvern is estimated at 2%.

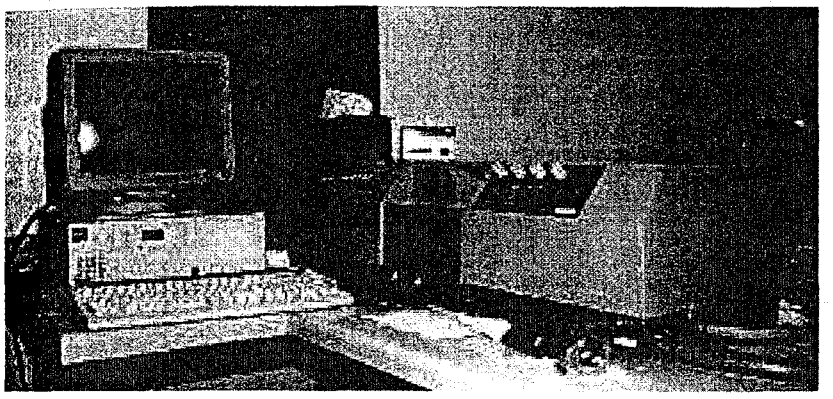

Fig. 4.4 The Malvern MasterSizer/E.

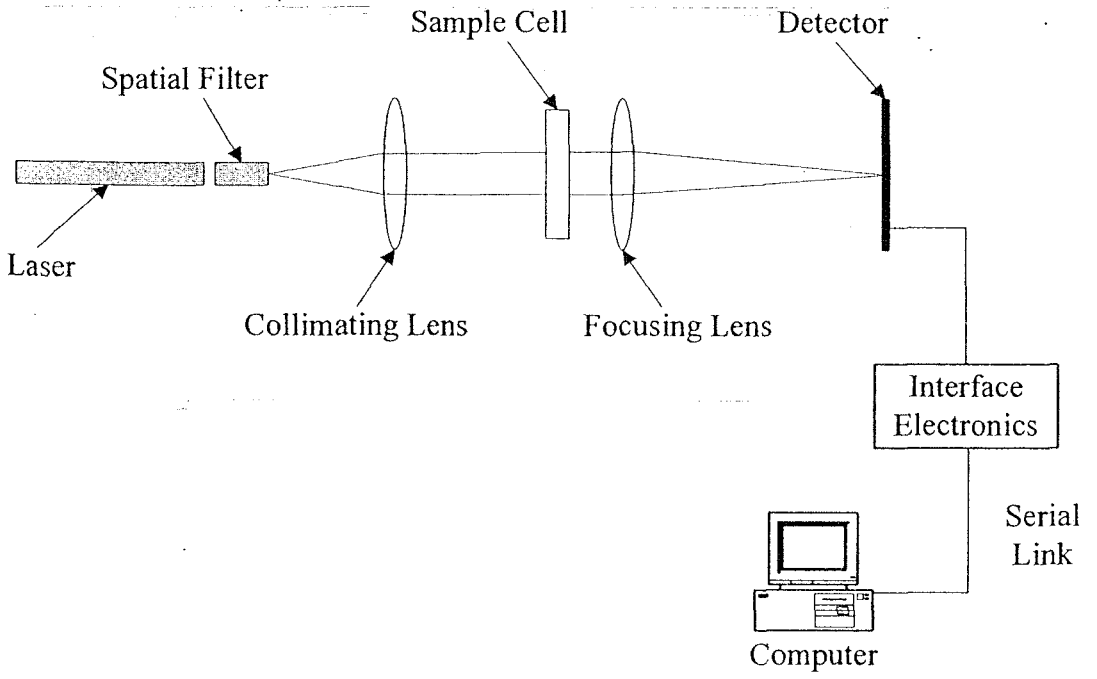

Fig. 4.5 The Malvern MasterSizer basic principle (redrawn from the Malvern manual).

4.2.6.2 Particle size measurement procedure

Approximately 16 ml of the dispersant (the preparation procedure is shown in Section 4.3.3) was placed in the stirred Malvern cell and the top opening of the cell was immediately covered with a plastic strip to prevent ethanol evaporation. The stirring level of magnetic star stirrer was set at the medium level (i.e. at 7), which is enough to suspend the crystals in the dispersant and not sufficiently fast to break the crystals by contacts with the bead. A beam alignment and background measurement, respectively, were taken prior to the addition of α-glucose monohydrate slurry. An alignment of the beam light is needed to check whether the system is ready for the measurement or not; if the Malvern fails this step the sample cell glass or lens are not clean enough. The background measurement must be subtracted from the sample measurement to get the actual scattering from the sample particles alone.

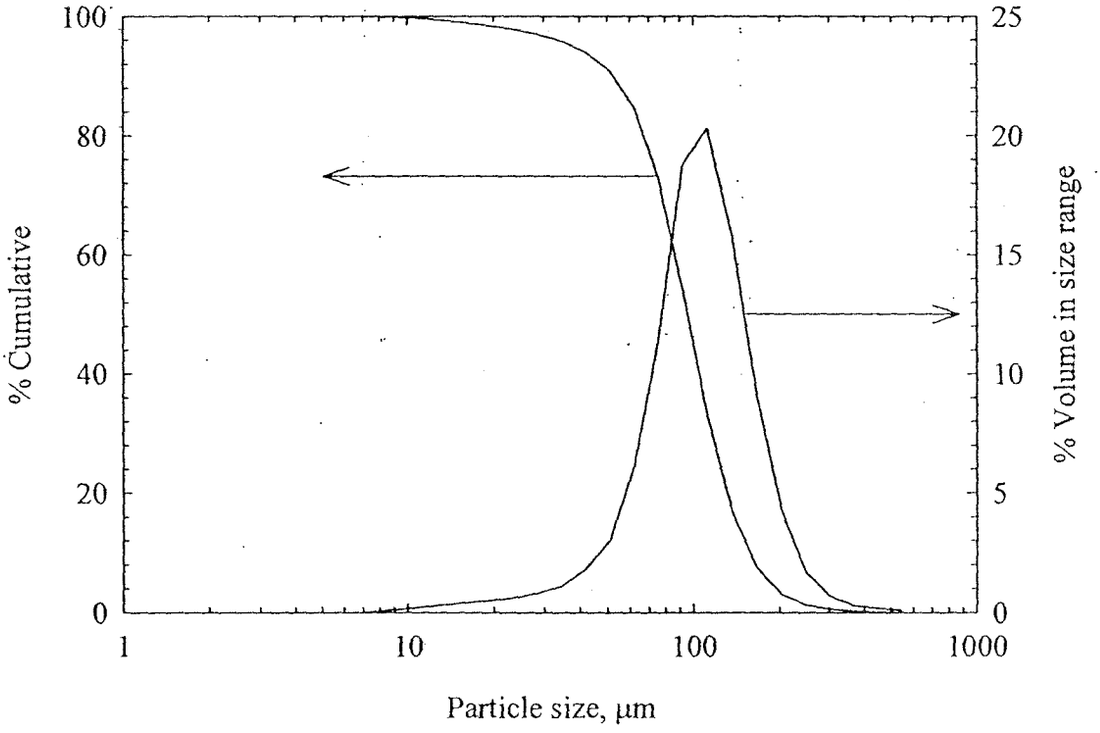

Fig. 4.6 The Malvern MasterSizer/E output (re-plotted) for the seed at 40°C

The volume of glucose slurry added was adjusted case by case to make the measured obscurations at approximately 0.2 since this value is the ideal value for the measurement. The obscuration is the fraction loss of energy from the laser beam caused by scattering from the particles. If the sample concentration is too high then light will

scattered by multiple particles, giving an incorrect angular reading. If the sample concentration is too low, the obscuration is low, leading to an insufficient sample count (compared to the background) for an accurate reading. More dispersant was added in cases where a high obscuration value was obtained, and, if the obscuration was too low (less than 0.15), more glucose monohydrate slurry sample was added to the sample cell. The results were read about a minute after adding the sample.

4.2.6.3 Crystal content calculation

For each measurement, the percent volume concentration was noted. This value is the predicted percent crystal content (by volume) in the sample cell. The crystal content in the crystallizer is calculated from the equation:

$$weight\ \%\ crystal = \frac{volume\ \%\ from\ Malvern \times (V_d + V_s) \times \rho_x}{V_s \times \rho_s} \tag{4.1}$$

where V_d is the volume of dispersant, V_s is the volume of slurry, ρ_x is the crystal density, and ρ_s is the density slurry. Crystal content (in the unit of kg particles per kg suspensions) can be determined from:

$$crystal\ content = \frac{volume\ \%\ from\ Malvern \times (V_d + V_s) \times \rho_x \times V_B}{100 \times V_s \times M_B} \tag{4.2}$$

where V_B is the crystallizer volume and M_B is the mass of crystallizer suspension.
The crystal content results were consistent with the increase in particle size due to crystal growth and also confirm that no nucleation inside the crystallizer.

4.3 Results and Discussion

Figure 4.7 shows an example of the PSDs from a batch run at 25°C plotted on a scaled log size basis. For the Common History Seed (CHS), where the relative growth rate of a crystal is proportional to its size, growth will not change the shape of the size distribution plotted on a log scale. Thus Figure 4.7 shows that the seed crystals are indeed CHS. The particle sizes have been scaled relative to the volume median size for each PSD

to illustrate the constant shape of the distribution. The results show two PSD duplicated for each time. The PSD results appear to be approximately normally distributed on a log size scale, except occasionally where there is a tail at the same size ranges. Particles from the crystallizer were visually inspected under a microscope at intervals during the crystallization, and no evidence of the nucleation (as evident from particles smaller than the seed crystals) was noticed, so it is likely that the tail is an artifact of the sizing technique. Distributions appearing normal on a log size plot will follow a log-normal distribution for linear size. A photomicrograph of crystal taken from one run of batch crystallization is shown in Figure 4.8 which shows a good shape of α-glucose monohydrate crystals and no evidence of nucleation. Figure 4.9 shows SEM pictures from one of the experimental run at 10°C. Figure 4.9 (a), which is of the seed crystals, shows very good uniformity of the seed crystals used in the experiment but the shape may be not good because of the breakage during the sieve process. Figure 4.9 (b), taken at 2 hours after seeding, shows a good shape of this sugar under the operating condition. Please note that, due to the sample used for the SEM should be a dry sample, it is very difficult to avoid the surface nucleation if the solvent is evaporated.

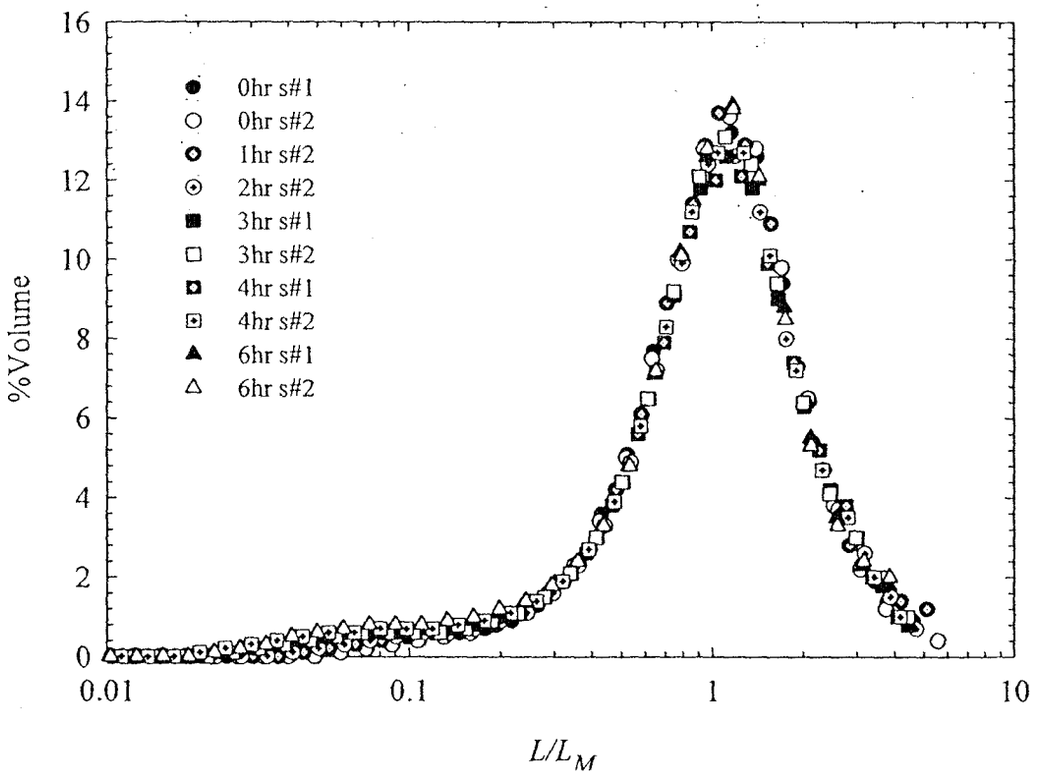

Fig. 4.7 Scaled particle size distributions from a batch run at 25°C, with duplicate samples represented by filled and open symbol.

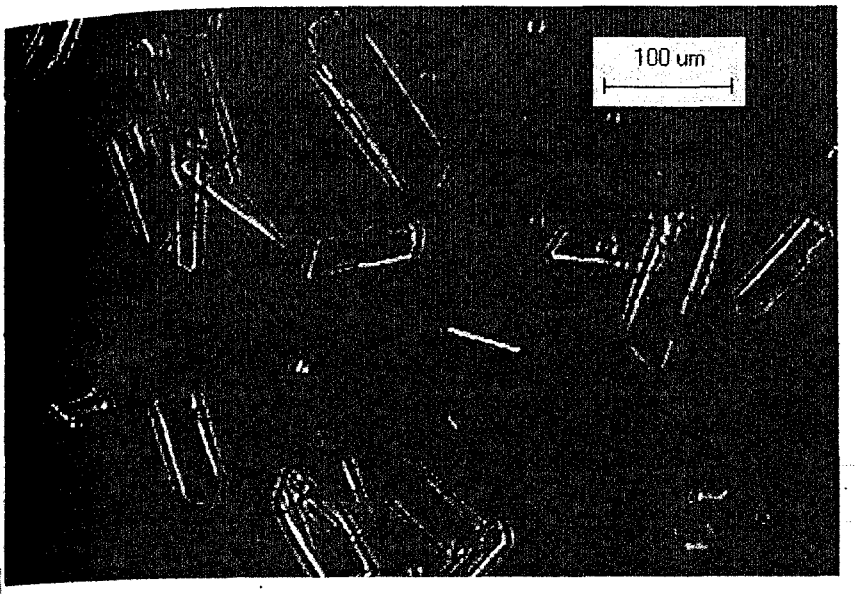

Fig. 4.8 Photomicrograph of crystals taken from the isothermal batch crystallization eight hours after seeding. The conditions for the crystallization were 25°C, agitation at 500 rpm, and the initial relative supersaturation was 0.027.

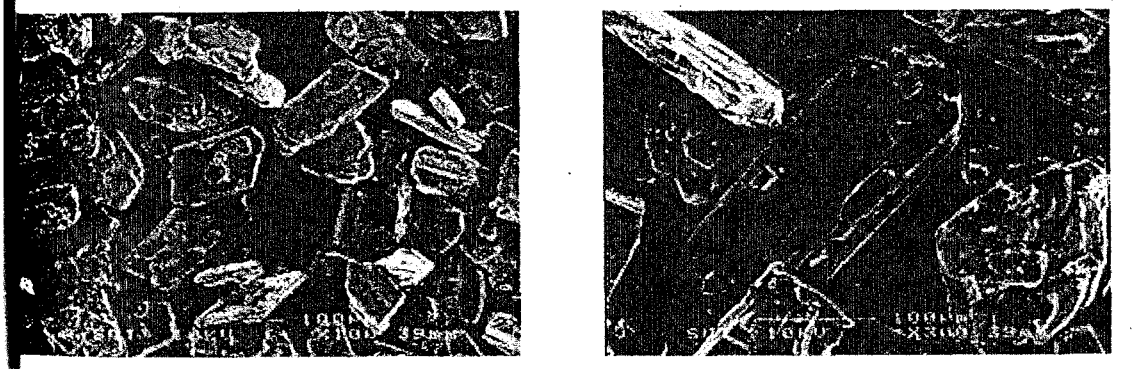

(a) (b)

Fig. 4.9 SEM pictures of (a) seed crystals and (b) crystals after 2 hours growth in the batch crystallizer.

4.3.1 Effect of stirring speed on crystal growth

The crystallization experiments of glucose monohydrate with varying stirring speed were performed to determine what stirring speed is required for the crystal growth mechanism to be surface integration controlled crystal growth. The result is shown in Figure 4.10 where the volume median size is plotted against the experimental time. The slopes of this plot in time range of 1 hour to 6 hour were determined and noted as the

volume based growth rates. There are two groups of results for each stirring speed; 40 rpm and 550 rpm, and 500 rpm. This is due to the difference in seeds used. The seed use for the experiment at 500 rpm was the same as used for all the experiments at 25°C, whil the experiments at 400 and 550 rpm used the same seed as the experiments at 10 and 40°C The difference in these two groups of the seed is shown in Section 4.4.3. However, ther is no significant difference between the growth rates calculated from these two groups o data, as can seen from them having almost the same of slopes between volume median siz with respect to time (Figure 4.10) and also directly from the growth rate values wit respect to stirring speed as Figure 4.11. Figure 4.11 shows the volume growth rates ove this stirring range are within 0.07 to 0.16 μm/min with an average value of 0.125 μm/mi It is also concluded that the growth rate of glucose monohydrate in this region (400 to 55 rpm) is surface integration controlled. A stirring speed of 500 rpm was chosen to for th other crystallization experiments in order that they determine integration controlled growt kinetics.

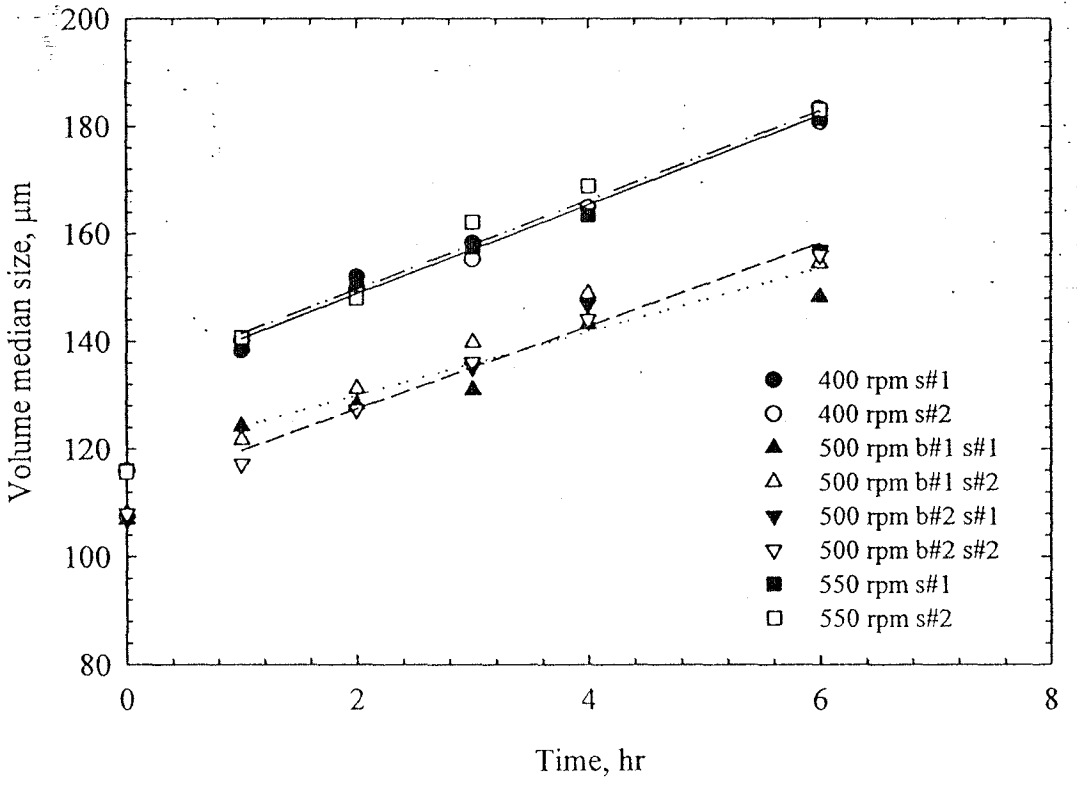

Fig. 4.10 Volume median sizes as a function of time at the operating conditions of 25° solution concentration of 57.62% (averaged from 4 batches), and seeding rate of 0.0024 glucose monohydrate/kg solution (averaged from 4 batches)

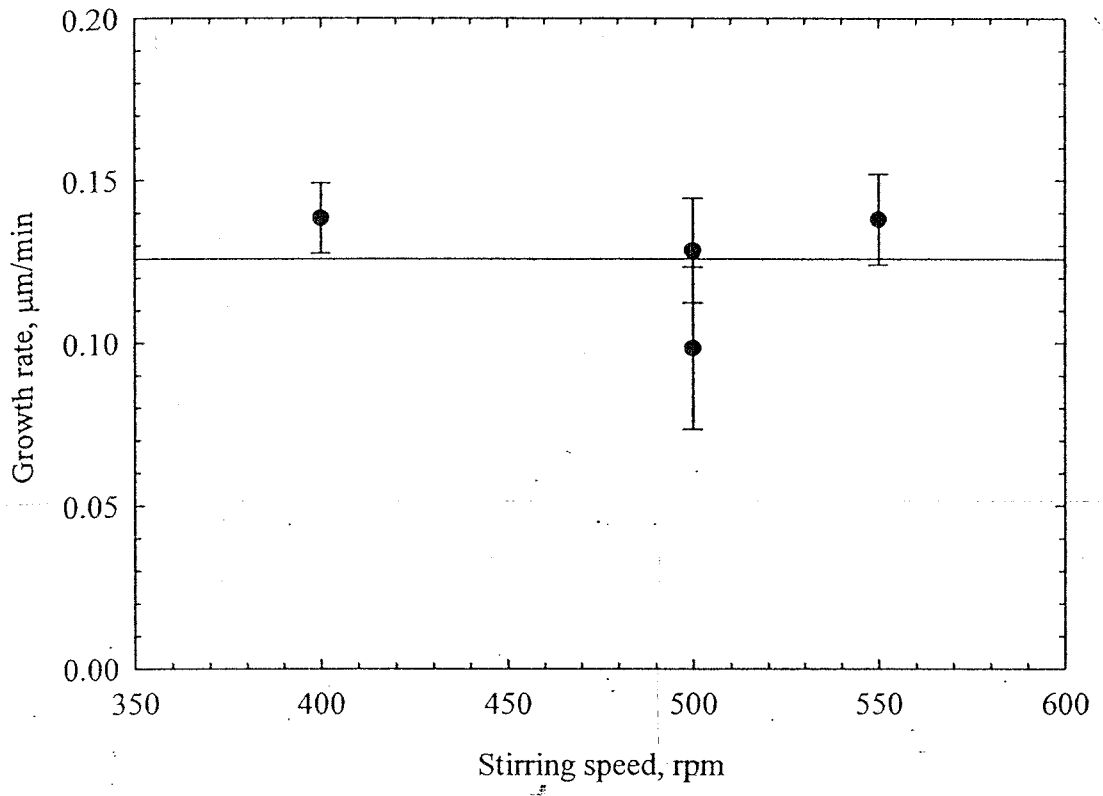

Fig. 4.11 Volume growth rates as a function of stirring speed.

5.3.2 Crystallization kinetics

If the volume distribution (or mass distribution) is log-normal, the number distribution is also log-normal with the same geometric standard deviation[40]. The number mean size may then be calculated from the relationship:

$$\ln x_{NL} = \ln x_{gV} - 2.5 \ln^2 \sigma_g \tag{4.3}$$

where x_{NL} is the mean particle size, x_{gV} is the median of the volume distribution, and σ_g is the geometric standard deviation of the volume distribution. These results were confirmed by discretizing the volume density distribution into small elements (of 1 μm width) and calculating the number of particles in each element, and from that, the number mean particle size. The geometric standard deviation of the volume distribution was essentially constant over the time period of the experiment, confirming there was growth rate dispersion and that the seeds were CHS. The growth kinetics was determined based on the number mean particle size.

Due to the constant solution concentration during the crystallization process, the mea growth rate was calculated directly from the slope of the plot between the number mea crystal size and time. The growth rate of α-glucose monohydrate from aqueous solutio was found to be unusually high in the first period of the experiments (i.e. the first hou and then followed an expected linear relationship, as illustrated in Figure 4.10. An unusu accelerated rate of crystal growth at the initial stage of batch crystallization may be due t repair of the crystal surface[41] or poisoning from unidentified impurities[3], or a roughenin transition[42]. The growth rates shown here were calculated based on the linear rates evide after the first hour of growth.

Duplicated crystallizations were performed simultaneously for almost a experiments. The results at 40°C (Figure 4.12) showed that, at the same conditions, t number sizes were essentially the same for all four measurements (two batches with tw measurements each), and the same mean crystal growth rates were obtained. Thus, t reproducibility was good and within the estimated measures of uncertainty.

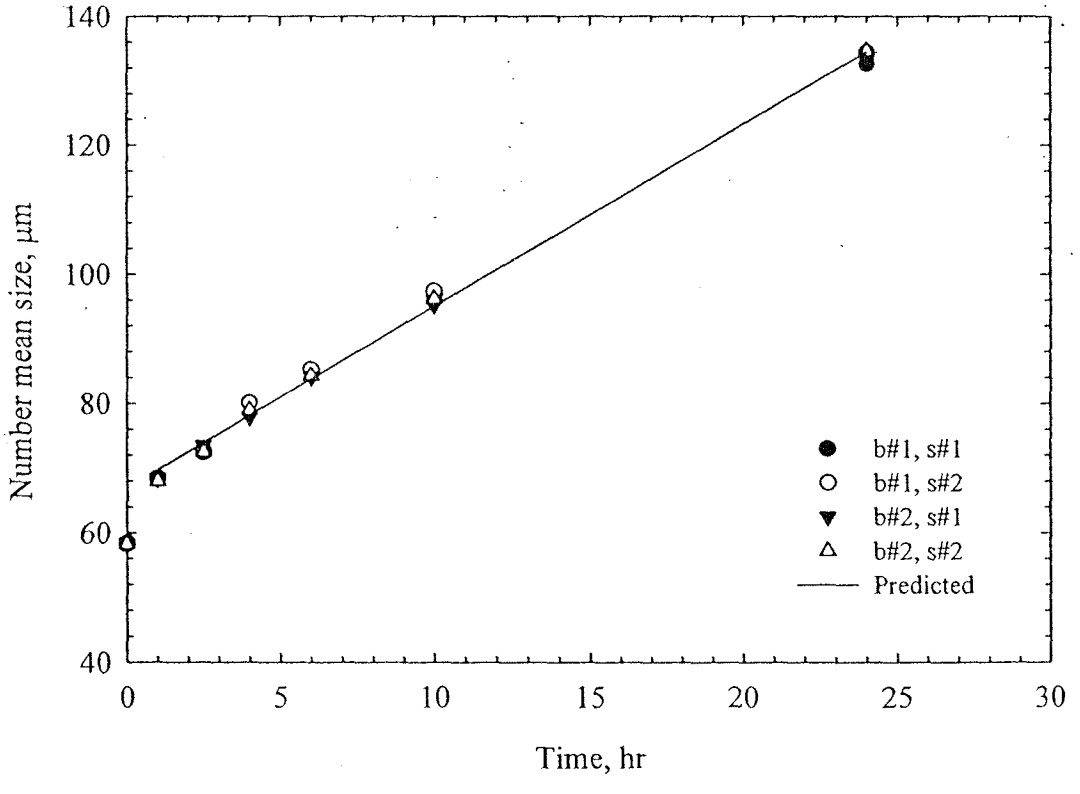

Fig. 4.12 Number mean sizes of α-glucose monohydrate as a function of time at 40 operating concentration as 65.81 ± 0.25%.

The plot between the mean crystal growth rates and relative supersaturation (Figure 4.13) for the three temperatures gives the growth rate constants for the experimental temperatures. It is clear that a growth rate order of 1 fits the data acceptably. The growth rate constant increases significantly with increasing temperature. The growth rate constant was modeled by an Arrhenius relationship (Figure 4.14), as the relationship $\ln k_g = 19.2 - 6010/T$, indicating an activation energy of 50 ± 2 kJ/mol. This value is typical for the crystallization of simple sugars. Previous research on crystal growth of sucrose[43] for example, gives activation energy of growth rate as 28.9 to 33.1 kJ/mol for growth from pure solutions, and 45.6 to 57.7 kJ/mol for growth from solutions having raffinose as an impurity.

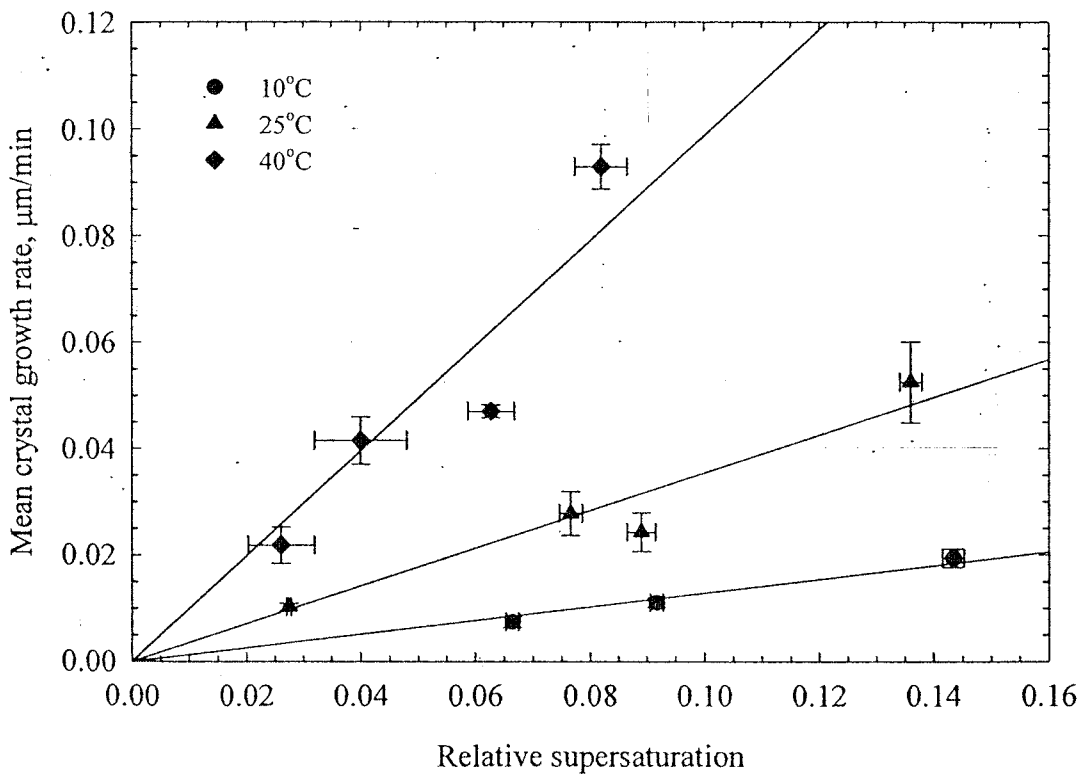

Fig. 4.13 Mean size crystal growth rates for α-glucose monohydrate as a function of relative supersaturation.

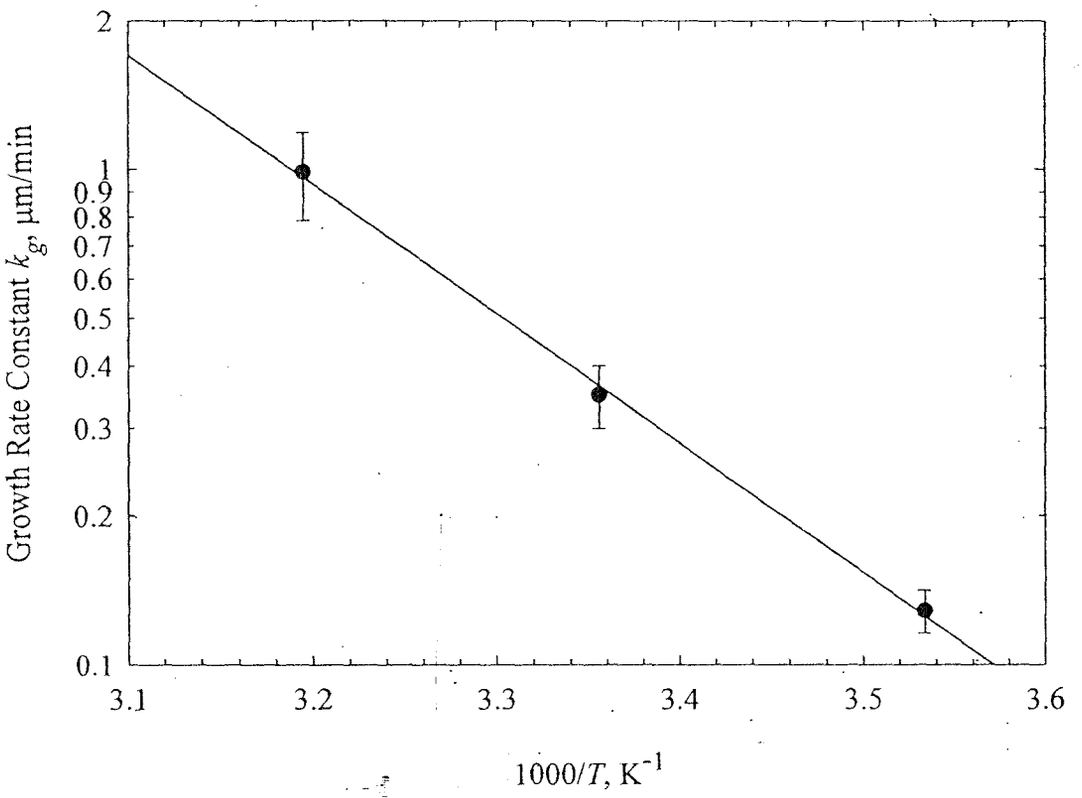

Fig. 4.14 An Arrhenius plot of the growth rate constants.

4.3.3 Crystal growth rate dispersion

Crystal growth rate dispersion (GRD) in the batch crystallizations was measu based on the time dependent number based PSDs. Figure 4.7 shows that on a log s scale, the shape of the PSD was unchanged as the crystals grew and so the seed was Cl The growth rates shown in Figures 4.12, 4.13, and 4.14 are for the number mean s crystal. The growth rates for other sizes are this value multiplied by the ratio of the siz the crystal to the mean crystal size. The range of growth rates for this sieved seed can expressed by the CV (= standard deviation / mean growth rate) of the growth distribution which for CHS is identical to the CV of the PSD. These can be on a nun basis, as was used in the current study, or on a weight (volume) basis. The stanc deviation of the number based PSD was calculated by discretizing the volume based P in 1 µm intervals and converting the results to a number basis. The geometric stanc deviations of the volume based PSDs (on a log size scale) were constant throughout experiments (Figure 5.15), but this transforms into significant increases in the stan deviations of the number based PSDs on a linear size scale, as the experiments progre where for CHS, the standard deviation should be proportional to the mean size anc

slope gives the associated CV. An example of a plot to determine the crystal growth rate dispersion is shown in Figure 4.15 for an experiment at 40°C and relative supersaturation equal to 0.082. There was very good reproducibility between duplicate samples in individual experiments, and between duplicate experiments. Table 4.1 gives values of the crystal growth rate dispersion CV on a number basis for all conditions studied.

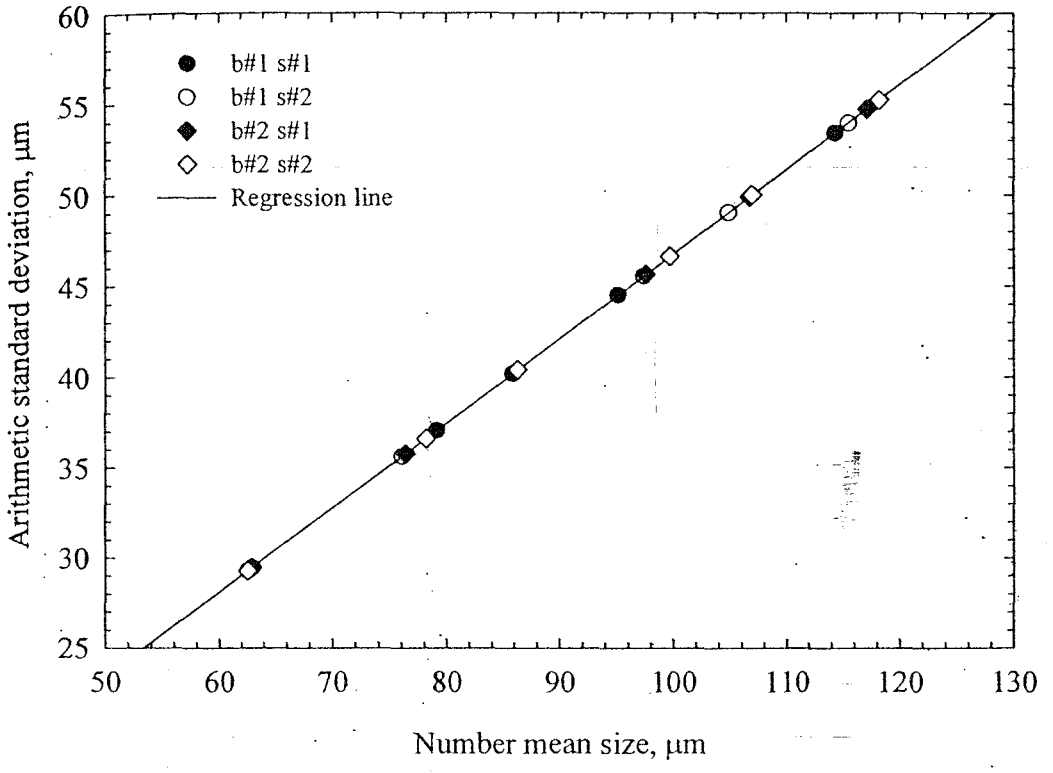

Fig. 4.15 Plot of the arithmetic standard deviation of the number distribution against number mean size for the experiment at 40°C and relative supersaturation equal to 0.082. The slope of this plot is the crystal growth rate dispersion CV for this condition.

The crystal growth rate dispersion CV is difficult to determine with very high accuracy due to the variability in the measured volume based PSDs. In the raw volume based PSD data there are small random changes in the geometric standard deviations through the experiment, but we have smoothed the data by assuming a constant geometric standard deviation, which is justified by the scaled volume based PSD plots, of which Figure 4.7 is an example. It is believed that the 95% confidence interval uncertainty on CV for a particular experiment is of the order of 0.10. Assuming that the CV measured come from identical distributions with the use of the same seed, it is possible to calculate the CV as 0.47 ± 0.06, for the results at 10 and 40°C (which used seed crystals from a

single preparation), and 0.59 ± 0.05 for the seeds at 25°C, which had a wider PSD. Thes results can be used to determine 95% ranges of growth rates (G97.5%/G2.5%), for the tw seeds. The seeds used in the 10 and 40°C experiments had a 95% range of growth rates o 5.8 ± 1.0 times, and those used in the 25°C experiment had a 95% range of growth rates o 8.5 ± 1.2 times. The bulk crystals, from which the CHS were prepared, had a numbe mean size of 92 μm and a number based standard deviation of 45 μm, resulting in a CV o 0.49. Thus, it can be concluded that the CV of the growth rate distributions predicted i the current study would be very similar to the CV of the growth rate distribution of th bulk particles from which the seeds were fractionated. Note that although the sieve fraction and the bulk material had similar CVs, the bulk had a mean size almost twice tha of the sieved seed, so the mean growth rate would have been larger by the same ratio. Tha the CVs of bulk and fraction are similar is not implicit in the seed preparation method, bu results from the coincidence that when the seed was prepared the reduction in the mea crystal size was by the same factor as the reduction in the standard deviation of the PSD this resulted in an approximately constant value of the CV, and hence a similar 95% rang of the growth rate distribution.

Table 4.1 Crystal growth rate dispersion number based CVs for glucose monohydra crystallized from aqueous solutions, all runs.

Temperature (°C)	Relative supersaturation (-)	CV (Batch 1) (-)	CV (Batch 2) (-)
10	0.067	0.50	0.50
	0.092	0.48	0.48
	0.143	0.46	0.46
25	0.027	0.56	0.56
	0.077	0.61	*a*
	0.089	0.62	*a*
	0.136	0.60	0.60
40	0.026	0.44	0.44
	0.040	0.44	0.44
	0.063	0.52	0.52
	0.082	0.47	0.47

a Only one batch was performed for these conditions.

The growth kinetics for a small number of other sugars have been measured previously, and these are also suitable for use in the simple model (however not the two dimensional model which requires a more complete measurement of the full crystal growth rate distribution rather than only the mean crystal growth rate). The following equations represent the previously measured data.

For xylose growth from aqueous solutions at 25°C[35]: (4.4)

$$G = 1.94\sigma^{1.7} \text{ (μm/min)}$$

The same sugar grown from aqueous ethanol at 25°C has the kinetics[35]

$$G = 0.071\sigma^{1.5} \text{ (μm/min)} \quad (4.5)$$

These both represent very low growth rate kinetics (an order of magnitude lower than fructose at the same level of supersaturation), and this indicates that xylose would need to be seeded at very high rates in order for the crystallization to be mutarotation rate controlled.

For fructose grown from aqueous solutions[34]:-

$$G = 2.5\times10^{5} \exp(-25500/RT)\sigma^{1.3} \text{ (μm/min)} \quad \text{[SI Units for R]} \quad (4.6)$$

At 25 °C this equations to $G = 8.52\sigma^{1.3}$, which allows the relative rates of fructose and xylose to be compared.

For fructose grown from aqueous ethanol solutions[3] it was noted that the effect of temperature and ethanol content in the solvent on the rate constant was not large. At low ethanol content and solvent the rate could be modeled as:

$$G = 2.5\sigma^{1.0} \text{ (μm/min)} \quad (4.7)$$

While at high temperature (40 °C) and ethanol content (90%), the rate increased to

$$G = 2.5\sigma^{1.0} \text{ (μm/min)} \quad (4.8)$$

The rates of galactose crystallization from aqueous solutions[32] are given in terms of a rate of mass change divided by the crystal surface area. It is possible to convert these to similar units as above with the crystal density.

$$\frac{dm}{dt}\frac{1}{A} = 20.0\sigma^{2.6} \quad (\mathrm{g/m^2min}) \tag{4.9}$$

Values for the other mutarotating sugars (including common sugars such as mannose) a
unfortunately not measured up to the present time.

Chapter V

Modeling of the Effect of the Mutarotation Reaction on the Aqueous Crystallization of Glucose Monohydrate

5.1 Introduction

There are currently few published models for industrial aqueous crystallization of sugars where the mutarotation reaction has been considered, despite the fact that accurate designs can only be achieved by taking this reaction into consideration. This study aims to generate this model and specify the conditions where the mutarotation kinetics plays an important role in the system. The model proposed is general for any sugar, but the data developed in the previous chapters (particularly mutarotation rates and equilibrium, and crystal growth kinetics and equilibria) are necessary. For this reason the model shown here uses the glucose monohydrate system as an example, and so based on the mutarotation and crystal growth parameters already measured in this study. Five ordinary differential equations were written to describe the system and then solved using the ODE45 routine in MATLAB together with the necessary initial conditions. The results show the mass deposition of glucose onto the crystal surface (which is implied from the crystal mass obtained) is faster in cases using small seed sizes, higher seeding rates, and higher temperatures. The depletion of α-glucose is rapid in cases using small seed size, high seeding rate, and low temperature. In summary, the conditions where the mutarotation may be the rate limiting step, or partially rate limiting, can be easily determined via the model. Unfortunately because of the small supersaturation values possible in this system (which are determined from the value of the long term secondary nucleation threshold) the reduction in the fraction of α-glucose monohydrate which results in almost complete cessation of crystal growth is only approximately two percent less than the equilibrium alpha fraction. A change in the anomer composition this small is not accurately measurable by ^{13}C N.M.R., which makes the model predictions of the anomer compositions impossible to verify experimentally. Despite this, since the model is based solely on balance and mechanistic models, without any fitted parameters, the model predictions must be an accurate reflection of what occurs in the crystallizer.

5.2 Simple (One Dimensional) Model for the Crystallization of Sugars

Experiments performed to collect data on the kinetic parameters used in the model have been described previously[44,45] and shown in Chapter 2 and 4, for mutarotation data and crystal growth kinetics, respectively. The secondary nucleation threshold (described in Chapter 3) and composition dependence of the crystal growth rates (under surface integration controlling conditions) were measured at 10, 25, and 40°C to obtain models of the temperature and composition dependence of these variables in pure aqueous solutions over the approximate range of temperatures of α-glucose monohydrate crystallization. The temperature and composition dependence of the mutarotation kinetics and equilibria were measured in aqueous solutions in the same range of temperatures to model the temperature and composition dependence of these variables. There is also reported the effect of pH on the mutarotation rates[8], but this is not significant in the narrow range of pH used for the industrial crystallizations.

The solubility of the different crystal forms of glucose (α-glucose monohydrate, anhydrous α-glucose, and anhydrous β-glucose) in water are already well known[24] and re-plotted in Figure 3.1 and also in Figure 3.10 where the metastable zone for secondary nucleation region is specified. The solubility in terms of the crystallization temperature (in °C) has been modeled by fitting a cubic equation through the data of Young, giving

$$C^* \text{ (kg glucose/kg soln.)} = 0.01\ (33.82 + 0.6484\ T + 0.00135\ T^2) \qquad (5.1)$$

The mutarotation reaction is modeled as a first order reversible reaction of α- to β-glucopyranose (a simplification which is well justified by the experimental results). The simplified kinetics are represented by Figure 4.1 (a), where the crystallization is not considered, with the forward reaction (from α-glucose to β-glucose) having a rate k_1 (s^{-1}) and the backward reaction having a rate k_2 (s^{-1}). The overall rate of reaction (which is the apparent rate as fitted in a first order decay curve) is

$$k = k_1 + k_2 \qquad (5.2)$$

The equilibrium constant is represented by

$$K = \frac{x_\beta}{x_\alpha} = \frac{k_1}{k_2} \qquad (5.3)$$

The overall rate constant is modeled through the Arrhenius relationship, and there is no significant concentration dependence in the range of compositions we are modeling (as would be predicted for a true first order reaction), thus

$$\log k\,[s^{-1}] = 10.8 - \frac{4210}{T\,[°C] + 273.15} \tag{5.4}$$

The equilibrium constant may be assumed to be independent of both temperature and glucose composition, and have a value of 1.50. The previous relationships can be used to determine forward and reverse reaction rate constants

$$k_1 = \frac{kK}{1+K} \quad \text{and} \quad k_2 = k - k_1 \tag{5.5}$$

The last kinetic rate needed for the model is the model for the crystal growth kinetics. A large series of crystallization experiments has shown that the surface integration crystal growth kinetics is first order with respect to relative supersaturation defined in terms of weight fractions

$$G\,[m/s] = k_g \sigma \qquad \text{with} \qquad \sigma = \frac{C_{\alpha\text{-gluc}} - C^*_{\alpha\text{-gluc}}}{C^*_{\alpha\text{-gluc}}} \tag{5.6}$$

The constant k_g depends only on the temperature, since we are considering surface integration controlled kinetics in pure solutions, and it can be adequately modeled using an Arrhenius relationship

$$\log k_g\,[\mu m/s] = 8.33 - \frac{2610}{(T\,[°C] + 273.15)} \tag{5.7}$$

Sugars are typically crystallized in seeded batch crystallizers operated within the secondary nucleation threshold to minimize the formation of false grain; hence the model assumes no nucleation occurs in the crystallizer. Figure 3.10 which is the glucose-water phase diagram also shows the valid region for this model (which is the region over the solubility line and under the metastable limit for secondary nucleation). In order to further simplify the modeling of the system, the seeds are treated as monosize seeds, and it is assumed that there is negligible growth rate dispersion. Crystal size is assumed to be the spherical average crystal diameter. These assumptions simplify the problem by allowing the crystal size distribution to be monodisperse, thus reducing the complexity of the population balance.

The differential equations used to describe a batch crystallization of α-glucose monohydrate, with a basis of 1 kg of solution, are:

1. The equation to describe the change in crystal size due to crystal growth

$$\frac{dL}{dt} = k_g \frac{C_{\alpha-gluc}\, C^*_{\alpha-gluc}}{C^*_{\alpha-gluc}} = k_g \frac{x_{\alpha-gluc} C_{gluc}\, x^*_{\alpha-gluc} C^*_{gluc}}{x^*_{\alpha-gluc} C^*_{gluc}} \tag{5.8}$$

This equation is derived from the crystal growth rate (equation 5.6) with substitution of relative supersaturation based on the crystallizing (α-glucose). Here, the supersaturation is with respect to the crystallizing anomer. The variable $x_{\alpha\text{-}gluc}$ is the fraction of glucose that is in the α-form, and can vary during the crystallization if the crystal deposition rate is higher than the rate of replacement through mutarotation. The variable C_{gluc} represents the total concentration of both forms of glucose.

2. The rate of change in crystal mass deposition (mass of glucose deposit onto the crystal surface) is derived with the assumption that the crystal is spherical with characteristic size of L.

Mass of a sphere: $$m_{cryst} = \rho_{cryst} \frac{\pi L^3}{6} \tag{5.9}$$

(The volume of a sphere is used because the sizing equipment used, the Malvern Mastersizer, represents size using the spherical average diameter). Differentiating equation 6.9 with respect to change in size L to $L + dL$ and from time t to $t + dt$ gives the change in total mass of N crystals due to the deposition of glucose as shown in equation 5.10.

$$\frac{dm_{cryst}}{dt} = \frac{1}{2} \rho_{cryst} N \pi L^2 \frac{dL}{dt} \tag{5.10}$$

3. The rate of change in solution mass (equation 5.11) is equal to the rate of mass lost by the deposition which follows the mass conservation rule. The minus sign shows the

opposite directions of the mass change, i.e. mass leaving the solution is equal to the mass deposition onto the crystal surface, but in the opposite direction.

$$\frac{dm_{soln}}{dt} = -\frac{dm_{cryst}}{dt} \tag{5.11}$$

4. Because the crystal form is glucose monohydrate, the crystal contains just over 9% water in the lattice. Glucose monohydrate has the molecular weight of 198, whereas glucose anhydrous has a molecular weight of 180, so the portion of glucose in glucose monohydrate crystal is equal to 180/198. Thus, the rate of change in the mass of glucose in solution is equal to the rate of mass deposition onto the crystal surface corrected by the fraction of the crystal which is water, as shown as equation 5.12.

$$\frac{dm_{gluc}}{dt} = -\frac{180}{198}\frac{dm_{cryst}}{dt} \tag{5.12}$$

5. Considering Figure 5.1 (a), where the crystallizing species is considered to be only glucose monohydrate in the valid temperature range, and without any phase transformation, there are two reactions occurring simultaneously. They are the reversible mutarotation reaction and an irreversible crystallization process that complete against each other in the system. Thus, the rate of change of the fraction of glucose in the α-form in solution is given by the difference between the rates away from this form (due to the forward mutarotation reaction and the crystallization) and the rates towards the form due to the backward mutarotation reaction from β-glucose to α-form.

$$\frac{dx_{\alpha-gluc}}{dt} = \frac{k_1}{K}(1 - x_{\alpha-gluc}) - k_1 x_{\alpha-gluc} + \frac{1}{C_{gluc}}\frac{dm_{gluc}}{dt} \tag{5.13}$$

The solution of the previous five differential equations requires the temperature of the batch to be known as well as the following initial conditions

1. $L(t=0)$, which is determined by measurement of the sieved seed crystals. The number of seed crystals, which is also required by the model, is determined from the initial size and the mass of seed crystals added.
2. $m_{cryst}(t=0)$, the mass of seed added to the batch.
3. $m_{soln}(t=0)$, the mass of solution in the batch before initiation of crystallization.
4. $m_{gluc}(t=0)$, the mass of glucose in the solution before initiation of crystallization, which may be calculated from the initial concentration.
5. $x_{\alpha\text{-}gluc}(t=0)$, the initial fraction of α-glucose in the crystallizer. Usually this is determined from the equilibrium constant, as industrial crystallizations will be initiated on equilibrium solutions. In research crystallizers, this fraction is determined by whether the α-form or the β-form was initially dissolved to create the solution, and the temperature-time profile of the cooling before the addition of seed crystals.

Other parameters necessary for modeling the crystallization, in particular the concentrations of particular species, can be determined using the variables found via solution of the equations above.

5.2.1 Results and Discussion for the Simple Model

The model was used to simulate the crystallization of α-glucose monohydrate in a batch crystallizer for a range of different conditions, concentrating on the effect of variation in the size of seed crystals, the amount of seed crystals added, and the crystallization temperature. These three variables are the key to determining whether the rate of mutarotation reaction will be sufficiently low as to have crystallization inhibited by low levels of replacement of α-glucose. It is not reasonable to vary the initial α-fraction and observe the change in the other parameters since in industry the operation always starts with a solution at the mutarotational equilibrium. Initial glucose concentrations were set at 10% relative supersaturation, as this is a relatively high supersaturation for this system, but us within the short-term secondary nucleation threshold for all temperatures in the system.

5.2.1.2 The Effect of Seed Crystal Size

The effect of seed crystal size on the crystal growth of α-glucose monohydrate in a batch using 200 g seed/kg initial mother liquor, batch temperature equal to 10°C, and 10% initial relative supersaturation, is shown in Figure 5.1. The two

parameters plotted are the mass of crystals in the vessel (showing the rate of crystal deposition) and the fraction of glucose that is in the α-form, as functions of batch time, which is an indication of whether the rate of crystal mass deposition is faster than the rate of replacement by mutarotation.

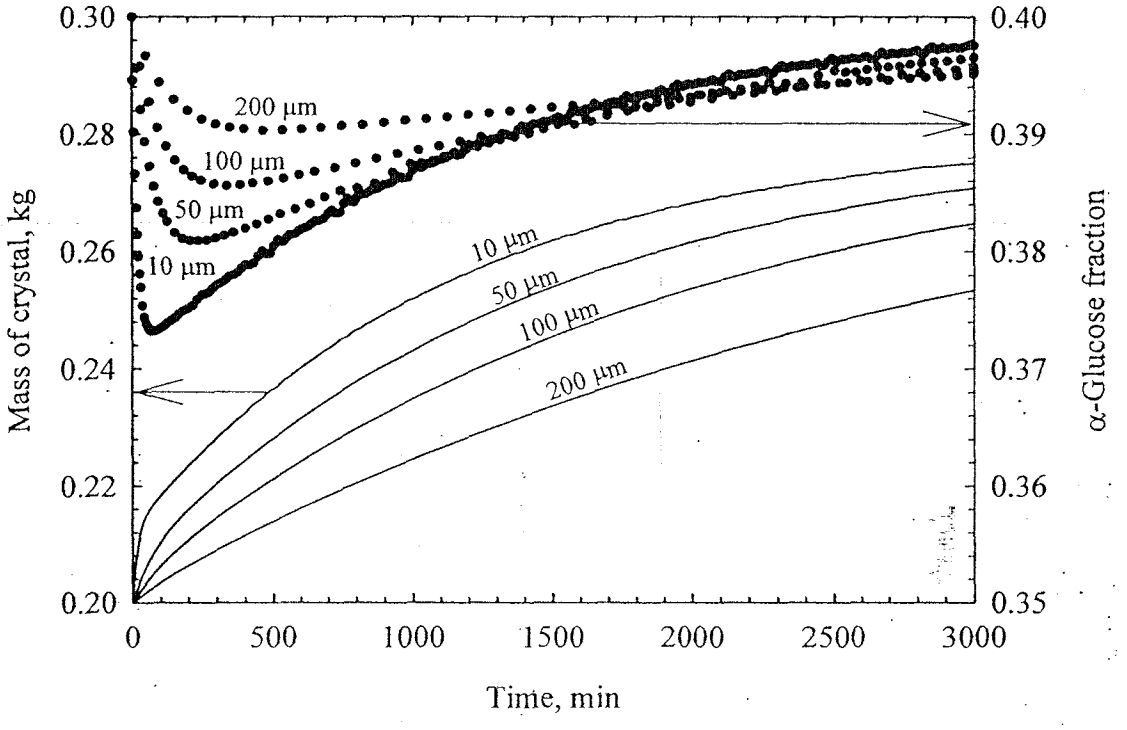

Fig. 5.1 The effect of seed size on the change in crystal mass in the mother liquor and fraction of glucose in the α-form for batch aqueous crystallization of α-glucose monohydrate. Simulated conditions are, T = 10°C, initial relative supersaturation = 10%, and seeding rate = 200 g seed/kg of mother liquor.

The initial rate of crystal mass deposition is significantly higher for smaller seed crystals, based on the same mass of seed. The crystal deposition rate depends on the driving force (i.e. the supersaturation) and the surface area of the crystals in the liquor; the surface area of the small crystals is larger than the surface area of larger crystals (for the same mass). The higher rate of mass deposition causes a significant decrease in the proportion of α-glucose in the crystallizer when 10 μm seeds are added. The change in the α-glucose fraction appears small, changing from the equilibrium value of around 0.4 down to a minimum of around 0.373 (at about 75 minutes), but this change is very significant with respect to the relative supersaturation, and therefore the crystal growth rate. The

glucose concentration at this point is 0.4370 kg glucose/kg solution, with equilibrium o 0.4044 kg glucose/kg solution. The relative supersaturation of α-glucose at this point i 0.00803, while if the relative supersaturation is calculated on a total glucose basis it i 0.0806: the relative supersaturation in the crystallizer is effectively only 10% of wha would be expected because of the removal of α-glucose without adequate replenishmen from the β-form.

The difference between the true supersaturation (in terms of the α-glucos concentration) and the apparent supersaturation (measured in terms of total glucose in th crystallizer) is illustrated in Figure 5.2. Even for the simulation with a very small see size, the total glucose concentration smoothly decreases towards the apparent glucos solubility, not approaching the solubility very closely even after 3000 minutes. The tru supersaturation, that of α-glucose, decreases very rapidly however, and there is almost zer driving force for crystal growth very quickly during the batch using the 10 μm seed. Afte 100 minutes the crystallization is essentially entirely controlled by the mutarotatio reaction giving up α-glucose for crystallization.

5.2.1.2 The Effect of Seeding Rate

The effect of seeding rate (the amount of seed crystals added to the system) on th crystallization of α-glucose monohydrate is shown in Figure 5.3 where the conditio temperature is 10°C, seed size of 100 μm, and the initial relative supersaturation is 10% The seeding rates are varied from approximately 5 to 20% of fresh mother liquor which i the industrially used range[38,46]. This graph indicates the mutarotation reaction will be mor significant at higher seeding rates, which cause a more rapid depletion in the α-glucos anomer. A larger seed amount (with the same seed size) gives a larger surface area an therefore a higher mass transfer rate at a given value of the mass transfer flux, and thi causes a faster crystal mass deposition rate. In this case, again, the conversion of β glucose anomer in solution phase is not quick enough to replace the α-glucose anomer los from the solution phase due to the crystallization process. This also causes the drop in th crystallization driving force in terms of the crystallizing species.

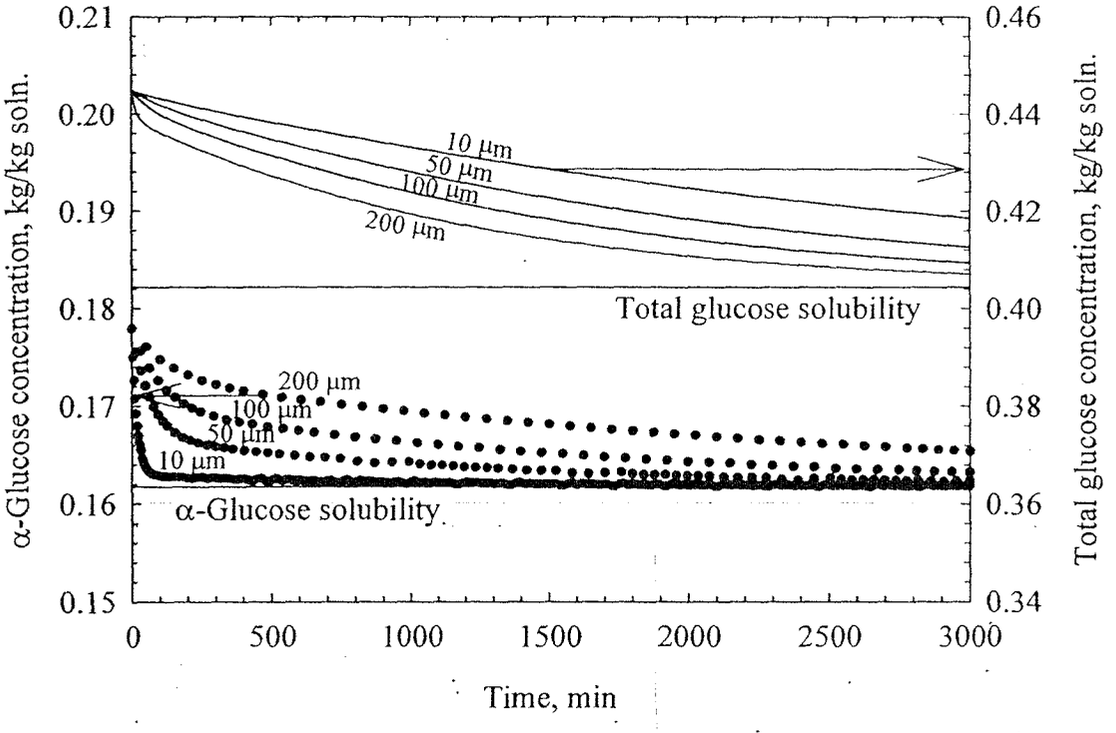

Fig. 5.2 Plots of the concentrations of α-glucose and total glucose in the crystallization with reference to the solubility of the species during batch crystallization. Simulated conditions are, T = 10°C, initial relative supersaturation = 10%, and seeding rate = 200 g seed/kg of mother liquor.

Normally, in α-glucose monohydrate manufacturing part of the crystalline suspension of the previous batch is left for the coming batch in order to induce the crystallization process. This seeding suspension is sometimes called "foots"[46] and the particles inside the solution act as seed for the coming batch. Preferred amount of foots (which is about 10 to 40% of solid) will be approximately 40% of the new batch, and this is used to calculate that the batch uses 4 to 16% seed. This value is close to that given by another patent[38], which suggests 3 to 15% seed for the crystallization of this sugar.

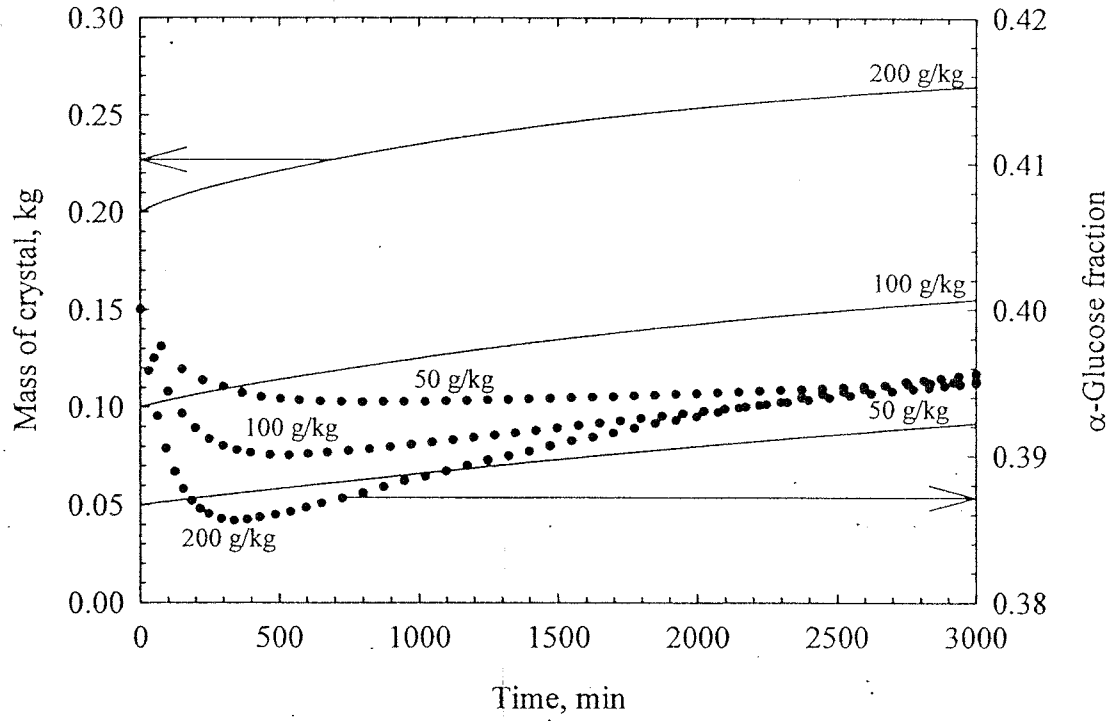

Fig. 5.3 The effect of seed mass on the change in crystal mass in the mother liquor and fraction of glucose in the α-form for batch crystallization of α-glucose monohydrate. Simulated conditions are, T = 10°C, seed size = 100 μm, and initial relative supersaturation = 10%.

5.2.1.3 The Effect of Temperature

The effect of batch temperature on the crystallization of α-glucose monohydrate is shown in Figure 5.4 where the seeding rate is fixed at 200 g seed/kg solution, seed size of 100 μm, and the initial relative supersaturation is 10%. The graph shows that at higher temperature, the crystal mass deposition is initially higher, which is due to the surface integration kinetics that will be higher at higher temperature[27]. The other result observed from this graph is that the mass of crystal formed at higher temperatures is always higher than that at lower temperatures at the same time, including at the equilibrium, even when the same amount of seed crystal is used. This is because there is higher solubility at higher temperature; therefore 10% relative supersaturation at 40°C represents a much higher amount of glucose able to be crystallized from solution than that at 25 and 10°C. From the calculation, at 10% relative supersaturation, there are approximately 0.04, 0.05, and 0.06 kg of glucose per kg of solution in excess of the equilibrium at 10, 25, and 40°C, respectively.

The change in α-fraction is more rapid and more pronounced at lower temperature, with a maximum depletion from the equilibrium value of 0.4 down to 0.384 at 10°C. At the conditions plotted in Figure 6.4 and at 40°C, the fraction of α-glucose is almost unchanged. The temperature changes both the crystallization kinetics and the mutarotation kinetics, but the mutarotation kinetics has a significantly higher value of the activation energy (the activation energy is 50 kJ/mol for crystallization kinetics and 80 kJ/mol for the mutarotation kinetics), and so the mutarotation rate increases far more than the crystallization rate as the temperature increases, thus making the system less mutarotation rate controlled.

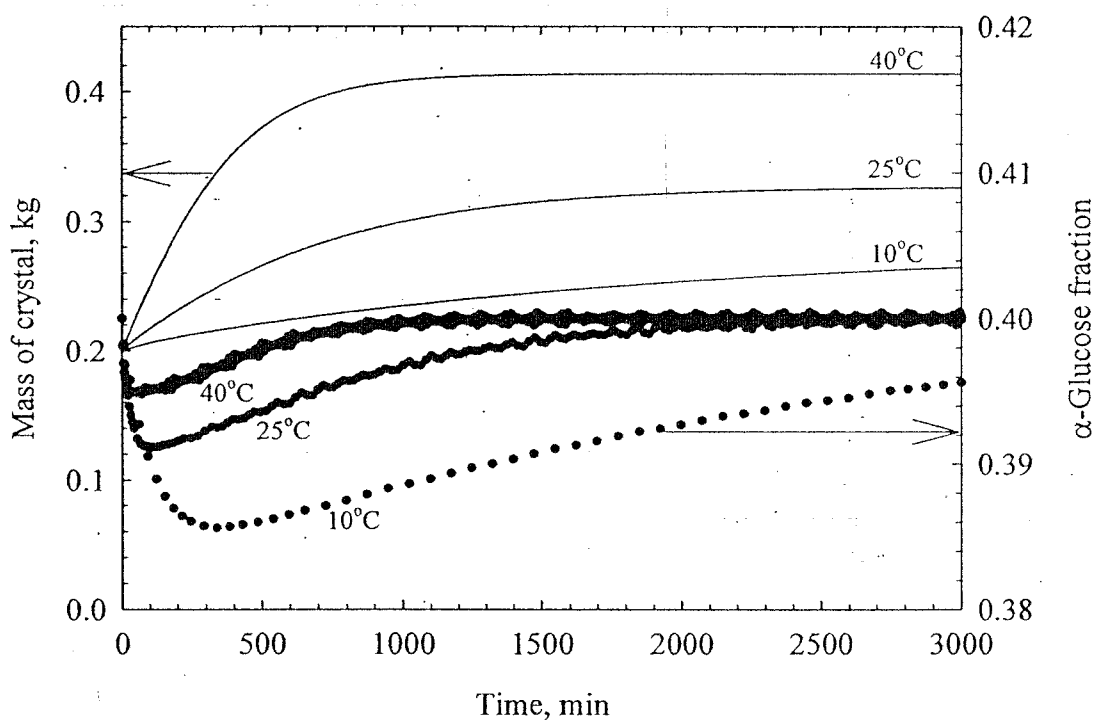

Fig. 5.4 The effect of temperature on the change in crystal mass in the mother liquor and fraction of glucose in the α-form for batch crystallization of α-glucose monohydrate. Simulated conditions are, seed size = 100 μm, initial relative supersaturation = 10%, and seeding rate = 200 g seed/kg of mother liquor.

5.2.1.4 Comparison with Literature Results

There are few literature models generated for the different sugars[2,31,32]. Both groups generated simple mathematical models similar to that generated in this work but for batch cooling aqueous crystallization of galactose and seeded batch aqueous-ethanolic

crystallization of fructose by Beckmann's group and White's group respectively. The models of both groups were generated by a balance of the system considering both crystallization and the mutarotation reaction. Galactose and fructose undergo a complex mutarotation reaction concerning their tautomers. The group of Beckmann simplified mutarotation of galactose into the simple kinetics concerned of only two main forms that are the pyranoses, and three forms for fructose that are β-fructopyranose (the crystallizing anomer) and α- and β-fructofuranose were proposed by Flood et al.. Both models found the reasonable change of the crystallizing anomer fraction in solution predicted by the model and the models also good agree with the experimental results.

5.3 The High Accuracy (Two-Dimensional) Model of the Crystallization

Modeling of crystallization processes in general requires simultaneous solution of mass balances, the energy balance, and also the population balance. In isothermal systems, as considered in the current work, the energy balance is not necessary. The population balance is a conservation balance for particles as a function of their size (or another property in certain cases), and for a macroscopic system that is well mixed, is given by

$$\frac{\partial n}{\partial t}+\frac{\partial (Gn)}{\partial L}+\frac{\partial (\log V)}{\partial t}+D-B+\sum_{k}\frac{Q_k n_k}{V}=0 \tag{6.14}$$

The solution of the population balance gives the population density distribution $n=n(L,t)$. In a batch crystallizer there are no inflow (Q_{in}) or outflow (Q_{out}) streams, nor birth of new crystals of finite size (B) (assuming nucleation at zero size can be treated with a boundary condition) or death of crystals, disregarding crystal breakage. If the model is performed using a suspension basis, the change in volume with respect to time is negligible. In addition, in most crystallizers we can assume a size independent growth rate, such that $G \neq G(L)$, although the growth rate is still time-dependent due to the solute concentration change during the batch. The full population balance for a crystallizer such as modeling here is given by

$$\frac{\partial n}{\partial t}+G\frac{\partial n}{\partial L}=0 \tag{6.15}$$

which is a partial differential equation with a non-constant coefficient. The coefficient G is determined from the crystal growth rate equation, and is a function of the time-dependent solute concentration. The solute concentration is determined through the addition of a mass balance to the system, which balances the amount of solute remaining in solution with the

increase in the mass of crystals, which may be determined from the population density, through integral equations.

Using the population density the mass of crystals present can be calculated from the third moment of the normalized distribution, defined as:

$$\mu_3 = \int_0^\infty L^3 f(L) dL \tag{6.16}$$

Here, $f(L)$ is the normalized population density, from which the population density may be calculated by $n(L) = N \cdot f(L)$. The mass of crystals per volume can be calculated by

$$M_T = \rho_{cry} k_v N \mu_3 \tag{6.17}$$

The parameter ρ_{cry} is the crystal density, k_v is the volume shape factor for the crystals, and N is the total number of crystals per unit volume. If the population distribution is a normalized distribution, then the results must be multiplied by the total number of crystals present per unit volume.

Alternatively, the change in the mass of crystals over a differential time increment can be calculated from the growth rate of the crystals (G = dL/dt, where L is the volume equivalent size) and their surface area, which is related to the second moment of the normalized particle size distribution.

$$\mu_2 = \int_0^\infty L^2 f(L) dL \tag{6.18}$$

$$A_T = k_a N \mu_2 \tag{6.19}$$

The change in the mass of crystal per unit volume is given by

$$\frac{dm_{cry}}{dt} = \tfrac{1}{2} \rho_{cry} N k_a \mu_2 \frac{dL}{dt} \tag{6.20}$$

The parameter k_a is the surface area shape factor. The factor of ½ is required because the crystal growth rate is based on the volume equivalent diameter of the particle (L), whereas the mass balance requires the surface area to be multiplied by the change in the radius of the particle. N is the total number of crystals per unit volume, and is needed if the second moment is based on a normalized distribution. The crystal growth rate is usually modeled in terms of the relative supersaturation and temperature using a model of the type

$$G = k_g(T) \cdot \left(\frac{C - C^*}{C^*} \right)^n = k_g(T) \cdot \sigma^n \tag{6.21}$$

where the dependence of the crystal growth rate constant, k_g, on temperature is modeled using an Arrhenius relationship, and the exponent is predicted by theoretical models to be between 1 and 2. These parameters have been measured in a previous study[45] (Srisa-nga et al., 2006).

Batch crystallizations are intrinsically time dependent, and hence the population balance required is a partial differential equation with respect to time and particle size, which is then difficult to solve with the mass balance (an integro-differential equation), and energy balance.

One way to avoid this complication is to assume that the particle population is monosize throughout the time of the batch crystallization, which means that it is only necessary to model the mean size of the distribution with respect to time in order to obtain the mass of crystal, which reduces the model (for this type of crystallizer) to an ordinary differential equation giving the solution $\bar{L}(t)$, the mean crystal size. However this is only strictly true if monosize seed is used, and if the system is completely free of crystal growth rate dispersion. A previous model of glucose monohydrate crystallization (discussed in the previous section), and a model for aqueous-ethanolic crystallization of fructose[2] (Flood et al., 1996) use this form.

Recently it has been shown that the crystal growth rate of glucose monohydrate has considerable growth rate dispersion, and furthermore, that the GRD measured was displayed common history seed behavior. In this behavior, seed crystals originating at the same time ($t = 0$) have a distribution of growth rates G. Since the crystals began growth at the same time, and each crystal maintains a constant crystal growth rate (although this growth rate is only part of the growth rate distribution, and is different to the other crystals in the population) the distribution of crystal sizes at any time must be equal to the distribution of crystal growth rates multiplied by the time of crystallization. The crystal growth rate distribution measured in the previous work was a log-normal distribution with a mean growth rate predicted by equations 5.6 and 5.7 and having a constant CV of 0.50[45]. Based on these measurements we can model the growth rate distribution in the crystallizer as a log-normal distribution: this also means that the particle size distribution will be log normal, since the α-glucose monohydrate crystals have been shown to act according to the common history seed behavior. The fact that the growth rate distribution was log-normal is fortunate because the log normal distribution has some interesting properties, as described following.

The normalized log-normal distribution is described by the population density function

$$f(x;\mu_g,\sigma_g)=\frac{1}{x\sigma_g(2\pi)^{1/2}}\exp(-(\ln x-\mu_g)^2/2\sigma_g^2) \tag{6.22}$$

where in the current work, the independent variable x in the above distribution may be either the particle size (L), or the crystal growth rate (G). The parameter μ_g is the natural log of the median of the distribution, and σ_g is the natural log of the geometric standard deviation of the distribution.

The number mean of the distribution can be calculated from the distribution parameters by

$$\mu_1=\exp(\mu_g+\sigma_g^2/2) \tag{6.23}$$

And the variance by

$$m_2=\exp(2\mu_g+2\sigma_g^2)-\exp(2\mu_g+\sigma_g^2)=(\exp(\sigma_g^2)-1)\exp(2\mu_g+\sigma_g^2) \tag{6.24}$$

The standard deviation of the distribution is the square root of the variance.

Rearranging the equations above results in the ability to determine parameters in the distribution from measured or predicted mean and standard deviation values. These are significant equations since crystal growth rate models predict the mean crystal growth rate (rather than the geometric mean) and the standard deviation, or possibly the CV of the growth rate distribution (rather than the geometric standard deviation). This means that a population balance model of a crystallization process will predict the mean and standard deviation of a CSD, where the parameters in the distribution are needed to calculate the second and/or third moments which are required for the mass balance in the crystallizer. The equations determining the parameters from the mean and standard deviation are

$$\mu_g=\ln\left(\frac{\mu_1^2}{(\mu_1^2+\sigma^2)^{1/2}}\right) \tag{6.25}$$

$$\sigma_g=\left(\ln\left(\left(\frac{\sigma}{\mu_1}\right)^2+1\right)\right)^{1/2} \tag{6.26}$$

The common history mechanism provides for a constant CV (= σ/μ) value. From the mean crystal size (the change in which is determined from the mean crystal growth rate) it is possible to calculate the standard deviation of the distribution, and hence the distribution parameters.

In this research we concentrate on the effects of crystallization temperature an initial supersaturation of glucose on the crystallization, using typical conditions for th other key parameters, namely a seeding rate of 100 g seed crystal per kg of initial solutior a mean seed crystal size of 50 μm (and therefore a seed crystal distribution having a standard deviation of 25 μm, since the growth is constant history with a CV of 0.5). Th results of the improved model, containing the accurate model of the crystal growth rat dispersion and the accurate mass balance, are compared to the results predicted by th previous model.

The simulation results at a temperature of 10 °C, which is the lowest temperature at which crystal growth kinetics and crystal growth rate dispersion were measured, and an initial relative supersaturation of 0.15, which is the highest supersaturation measured in the recent growth rate study, are shown in Figure 5.5. The graphs show the evolution of the mass of crystals (Figure 5.5a), the decrease in the glucose concentration in solution (Figure 5.5b), the change in the fraction of glucose present in the α-D-glucopyranose form (Figure 5.5c), the mean crystal growth rate (Figure 5.5d), and the evolution of the particle size distributions (Figure 5.5e).

The first matter which is evident from these results is that there is a significant difference between the evolution of the crystallization predicted by the two models (see Figure 5.5a), with the improved model showing a slower approach to the equilibrium, i.e. a lower overall crystallization rate, than the old model based on the monosize seed crystals with no GRD. This is counter-intuitive: it was expected that the seed crystals with the wider distribution, the new model, would result in a higher specific surface area for the seed, and therefore a higher crystal mass deposition rate. Upon closer inspection, the reason that this did not occur is that the same mass of monosize seed has a much higher number of crystals than the log-normal distribution of the same weight and mean size. 100 g of a monosize seed of 50 μm is equivalent to 9.79×10^8 crystals, whereas 100 g of the log-normal distribution seed with a mean of 50 μm and a standard deviation of 25 μm is equivalent to 5.01×10^8 crystals. This indicates that the total surface area of the 100 g of monosize seed (7.69 m^2) is significantly larger than the total surface area of the 100 g of log-normally distributed seed (4.92 m^2) so that the initial rate of mass deposition on the seed is higher in the case of the monosize seed, due to the higher number of seeds per weight.

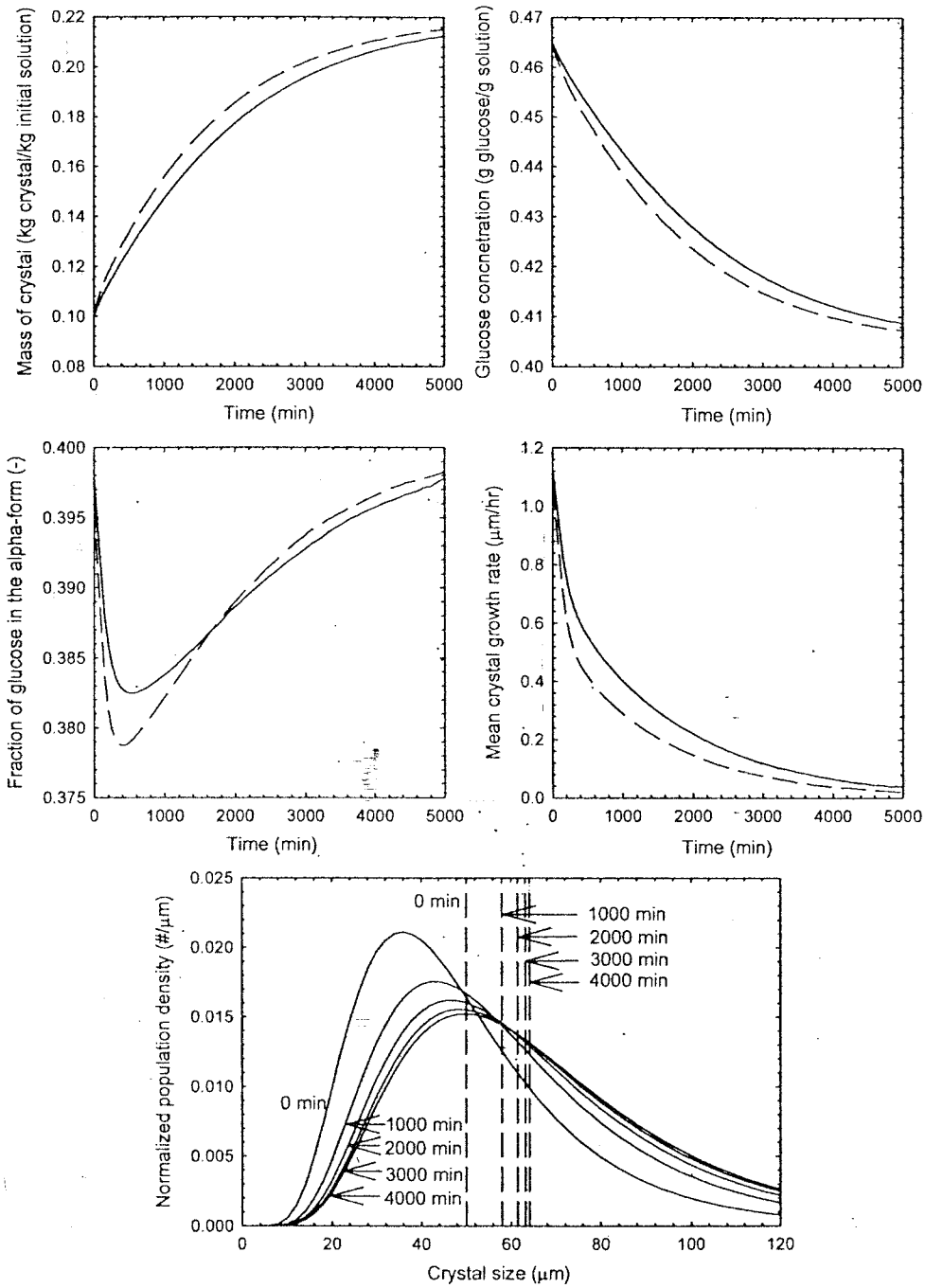

Fig. 5.5 Evolution of (a) the mass of crystals, (b) the glucose concentration, (c) the fraction of glucose present in the α-form in solution, (d) the mean crystal growth rate, and (e) the particle size distribution, based on 100 g seed crystals (mean size = 50μm) per 1 kg of solution, crystallized at 10°C, initial relative supersaturation = 0.15, and mean seed size = 100 μm. The GRD is characterized by a C.V. = 0.5. Lines represent predictions of the new model, and dashed lines represent predictions of the old model.

Since the older model predicts a higher rate of crystal mass deposition, then it also predicts too high a rate of depletion of glucose from the solution, as evident from Figure 5.5b.

The result of the older model overestimating the rate of crystal mass deposition, is that it also overestimates the decrease in the fraction of the α-D-glucopyranose form: the rate of crystallization and mutarotation are competitive, and if the crystal mass deposition rate is high then the mutarotation reaction is not sufficiently fast in producing the α-form to maintain the mutarotational equilibrium: this is shown in Figure 5.5c. The improved model also predicts a decrease in the fraction of the α-form, but not as severe as in the previous model. Note that the initial fraction of the α-form is a model input, but this is usually assumed to be 0.4, which is the mutarotational equilibrium, as this should be the case before the initiation of crystallization.

Crystal growth rates predicted by the two models are shown in Figure 5.5d. The two models predict the same initial growth rate since the initial supersaturation values are equal. However the newer model has a slower mass deposition rate, and hence the rate of supersaturation decrease is lower, and therefore the rate of decrease of the crystal growth rate is also lower. The crystal growth rates of this form of glucose are very low, with the highest growth rates at 10°C being only around 1.17 μm/hr (0.0195 μm/min).

The evolution of the CSD are shown in Figure 5.5e. The older model does not predict the full crystal size distribution and so the model is shown by impulses representing the monosize particles at different times. The newer model predicts the full CSD as a function of time, and these are plotted for the seed, and at 1000, 2000, 3000, 4000, and 5000 min. The CSD at 4000 and 5000 min are very similar, indicating that this is close to the end of the batch, or in other words, close to equilibrium. This equates to a batch time of about 3.5 days, which is substantially longer than industrial batches (1-2 days) which are operated at higher temperatures. The CSD also show substantial widening of the CSD as time increases due to the relatively large amount of GRD in this system. Note that the CV is constant during the crystal growth process, since the growth is common history, however this results in a significant increase in the standard deviation of the CSD as the mean crystal size increases. It is extremely important to be able to model the evolution of the CSD accurately, because the CSD of the final product is an extremely important determinate of its commercial value.

It is also interesting to use the model to analyze the competitive reaction and crystallization processes occurring in the crystallization of glucose monohydrate. Crystallization removes the α-D-glucopyranose form from solution, whilst the mutarotation reaction attempts to replace this form, using conversion from the β-form, to maintain the equilibrium of the mutarotation. If the mass rate of crystallization is very large compared to the mutarotation rate, due to any or all of high seeding rates, high growth kinetics, or low mutarotation kinetics, then the mutarotation reaction will not be able to maintain the mutarotation equilibrium, and the fraction of the α-form in solution will decrease (as evident in Figure 5.5c). This will result in the apparent supersaturation, as measured with respect to total glucose concentration, defined as

$$\sigma_g = \frac{C_g - C_g^*}{C_g^*} \tag{6.34}$$

being significantly different to the true supersaturation, which is with respect to the α-form

$$\sigma_{\alpha-g} = \frac{x_{\alpha-g} C_g - x_{\alpha-g}^* C_g^*}{x_{\alpha-g}^* C_g^*} \tag{6.35}$$

The supersaturation with respect to total glucose is the value that is readily measurable, since the glucose anomers are difficult to quantify independently, and is also the one that is commonly measured in industrial practice. However the supersaturation with respect to the α-form is the true driving force for the crystallization. These two measurements of the driving force can be ascertained from the model, and a comparison between them for different initial supersaturation levels (but otherwise using the same initial conditions as in the example used in Figure 5.5) is shown in Figure 5.6. The 45° line in the figure indicates where the two driving forces have equal values. The initial supersaturation values are the same for both measures of supersaturation because the system is initially at the mutarotational equilibrium, and so $x_{\alpha-g} = x_{\alpha-g}^*$ and equation (6.35) can be simplified to equation (6.34) at this point.

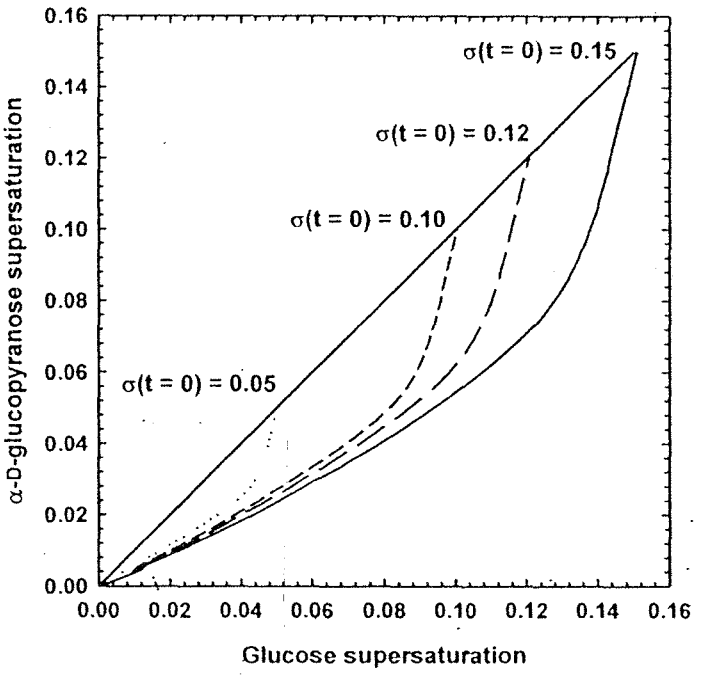

Fig. 5.6 Differences in the supersaturation with respect to total glucose and with respect to α-D-glucopyranose as a function of the initial supersaturation based on 100 g seed crystals (mean size = 50μm) per 1 kg of solution, crystallized at 10°C, and mean seed size = 100 μm. The GRD is characterized by a C.V. = 0.5.

It can be seen from this figure that the higher the initial supersaturation, the larger the maximum deviation between the two measures of the driving force are. This is due to the faster crystallization kinetics at high supersaturation, which makes the overall scheme far more mutarotation rate controlled, i.e. the ratio of the crystal mass deposition over the rate of replacement by mutarotation becomes larger. At 10°C it is evident that the crystallization is significantly controlled by the slow rate of the mutarotation reaction, and that the assumption that the total glucose driving force could be used to represent crystal growth rates would be significantly incorrect.

In order to investigate the effect of temperature on the crystallization process, more simulations were performed at 40°C, which is near the maximum temperature at which this form of glucose can be reliably crystallized. The transition point from α-glucose monohydrate crystal to anhydrous α-glucose crystal is at approximately 50°C, but the

crystallization cannot be run at this point because a certain initial supersaturation (or sub-cooling) is required, and because the process should be immune to small temperature fluctuations. The results of these studies are shown in Figures 5.7 and 5.8.

The results have the same trend as those at 10°C, however it is possible to make a number of conclusions about the effect of temperature. The first conclusion is that the process is much faster at the elevated temperature, with the process reaching equilibrium within 1000 min (around 17 hr) when the other initial conditions are equivalent to the 10°C simulations: 17 hr is typical of industrial crystallization batch times for this sugar. There is still considerable deviation between the improved predictions of the new model and the older model, with a similar magnitude of difference to the case studies at 10°C. The crystal growth kinetics at 40°C are (not surprisingly) much higher than those at 10°C, with initial crystal growth rates of 9 μm/hr (0.15 μm/min), due to the strong temperature dependence of the crystal growth rate constant, k_g. The mutarotation kinetics also increase significantly due to the effect of temperature, and it can be seen in Figure 5.5c that the reduction in the α-form fraction is much less than it was at 10°C. This is due to the mutarotation rate constant having a much stronger temperature dependence than the crystal growth rate constant, making the overall scheme less mutarotation rate controlled at higher temperatures. This can be confirmed by the magnitudes of the activation energies for the two processes (crystallization and mutarotation) which were given in parameter equations in the theory section. This is also evident in Figure 5.8, where the differences in the two forms of the driving force are much smaller than they were at 10°C. The overall scheme is still partly mutarotation rate controlled, but to a much small extent than at the lower temperature.

5.4 Conclusions

The current study has used previously measured kinetics for the mutarotation reaction of glucose, crystallization kinetics of α-glucose monohydrate in the temperature range that is the stable crystal phase, and other data including secondary nucleation thresholds and solubility data to construct a model of the batch crystallization of this sugar. Although the changes in the fraction of the α-glucose anomer are relatively small during most of the simulated batch crystallization, changing only from the equilibrium value of 0.40 to a minimum of about 0.37, this change is very significant when the relative supersaturation is considered.

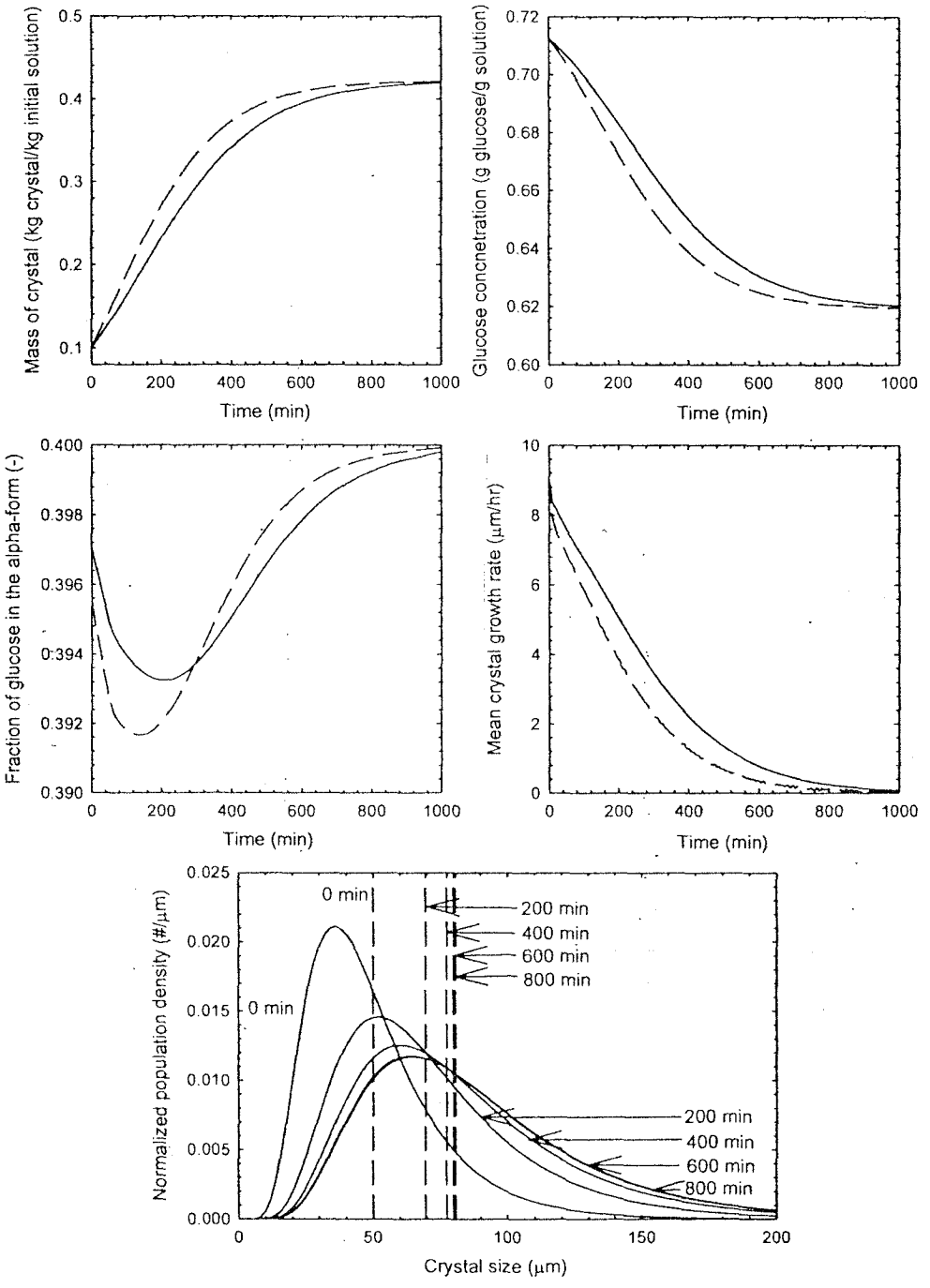

Fig. 5.7 Evolution of (a) the mass of crystals, (b) the glucose concentration, (c) the fraction of glucose present in the α-form in solution, (d) the mean crystal growth rate, and (e) the particle size distribution, based on 100 g seed crystals (mean size = 50μm) per 1 kg of solution, crystallized at 40°C, initial relative supersaturation = 0.15, and mean seed size = 100 μm. The GRD is characterized by a C.V. = 0.5. Lines represent predictions of the new model, and dashed lines represent predictions of the old model.

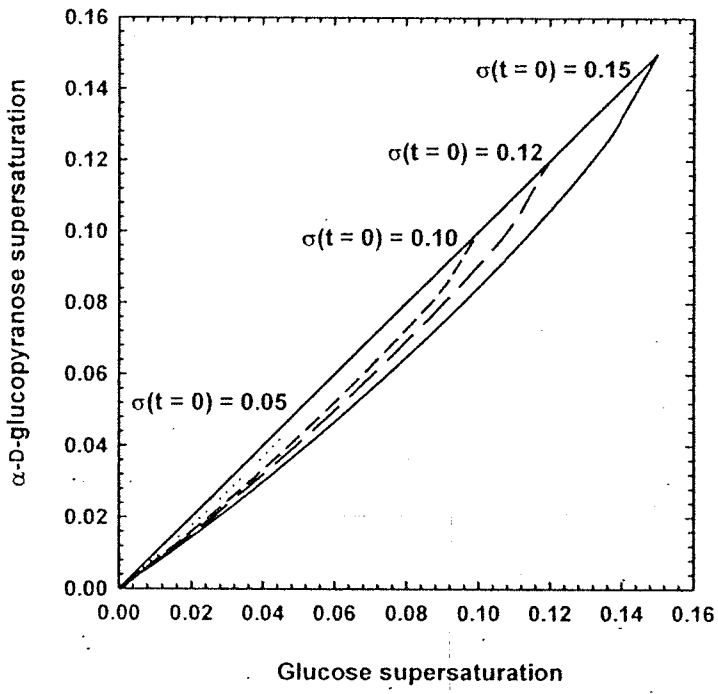

Fig. 5.8 Differences in the supersaturation with respect to total glucose and with respect to α-D-glucopyranose as a function of the initial supersaturation based on 100 g seed crystals (mean size = 50μm) per 1 kg of solution, crystallized at 40°C, and mean seed size = 100 μm. The GRD is characterized by a C.V. = 0.5.

The relative supersaturation of α-glucose was as low as 10% of the supersaturation expected from the total concentration of glucose in the crystallizer. This indicates that under some conditions the crystallization is almost entirely mutarotation rate controlled. The main variables affecting the response of the α-glucose anomer are the seed size, seeding rate, and the temperature. The mutarotation reaction may be the rate controlling step in processes where small seed size, higher seeding rate, and lower operating temperature are used. This phenomenon must be taken into account when designing industrial crystallizers for this sugar, which typically has very high seeding rates because of the slow crystallization kinetics, although the situation in industrial crystallizer may be complicated by various impurities having an effect on the rate of both the mutarotation reaction and the crystallization.

Chapter VI

Summary

The current study looks at the effect of the mutarotation reaction on the crystallization of simple carbohydrates, i.e. sugars, which are a very important class of materials both biologically and economically. Almost all sugars (with sucrose as the exception to the rule) exist in a range of forms in solution, which are named as tautomers if the forms have a different ring structure, or anomers if the forms only differ in orientation around the anomeric carbon in the sugar. The reaction which interconverts the forms is called the mutarotation reaction. All sugars produced commercially are crystallized as a purification step, and thus the crystallization rates are vital for designs of plants producing the sugars. Unfortunately under any set of conditions only one of the forms can crystallize from solution, thus making the interconversion of non-crystallizing forms to the crystallizing form a vital step in the purification of the sugar. If this reaction is slower than the potential rate of crystallization then the reaction rate will partially or totally control the overall rate of crystallization, and this will have serious consequences on the design of the crystallization operations. Unfortunately this effect has been little studied over the previous decade since it was first noted.

The current study has measure mutarotation rates and equilibrium for a range of monosaccharide and disaccharide sugars, with example of both aldose and ketose sugars being studied. The rates of aldose sugars are considerably lower than the rates of ketose sugars, meaning that the reaction is more likely to be rate controlling in the crystallization of the aldose sugars (for instance glucose, galactose, and mannose) than in the crystallization of ketose sugars (for instance fructose or sorbose). The number of rings in the sugar did not appear to effect the mutarotation rate, with the rate being determined by the type of sugar in the mutarotating ring. The equilibrium of the reaction is difficult to determine just be consideration of the type of sugar, since the equilibrium is substantially different even in two closely related sugars. Thus it is necessary to use measured values of the equilibrium constant: this is not difficult since the equilibrium for all the monosaccharide sugars is already published[10,11].

Due to the considerable time required to obtain crystallization kinetic data for sugars, glucose monohydrate has been used as a test case, and nucleation thresholds, mean crystal growth rates, and crystal growth rate distributions were measured for this sugar over the

range of temperatures for which it is likely to be crystallized (10-45°C). Crystal growth rate data which is required in the model is also available in the literature for other sugars such as fructose, anhydrous glucose, galactose, and xylose.

Using the data from the crystal growth studies and the mutarotation rate and equilibrium studies, two models have been developed to quantify the effect of the mutarotation reaction on the overall crystallization kinetics of sugars. The first model only uses mean crystal growth rates and gives a qualitative determination of the level of the effect. The more complex model uses the full crystal growth rate distribution, and gives an exact determination of the effect, along with particle size distributions, anomers and total sugar contents vs time, and crystal suspension density vs time. Use of the model shows that in many industrial crystallizations the overall crystallization rate will be partially or totally controlled by the mutarotation rate. The main operating variables determining the level of this effect are the seeding rate (with increased levels of seeding resulting in the reaction becoming more rate controlling), temperature (the effect is determined by whether the reaction rate constant or the crystallization rate constant has a larger temperature effect), and the initial supersaturation used in the crystallizer.

The model presented here will enable designers of industrial sugar crystallizers to better design the crystallizer, such that the product rates and crystal size distributions will better represent the design specifications.

References

1. Schenck, F. W. (1989). In Ullmann's Encyclopedia of Industrial Chemistry Vol. A 12 (pp 457-476), Weinheim: VCH.
2. Flood, A. E., Johns, M. R., and White, E. T. (1996). Mutarotation of D-fructose in aqueous-ethanolic solutions and its influence on crystallization. Carbohydr. Res. 288: 45-56.
3. Flood, A. E., Johns, M. R., and White, E. T. (2000). Crystal Growth Rates and Dispersion for D-Fructose from Aqueous Ethanol. AIChE J. 46(2): 239-246.
4. Hart, H., Craine, L. E., and Hart, D. J. (1999). Organic Chemistry: A Short Course. 10th Ed., Boston: Houghton Mifflin.
5. Boons, G.-J. (1998). Mono- and oligosaccharides: structure, configuration and conformation. In G.-J. Boons (ed.). Carbohydrate Chemistry (pp 1-20). London: Blackie Acadamic & Professional.
6. Beyer, H. and Walter, W. (1996). Handbook of Organic Chemistry. London: Prentice Hall.
7. Isbell, H. S. and Pigman, W. (1969). Mutarotation of sugars in solution. II Catalytic processes, isotope effects, reaction mechanism, and biochemical aspects. Adv. Carbohydr. Chem. Biochem. 24: 13-65.
8. Nelson, J. M. and Beegle, F. M. (1919). Mutarotation of glucose and fructose. J. Am. Chem. Soc. 41: 559-575.
9. Kraus, J. and Nyvlt, J. (1994). Crystallization of anhydrous glucose I. Mutarotation rate and solid-liquid phase equilibria. Zuckerind. 119(1): 24-29.
10. Bock, K. and Pedersen, C. (1983). Carbon-13 nuclear magnetic resonance data of monosaccharides. Adv. Carbohydr. Chem. Biochem. 41: 27-65.
11. Bock, K., Pedersen, C., and Pedersen, H. (1983). Carbon-13 nuclear magnetic resonance data for oligosaccharides. Adv. Carbohydr. Chem. Biochem. 42: 193-225.
12. Gray, G. R. (1976). Solution structures of the keto sugars and their biologically important phosphate esters. Acc. Chem. Res. 9: 418-424.
13. Barc'H, N. L., Grossel, J. M., Looten, P., and Mathlouthi, M. (2001). Kinetic study of the mutarotation of D-glucose in concentrated aqueous solution by gas-liquid chromatography. Food Chem. 74: 19-124.

14. Hudson, C. S. and Sawyer, H. L. (1917). The preparation of pure crystalline mannose and a study of its mutarotation. J. Am. Chem. Soc. 39(3): 470-478.

15. Hudson, C. S. and Dale, J. K. (1917). Studied on the forms of D-glucose and their mutarotation. J. Am. Chem. Soc. 39: 320-328.

16. Lowry, T. M. and Smith, G. F. (1929). The mutarotation of galactose. J. Am. Chem. Soc. 33(1): 9-21.

17. Pigman, W. and Isbell, H. S. (1968). Mutarotation of sugars in solution. I History, basic kinetics, and composition of sugar solutions. Adv. Carbohydr. Chem. 23: 11-57.

18. Lee, C. Y., Acree, T. E., and Shallenberger, R. S. (1969). Mutarotation of D-glucose and D-mannose in aqueous solution. Carbohydr. Res. 9: 356-360.

19. Nelson, R. G. and Johnson, W. C. Jr. (1976). Optical Properties of Sugar. 3. Circular Dichroism of Aldo-and Ketopyranose Anomers. J. Am. Chem. Soc. 98(14): 4290-4295.

20. Wertz, P. W., Garver, J. C., and Anderson, L. (1981). Anatomy of a complex mutarotation. Kinetics of tautomerization of α-D-galactopyranose and β-D-galactopyranose in water. J. Am. Chem. Soc. 103: 3916-3922.

21. Kraus, J. and Nývlt, J. (1994). Crystallization of anhydrous glucose IV. Batch Crystallization and Secondary Nucleation. Zuckerind. 119(5): 407-413.

22. Johns, M.R., Judge, R.A., and White, E.T. (1990). Kinetics of Ethanolic Crystallization of Fructose. In A.S., Myerson and K., Toyokura (eds.), Crystallization as a Separation Process (pp. 198 – 209). Washington DC: American Chemical Society.

23. Nývlt, J. and Kraus, J. (1993). Crystallization of anhydrous glucose II. Metastable Zone-width and Nucleation Rate. Zuckerind. 118(3): 219-222.

24. Young, F.E. (1957). D-Glucose-Water Phase Diagram. J. Phys. Chem. 61(5): 616-619.

25. Young, F.E., Jones, F. T., and Lewis, H. J. (1952). D-Fructose-Water Phase Diagram. J. Phys. Chem. 56: 1093-1096.

26. Randolph, A. D. and Larson, M. A. (1988). Theory of Particulate Processes (2nd ed.). New York: Academic Press.

27. Myerson, A. S. and Ginde, R. (2002). Crystal, Crystal Growth, and Nucleation, In A. S., Myerson (ed.), Handbook of Industrial Crystallization (2nd ed., pp.121-176). Boston: Butterworth-Heinemann.

28. Mullin, J. W. (2001). Crystallization (4th ed.). Oxford: Butterworth-Heinemann.

29. Mersmann, A. (1995). Crystallization Technology Handbook. New York: Mercel Dekker.

30. Srisa-nga, S. (2006). Ph.D. Thesis. Suranaree University of Technology, Nakhon Ratchasima, Thailand.

31. Beckmann, W., Boje, G., Rössling, G. and Arlt, W. (1996). Crystallization of Galactose from Aqueous Solutions: Influence of the α- and β-Anomers. In B. Biscans, and J. Garside (eds.). Proceeding of 13th Symp. on Industrial Crystallization (pp 497-502). LGC-CNRS: Toulouse, France.

32. Boje, G., Beckmann, W., Arlt, W., and Rössling, G. (1997). A Model for the Batch Cooling Crystallization of α- and β-D-Pyrano-Galactoses from Aqueous Solutions. In J. Ulrich (ed.). Proceeding of Fourth Int. Workshop on Crystal Growth of Organic Materials (pp 342-349). Shaker Verlag: Aachen, Germany.

33. Mulvihill, P. J. (1992). Crystalline and Liquid Dextrose Products: Production, Properties, and Applications. In F. W., Schenck and R. E., Hebeda (eds.). Starch Hydrolysis Products: worldwide technology production and applications (pp. 121-176) New York: VCH Publishers.

34. Chu, Y.D., Shiau, L.D., and Berglund, K.A. (1989). Effects of impurities on crystal growth in fructose crystallization. J. Cryst. Growth 97(3-4) 689-696.

35. Gabas, N. and Laguérie, C. (1992). Batch crystallization of D-xylose by programmed cooling or by programmed adding of ethanol. Chem. Engng. Sci. 47(12) 3148-3152.

36. Goldberg, R. N. and Tewari, Y. B. (1989). Thermodynamic and Transport Properties of Carbohydrates and Their Monophosphates: The Pentoses and Hexoses. J. Phys. Chem. Ref. Data. 18(2): 809-880.

37. Lloyd, N. E. and Nelson, W. J. (1984). Glucose- and Fructose-Containing Sweeteners from Starch: Chemistry and Technology (2nd ed., pp. 611-660). San Diego: Academic Press.

38. Mueller, H. (1970). Isothermal crystallization of dextrose. U. S. Patent 3,547,696.

39. Peres, A. M. and Macedo, E. A. (1997). Solid-Liquid Equilibrium of Sugars in Mixed Solvents. Entropie. 202/203: 71-75.

40. Allen, T. (1997). Particle Size Measurement: Volume 1 Powder Sampling and Particle Size Measurement (5^{th} ed.). the Dordrecht: Kluwer Academic.

41. Addai-Mensah, J. (1993). Crystallization of D-fructose from aqueous ethanolic solutions. Ph.D. Thesis. The University of Queensland, Brisbane, Australia.

42. Pantaraks, P. and Flood, A. E. (2005). Effect of Growth Rate History on Current Crystal Growth: A Second Look at Surface Effects on Crystal Growth Rates. Crystal. Growth Des., 5; 365-371.

43. Liang, B., Hartel, R. W., and Berglund, K. A. (1989). Effects of Raffinose on Sucrose Crystal Growth Kinetics and Rate Dispersion. AIChE J. 35(12): 2053-2057.

44. Srisa-nga, S. and Flood, A. E. (2004). Mutarotation Rates and Equilibrium of Simple Carbohydrates [CD]. In Proceeding of the APCChE 2004 (paper no. 3C-10). Kitakyushu, Japan.

45. Srisa-nga, S., Flood, A. E., and White, E. T. (2006). The Secondary Nucleation Threshold and Crystal Growth of Alpha-Glucose Monohydrate in Aqueous Solution. Cryst. Growth Des., 6;795-801.

46. Newkirk, W. B. (1925). Manufacture of Dextrose. U. S. Patent 1,521,830.

Appendix

Peer Reviewed Publications from the Research

CRYSTAL GROWTH & DESIGN
2006
VOL. 6, NO. 3
795–801

The Secondary Nucleation Threshold and Crystal Growth of α-Glucose Monohydrate in Aqueous Solution

Sukanya Srisa-nga,[†] Adrian E. Flood,*[,†] and Edward T. White[‡]

School of Chemical Engineering, Suranaree University of Technology, Nakhon Ratchasima, 30000, Thailand, and Division of Chemical Engineering, The University of Queensland, Brisbane, QLD, 4072, Australia

Received August 22, 2005; Revised Manuscript Received November 28, 2005

ABSTRACT: Investigation of the secondary nucleation threshold (SNT) of α-glucose monohydrate was conducted in aqueous solutions in agitated batch systems for the temperature range 10 to 40 °C. The width of the SNT decreased as the induction time increased and was found to be temperature independent when supersaturation was based on the absolute concentration driving force. Nonnucleating seeded batch bulk crystallizations of this sugar were performed isothermally in the same temperature range as the SNT experiments, and within the SNT region to avoid nucleation. The growth kinetics were found to be linearly dependent on the supersaturation of total glucose in the system when the mutarotation reaction is not rate limiting. The growth rate constant increases with increasing temperature and follows an Arrhenius relationship with an activation energy of 50 ± 2 kJ/mol. α-Glucose monohydrate shows significant crystal growth rate dispersion (GRD). For the seeds used, the 95% range of growth rates was within a factor of 3 for seeds with a narrow particle size distribution, and 8 for seeds with a wider distribution that was used at 25 °C. The results will be used to model the significance of the mutarotation reaction on the overall crystallization rate of D-glucose in industrial crystallization.

Introduction

Crystallization is one of the main separation and purification processes used in the production of a wide range of materials. It is used in many industries to remove a valuable substance from an impure mixture, glucose monohydrate from hydrolyzed starch, for example. Industrial crystallization processes in the chemical, pharmaceutical, and food industries mostly involve crystallization from solution. The crystallizing form can be anhydrous or hydrated depending on the operating conditions; however, usually only one crystal form is stable at a particular condition. D-Glucose, for example, can be crystallized from aqueous solution in three different forms: α-D-glucose monohydrate, anhydrous α-D-glucose, and anhydrous β-D-glucose. The first two forms are produced commercially, while the last one is available as a specialty chemical. In aqueous solutions, from the eutectic point at approximately −5 °C up to approximately 50 °C, the solution is in equilibrium with α-D-glucose monohydrate. Between 50 °C and approximately 115 °C, anhydrous α-D-glucose is the solid phase in equilibrium, whereas at temperatures above 115 °C the stable phase is anhydrous β-D-glucose.[1−3] At conditions near the transformation points (approximately 50 °C and 115 °C), the two most stable forms can exist simultaneously. Away from these points, the less stable phase is transformed to the more stable one. At just below approximately 50 °C, the hydrate-to-anhydrous transformation point, both hydrate and α-D-glucose anhydrous can be crystallized out.[4] This phenomenon occurs when the crystallizer is operated at a high supersaturation, well above the solubility of the anhydrous α-D-glucose form. However, the unstable anhydrous crystals dissolve later in the crystallization process to form the hydrate form, as the solubility concentration of the anhydrous form is above the solubility of the hydrate. In the same way, the phase transition of the anhydrous β form may occur near 115 °C, which is the α-anhydrous-to-β-anhydrous transformation point.

Supersaturated solutions often exhibit a metastable zone, where crystals can grow without significant birth of new crystals (nuclei). Further increases in the supersaturation will cause the solution to reach a value where secondary nucleation in the presence of prior crystals occurs; this limit is known as the metastable limit for secondary nucleation. The metastable limit or secondary nucleation threshold (SNT) is the upper limit of the metastable zone with regard to secondary nucleation. Nucleation is typically avoided or minimized in commercial crystallization processes since it is difficult to control and thus introduces undesired variability in the product size distribution. In batch processes, if possible, operation is usually undertaken in the metastable zone, and crystallization is initiated through the addition of seed crystals, thus avoiding large amounts of nucleation. Fortunately, the SNT of sugars such as glucose is usually quite large.[5,6]

The crystallization of D-glucose also involves mutarotation.[3] In solution, both α-D-glucose and β-D-glucose anomers exist simultaneously and undergo reversible mutarotation along with crystallization by the scheme shown in Figure 1a. The equilibrium ratio of the concentration of β-D-glucose to α-D-glucose in aqueous solutions is approximately 1.5 independent of temperature and total glucose concentration.[7] If a part of the α-anomer is crystallized out, part of the β-anomer slowly converts into the α-anomer and, if necessary, vice versa. If the rates of the mutarotation reactions are slower than the rates of crystallization, the crystallizing anomer will be depleted such that it is below the anomeric equilibrium in solution, leading to a decrease in the driving force for crystallization. Thus, mutarotation could have an important effect on the kinetics of crystallization of D-glucose in aqueous solution, by affecting the supersaturation.[3] This behavior has also been reported for fructose crystallized from aqueous ethanol solutions, where the mutarotation kinetics is particularly slow due to the less polar nature of the solvent.[8] Consequently, the authors reported the crystal growth rate with respect to the concentration of the crystallizing form (β-fructopyranose, in this case) instead of the total fructose in the system. The group of Arlt and Beckmann noted similar behavior for galactose, including initial nucleation

* To whom correspondence should be addressed. E-mail: adrianfl@sut.ac.th.
† Suranaree University of Technology.
‡ The University of Queensland.

10.1021/cg050432r CCC: $33.50
Published on Web 02/14/2006

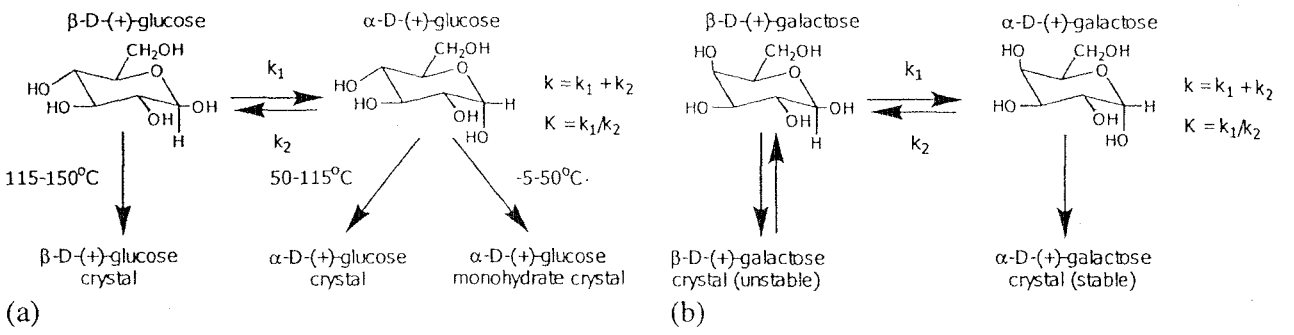

Figure 1. Reaction schemes for the crystallization including the mutarotation reaction of (a) D-glucose and (b) D-galactose.[9]

of the unstable crystalline form, followed by a solution-mediated (mutarotation controlled) phase transition to the stable crystalline phase.[9,10] They also defined the crystallization driving force with respect to the α-anomer, which is the stable crystalline form. The crystallization scheme including the mutarotation and an unstable phase transformation of galactose is shown in Figure 1b.

Mutarotation may be the rate-limiting step, depending on the relative rate constants of the mutarotation and crystallization kinetics. Whether this is the case or not depends on both the sugar and the solvent: on the basis of previously measured data,[11] crystallization of lactose from DMSO is most likely mutarotation rate controlled, but industrial crystallizations of lactose from whey are surface integration controlled.[12] The habit of the crystals may also be affected by the concentration of the noncrystallizing anomer.[11,13] The crystallization kinetics also depends on nucleation, but the secondary nucleation thresholds of industrial sugar crystallizations are large, so operation is mostly seeded and nonnucleating. In seeded batch crystallizations, the kinetics depend on the initial suspension density, which in industrial crystallization of glucose monohydrate is about 3 to 15 vol %.[14] However, to study the crystallization kinetics, where the mutarotation effect is to be neglected, the depletion of the crystallizing anomer due to the crystal growth needs to be significantly slower than the generation via mutarotation. This can be achieved using batches containing small numbers of seed crystals operating within the metastable zone.

The major objective of this study was to determine the crystal growth rate of glucose monohydrate in aqueous solution. The SNT of this system was determined to ensure that the system is operated under convenient nonnucleating conditions. The crystal growth rate data together with the mutarotation data, which we have measured previously,[7] will be used to generate a model to predict whether the mutarotation reaction has a significant effect on the overall crystallization of glucose monohydrate.

Here, the effects of temperature and supersaturation on the crystal growth were investigated. Pure aqueous solutions were crystallized in isothermal batch crystallizers to simplify the system studied. Because of the very slow crystal growth of this sugar, and the small amount of seed added, the supersaturation in the crystallizer was essentially constant during the crystallization.

Experimental Section

Materials. All glucose solutions were prepared from AR grade anhydrous D-glucose supplied by Chem-Supply Pty. Ltd., Australia, and water, treated by reverse osmosis (RO). The anhydrous D-glucose was confirmed to contain less than 2% moisture using a vacuum evaporation (dry substance method). The prepared solution was kept above the experimental temperature overnight to ensure the establishment of the mutarotation equilibrium and that no nuclei were present.

Seed crystals were prepared from D-glucose monohydrate supplied by Asia Pacific Specialty Chemical Limited (APS), Australia. As the later growth results show, these crystals were common history (CH) seeds,[15] in which the innate growth rate of each crystal was proportional to its size. This behavior results from crystals nucleating at the same time and having a common history of crystal growth conditions. The nuclei initially have a distribution of sizes that are negligibly small, and thus the size of the crystal at any later time is proportional to the innate growth rate of the particle under the crystallization conditions it experienced. This has implications for the growth rate dispersion (GRD) results in the present study.

Because of the possible formation of tiny crystals on the surface of the glucose monohydrate crystals, and also dust on the surface of the particles, a pretreatment process was performed before the seeds were introduced into the crystallizer. The pretreatment minimized dust-breeding secondary nucleation, which is a serious problem in industrial batch operation.[16] Seed crystals were prepared using a technique that initially sieved the commercial glucose monohydrate crystals through a set of sieves ranging from 45 to 250 μm. Sieving was performed to produce seed crystals with a narrow size distribution to reduce difficulties in sizing wide crystal size distributions and to avoid the larger crystals growing out of the size range measurable using the Malvern Mastersizer/E. The 63−90 μm dry-sieved fraction of the α-glucose monohydrate crystals was wet sieved in denatured ethanol using a 63 μm sieve to remove fine particles and dust from the particles. The wet-sieved product was then washed in 50% (by weight) aqueous glucose solution, which is undersaturated by a small amount, to remove the dust or surface nuclei from the surface of the particles. The appearance of the crystals was monitored by observation under a microscope, and no nuclei in the seed particles or on the crystal surface was seen, and the seed crystals displayed good shape and no evidence of dehydration, which typically produces a strongly altered crystal surface. Two samples of this slurry were taken to measure the particle size distribution (PSD) using the Malvern Mastersizer/E before each experiment, and these results were noted as the seed size. Two batches of seed crystals were produced, as the initial batch prepared, used for the 25 °C experiments, was insufficient to complete the experiments at 10 and 40 °C. The particle size distributions of the two batches of seed crystals prepared were slightly different, with the seed prepared for the 25 °C experiments having the same volume mean size (approximately) but a slightly larger coefficient of variation. Examples of the seed PSDs for the experiments at 10, 25, and 40 °C are shown in Figure 2. It was confirmed also that there was no difference between the seed size measured before, and immediately after, addition to the crystallizer.

The supporting medium (the dispersant) used in the particle size measurement was prepared from anhydrous ethanol (CSR Ltd., Sydney), RO water, and anhydrous D-glucose. An excess amount of glucose crystals was added to a solution that was 10% (by weight) water in ethanol. The mixture was agitated using a magnetic bar at 40 °C overnight. This solution was then kept under stagnant conditions until the solution temperature decreased to room temperature and only the clear solution was used as a dispersant. The glucose monohydrate crystals to be sized did not dissolve in this solution since it was saturated with glucose, and the water present in the mixture prevented dehydration of the crystals. Measurements of the PSD of glucose monohydrate

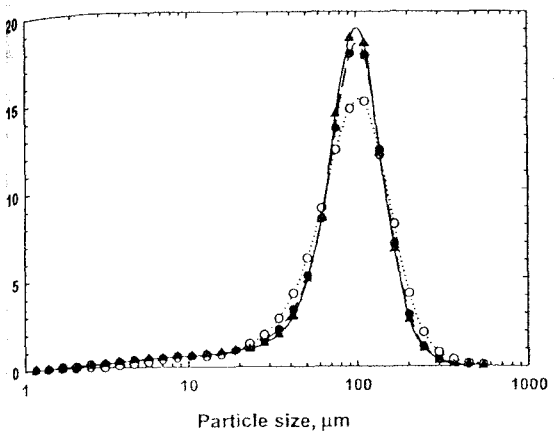

re 2. Typical volume based particle size distributions for seed als used in experiments at 10 ●; 25 ○; and 40 °C ▲.

als using the Malvern Mastersizer/E at successive time intervals d the crystals did not dissolve or dehydrate, since there was no ficant change in the distribution over time.

pparatus. The apparatus used for secondary nucleation threshold urements involved 50 mL stirring bottles located in a water bath e the temperature was controlled within ±0.5 °C. The stirring s were designed to minimize particle breakage due to crushing rticles between the bottom and the stirrer by use of a stirrer bar orted some distance above the base of the bottle using an axle ted on a hub in the bottom of the bottle. A multipoint submerged ng plate set at 200 rpm drove the stirrer bars. This stirring speed chosen since it was the stirring speed where the particles were suspended, and the stirrer caused no significant breakage of the cles. The equipment used in the SNT experiments is shown in re 3a.

l-L glass batch crystallizer was used in the batch crystallizations. 4 bladed impeller provided agitation at 500 rpm, except where tion limits were varied to confirm the growth kinetics were surface gration controlled. Two batch crystallizations were performed ltaneously to check reproducibility. The experimental temperature controlled within ±0.5 °C. A schematic drawing of the crystal- on equipment is shown in Figure 3b.

he PSD of the slurry crystals was measured using the Malvern lersizer/E (Malvern Instruments Ltd., England), which uses a light ering technique. The measurements were performed in the small me cell (15 mL) in which the sample is stirred by use of a magnetic stirrer. As indicated above, a 10% water in ethanol solution ated with glucose was used as the supporting dispersant. The racy of results from this equipment is expected to be within ±2% he volume median diameter.

he glucose concentration of the crystallizer solution was monitored g a digital refractometer (RFM 340, Bellingham & Stanley Limited, . The discrimination of the refractive index (RI) value is within 0001 RI units. A calibration curve of known concentration ions was used to determine total glucose concentrations from the ctive index measurements.

econdary Nucleation Experiments. Secondary nucleation experi- ts were performed at 10, 25, and 40 °C. Each secondary nucleation involved observation of the nucleation of a number of different rsaturated solutions containing α-glucose monohydrate seed crys- A series of supersaturated solutions were prepared and heated to C above the experimental temperature for 20 min to ensure that host nuclei remained in the solution. Approximately 1 mg of ucose monohydrate crystals larger than 180 μm in size, which could asily distinguished from the nuclei formed, was added to each tion to induce secondary nucleation. Nucleation was determined ally at later time intervals, with nucleation being indicated by ipitation or clouding due to the very fine nuclei particles. The ding occurring in the experiments was clearly visible and the ction between solutions that had precipitated at a particular surement time and those that had not was clear. The concentrations e highest concentration solution that had not nucleated and the st that had were recorded, concentrations being those of the initial concentration prior to nucleation. The experiments were duplicated (at 25 °C) or triplicated (at 10 and 40 °C) to check reproducibility.

Crystallization Experiments. The crystallization of α-glucose monohydrate was performed isothermally at 10, 25, and 40 °C. Initial crystallization experiments at varying agitation rates demonstrated that the crystallization was surface integration controlled at least at, and above, 450 rpm. It was important to achieve negligible attrition and/or breakage of seed crystals, so 500 rpm was chosen as the agitation speed for the crystallization experiments. The experiment was duplicated in a parallel crystallizer.

Batches were initiated by the addition of 10 mL of seed slurry into 500 g of prepared supersaturated glucose solution. Before the addition of the seed to the crystallizer, and during the batch run, duplicate samples were taken at various time intervals to measure the PSD. The total experimental time depended on how quickly the crystals grew under the given conditions but was chosen to be less than that for the secondary nucleation limit at the initial supersaturation to avoid undesired nucleation. Observation of samples under a microscope indicated that nucleation did not occur. The refractive index of the clear liquor was periodically monitored during the experimental run to ensure the concentration was essentially constant during crystallization: the low amount of seed added to the batch and slow growth kinetics should ensure that the batches were at constant composition within the accuracy of the measurements.

Results and Discussion

Effect of Observation Time and Temperature on SNT. The effect of temperature and observation time on the SNT is illustrated in Figure 4. In this figure, each data value consists of two data points joined by a vertical line: the upper point represents the lowest absolute supersaturation that had nucleated, and the lower point represents the highest absolute supersaturation that had not nucleated. The true value of the SNT must lie between these two points. The figure shows that the SNT decreases as the observation time (or induction time) increases. An initial time SNT in terms of absolute supersaturation is about 16 g of glucose/100 g of solution. At large induction times, greater than 50 h, the SNT is about 5 g of glucose/100 g of solution. Even after 2 days, some of the low supersaturated solutions had not nucleated.

The SNT at 10, 25, and 40 °C overlap when plotted in terms of the absolute value of the supersaturation, as in Figure 4. This allows a single line to represent the zone width for the three temperatures studied. This implies that temperature does not have a significant effect on SNT over the range of temperatures where glucose monohydrate is likely to be crystallized. Because the solubility of glucose is a strong function of temperature, this same result does not result if the data is plotted with respect to relative supersaturation, which is the more common measure of the driving force for crystal growth. In a limited number of the SNT experiments, both points are below or both points are above the line of best fit. This is thought to be due to the stochastic nature of the nucleation process. While a large number of experiments could have been done to locate the mean of the stochastic distribution with high accuracy, this was not considered worthwhile as the secondary nucleation experiments are very time-consuming and the results of the triplicate experiments (10 and 40 °C) and duplicate experiments (25 °C) were of acceptable accuracy for further use.

The line of best fit to the data is an exponential decay with three parameters (eq 1), where C represents the total glucose concentration in g of glucose/100 g of solution for the SNT, C^* is the solubility, and t is the observation time in hours.

$$\text{SNT width: } C - C^* = 5 + 11\exp(-0.11t) \quad (\text{for } 10\ ^\circ\text{C} < T < 40\ ^\circ\text{C}) \quad (1)$$

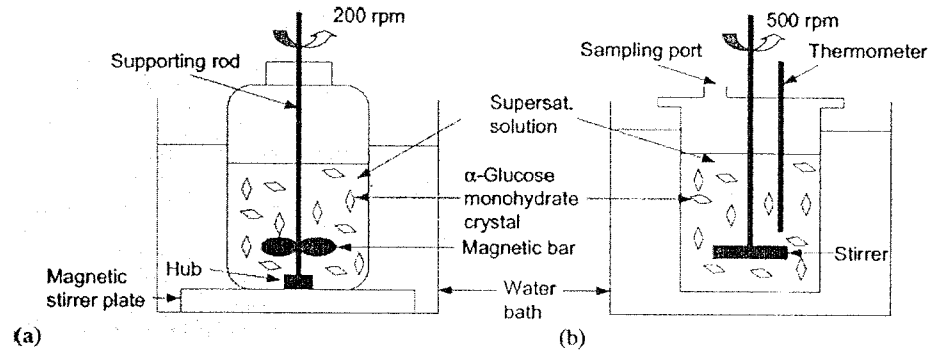

Figure 3. Schematic diagrams of the experimental apparatus: (a) SNT apparatus and (b) crystallization apparatus.

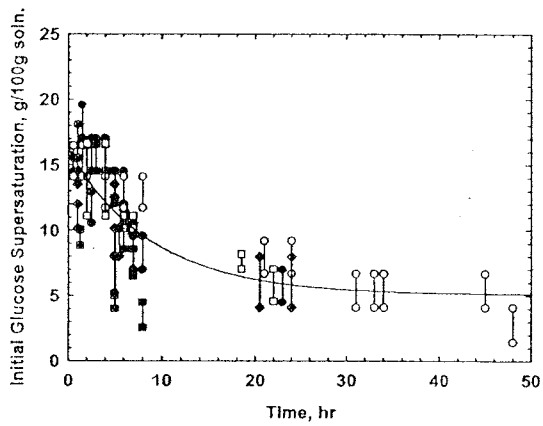

Figure 4. The time dependence of the secondary nucleation zone width based on anhydrous glucose concentrations. Filled symbols are for the triplicate experiments at 10 °C, open symbols are for the duplicate experiments at 25 °C, and open symbols containing a character are for the triplicate experiments at 40 °C.

Accurate solubility data for glucose monohydrate in water has already been published.[17] The solubility data in the temperature range of 0 to 50 °C was fitted using a quadratic polynomial equation, with the result shown in eq 2, where T represents the experimental temperature in degrees Celsius.

$$\text{solubility: } C^* = 33.8 + 0.65T + 0.0014T^2 \quad (\text{for } 0\ ^\circ\text{C} < T < 50\ ^\circ\text{C}) \quad (2)$$

Substitution of eq 2 into eq 1 gives the SNT concentration as a function of time (for temperatures between 10 and 40 °C), as shown in eq 3. Because the SNT is not a significant function of temperature, and glucose monohydrate is stable only between −5 and 50 °C, it is likely that this equation is a reasonably accurate representation of the SNT concentration over the entire range of conditions where glucose monohydrate crystallizes.

$$\text{SNT: } C = 39 + 0.65T + 0.0014T^2 + 11\exp(-0.11t) \quad (3)$$

Use of SNT in the Nonnucleated Batch Bulk Crystallization. Figure 5 replots the induction time dependent secondary nucleation thresholds of glucose monohydrate in aqueous solutions. This graph is very important in nonnucleating batch crystallizations because it shows limitations on either the operation concentration or the batch time to ensure that nuclei are not formed, so the system can be easily controlled. For instance, when crystallization occurs at 30 °C and the operating time is within 24 h, the initial concentration that can operate without a significant birth of new crystals is up to approximately

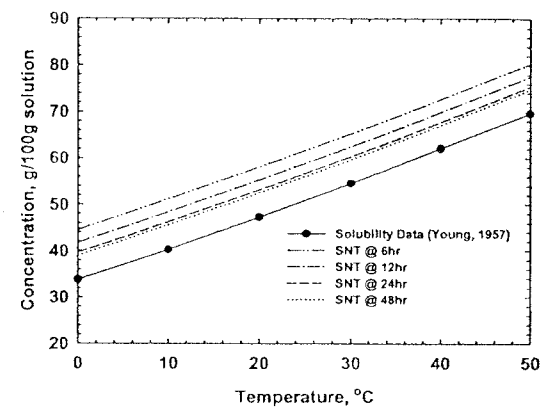

Figure 5. Secondary nucleation threshold (based on anhydrous glucose concentration) for α-glucose monohydrate at operating times of 6, 12, 24, and 48 h.

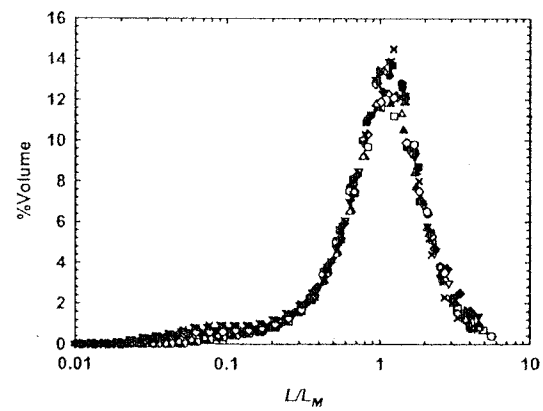

Figure 6. Scaled particle size distributions from a batch run at 25 °C, with duplicate samples represented by filled and open symbols. ● seed; ■ 1 h; ▲ 2 h; ▼ 3 h; ◆ 4 h; × 6 h.

60 g of glucose/100 g of solution. This initial concentration may be higher if the concentration decrease is rapid enough to ensure that the combination of concentration and time always puts the mother liquor at a point below the SNT.

Crystallization Kinetics. Figure 6 shows an example of the PSDs from a batch run at 25 °C plotted on a scaled log size basis. For CH seed, where the relative growth rate of a crystal is proportional to its size, growth will not change the shape of the size distribution plotted on a log size scale. Thus, Figure 6 shows that the seed crystals are indeed CH seed. The particle sizes have been scaled relative to the volume median size for each PSD to illustrate the constant shape of the distribution. The results show two PSD replicates for each time. The PSD

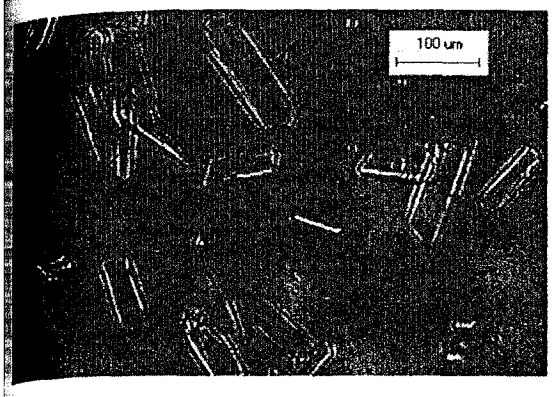

ure 7. Photomicrograph of crystals taken from the isothermal batch stallization 8 h after seeding. The conditions for the crystallization e 25 °C, agitation at 500 rpm, and the initial relative supersaturation s 0.027.

sults appear to be approximately normally distributed on a g size scale, except occasionally where there is a tail at the all size ranges. Particles from the crystallizer were visually spected under a microscope at intervals during the crystal-ation, and no evidence of nucleation (as evident from particles aller than the seed crystals) was noticed, so it is likely that e tail is an artifact of the sizing technique. Distributions pearing normal on a log size plot will follow a log-normal tribution for linear size. A photomicrograph of crystals taken om one isothermal batch crystallization is shown in Figure 7. If the volume distribution (or mass distribution) is log-normal, e number distribution is also log-normal with the same ometric standard deviation.[18] The number mean size may then calculated from the relationship:

$$\ln x_{NL} = \ln x_{mV} - 2.5 \ln^2 \sigma_g \qquad (4)$$

here x_{NL} is the number mean particle size, x_{mV} is the median the volume distribution, and σ_g is the geometric standard viation of the volume distribution. These results were con-med by discretizing the volume density distribution into all elements (of 1 μm width) and calculating the number of rticles in each element, and from that, the number mean rticle size. The geometric standard deviation of the volume tribution was essentially constant over the time period of the periment, confirming there was growth rate dispersion and l the seeds were CH. The growth kinetics was determined sed on the number mean particle size.

Because of the constant solution concentration during the rstallization process, the mean growth rate was calculated ectly from the slope of a plot between number mean crystal e and time. The growth rate of α-glucose monohydrate from ueous solution was found to be unusually high in the first riod of the experiments (i.e., the first hour) and then followed expected linear relationship, as illustrated in Figure 8. An usual accelerated rate of crystal growth at the initial stage of ch crystallization may be due to repair of the crystal surface,[19] isoning from unidentified impurities,[20] or a roughening nsition.[21] The growth rates shown here were calculated based the linear rates evident after the first hour of growth.

Duplicate crystallizations were performed simultaneously for experiments. The results at 40 °C (Figure 8) showed that, at same conditions, the number mean sizes were essentially same for all four measurements (two batches with two asurements each), and the same mean crystal growth rates re obtained. Thus, the reproducibility was good and within estimated measures of uncertainty.

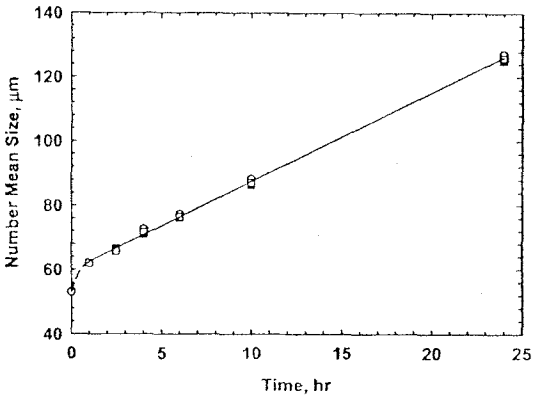

Figure 8. Number mean sizes of α-glucose monohydrate as a function of time at 40 °C, operating concentration = 65.81 ± 0.25%; batch 1 duplicates (●, ○); batch 2 duplicates (△, ▼).

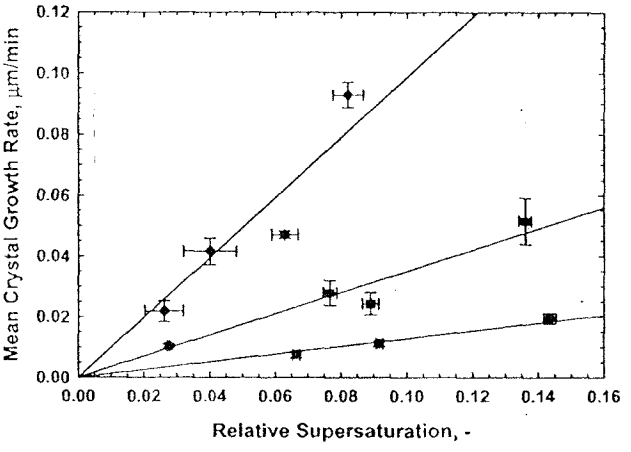

Figure 9. Mean size crystal growth rates for α-glucose monohydrate as a function of relative supersaturation at 10 (●), 25 (■), and 40 °C (◆).

The plot between the mean crystal growth rates and relative supersaturation (Figure 9) for the three temperatures gives the growth rate constants for the experimental temperatures. It is clear that a growth rate order of 1 fits the data acceptably. The growth rate constant increases significantly with increasing temperature. The growth rate constant was modeled by an Arrhenius relationship (Figure 10), as the relationship $\ln k_g = 19.2 - 6010/T$, indicating an activation energy of 50 ± 2 kJ/mol. This value is typical for the crystallization of simple sugars. Previous research on crystal growth of sucrose[22] for example, gives an activation energy of crystal growth as 28.9 to 33.1 kJ/mol for growth from pure solutions, and 45.6 to 57.7 kJ/mol for growth from solutions having raffinose as an impurity.

Crystal Growth Rate Dispersion. Crystal GRD in the batch crystallizations was measured based on the time-dependent PSDs. Figure 6 shows that on a log size scale, the shape of the PSD was unchanged as the crystals grew, and so the seed was CH. The growth rates shown in Figures 8−10 are for the number mean size crystal. The growth rates for other sizes are these values multiplied by the ratio of the size of the crystal to the mean crystal size. The range of growth rates for this sieved seed can be expressed by the CV (= standard deviation/mean growth rate) of the growth rate distribution which for CH seed is identical to the CV of the PSD. These can be on a number basis, as was used in the current study, or on a weight (volume) basis. The standard deviation of the number based PSD was calculated by discretizing the volume based PSDs in 1 μm

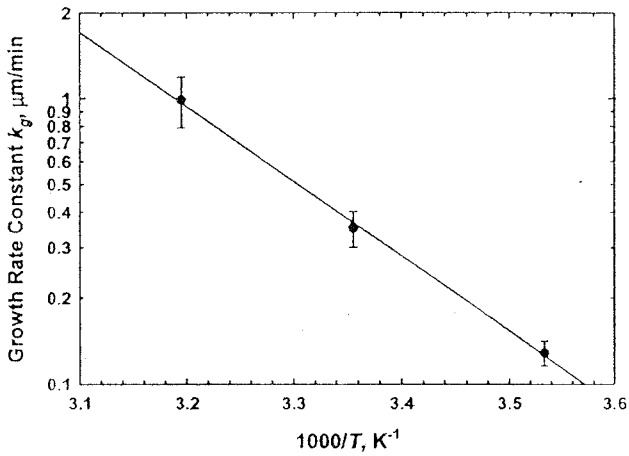

Figure 10. An Arrhenius plot of the growth rate constant for determination of the activation energy of crystal growth.

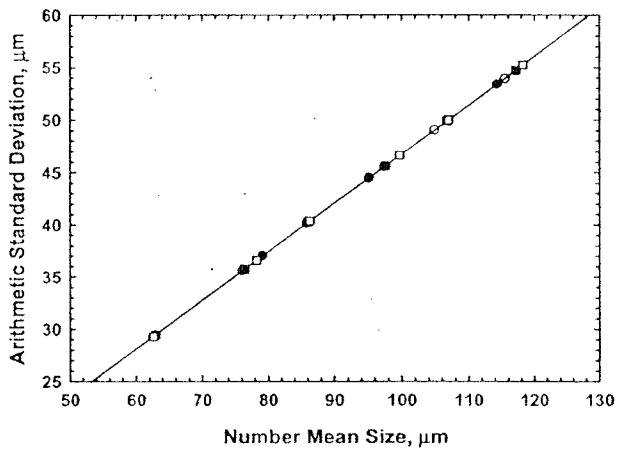

Figure 11. Plot of the arithmetic standard deviation of the number distribution against number mean size for the experiment at 40 °C and relative supersaturation equal to 0.082. Different symbols represent replicate data. The slope of this plot is the crystal growth rate dispersion CV for this condition.

intervals and converting the results to a number basis. The geometric standard deviations of the volume based PSDs (on a log size scale) were constant throughout the experiments (Figure 6), but this transforms into significant increases in the standard deviations of the number based PSDs on a linear size scale, as the experiments progressed. For CH seed, the standard deviation should be proportional to the mean size and the slope gives the associated CV of the growth rate distribution. An example of a plot to determine the crystal growth rate dispersion is shown in Figure 11 for an experiment at 40 °C and relative supersaturation equal to 0.082. There was very good reproducibility between duplicate samples in individual experiments, and between duplicate experiments. Table 1 gives values of the crystal growth rate dispersion CV on a number basis for all conditions studied.

The crystal growth rate dispersion CV is difficult to determine with very high accuracy due to the variability in the measured volume based PSDs. In the raw volume based PSD data, there are small random changes in the geometric standard deviations through the experiment, but we have smoothed the data by assuming a constant geometric standard deviation, which is justified by the scaled volume based PSD plots, of which Figure 6 is an example. It is believed that the 95% confidence interval uncertainty on CV for a particular experiment is of the order of 0.10. Assuming that the CV measured come from identical distributions with the use of the same seed, it is possible to calculate the CV as 0.47 ± 0.06, for the results at 10 and 40 °C (which used seed crystals from a single preparation), and 0.59 ± 0.05 for the seeds at 25 °C, which had a wider PSD. These results can be used to determine 95% ranges of growth rates ($G_{97.5\%}/G_{2.5\%}$), for the two seeds. The seeds used in the 10 and 40 °C experiments have a 95% range of growth rates of 5.8 ± 1.0 times, and those used in the 25 °C experiment had a 95% range of growth rates of 8.5 ± 1.2 times.

Table 1. Crystal Growth Rate Dispersion Number Based CVs for Glucose Monohydrate Crystallized from Aqueous Solutions, All Runs

temp (°C)	relative supersaturation (−)	CV (batch 1) (−)	CV (batch 2) (−)
10	0.067	0.50	0.50
	0.092	0.48	0.48
	0.143	0.46	0.46
25	0.027	0.56	0.56
	0.077	0.61	*a*
	0.089	0.62	*a*
	0.136	0.60	0.60
40	0.026	0.44	0.44
	0.040	0.44	0.44
	0.063	0.52	0.52
	0.082	0.47	0.47

a Only one batch was performed for these conditions.

The bulk crystals from which the CH seeds were prepared had a number mean size of 92 μm and a number based standard deviation of 45 μm, resulting in a CV of 0.49, which is similar to that of the seeds that were fractioned from the bulk crystals. Thus, it can be concluded that the CV of the growth rate distributions predicted in the current study would be very similar to the CV of the growth rate distribution of the bulk particles from which the seeds were fractionated. Note that although the sieved fraction and the bulk material had similar CVs, the bulk had a mean size almost twice that of the sieved seed, so the mean growth rate would have been larger by the same ratio. That the CVs of bulk and fraction are similar is not implicit in the seed preparation method, but results from the coincidence that when the seed was prepared the reduction in the mean crystal size was by the same factor as the reduction in the standard deviation of the PSD: this resulted in an approximately constant value of the CV and hence a similar 95% range of the growth rate distribution.

Conclusions

The SNT of α-glucose monohydrate in aqueous solution is large but decreases with increasing induction time. The instantaneous (short time) secondary nucleation threshold (the SNT immediately after parent crystal addition) is approximately 16 g of glucose/100 g of solution for all temperatures studied. The SNT in these measurement units is temperature independent for all induction times. The crystallization of α-glucose monohydrate from aqueous solution should be operated within the SNT region if nucleation is to be avoided. The crystal growth rate order is 1, and the growth rate constant is temperature dependent with activation energy of 50 ± 2 kJ/mol. Growth rate dispersion was observed. For the sieved seeds used, the 95% range of growth rates ($G_{97.5\%}/G_{2.5\%}$) was 5.8 ± 1.0 for crystallizations using the seeds prepared for the 10 and 40 °C experiments, and 8.5 ± 1.2 for the seeds prepared for the 25 °C experiments, which had a slightly wider initial PSD. This is evidence that growth rate dispersion is significant for this system. The seeds were prepared from a sieve fraction from commercial α-glucose monohydrate, suggesting that the 95% range of growth rates

commercial crystals is also nearly an order of magnitude. basis of the crystallization kinetics from the current work, netics and equilibrium for the mutarotation reaction[7] it is le that the mutarotation reaction kinetics will be signifi- or the industrial crystallization of glucose monohydrate high seeding rates are employed.

knowledgment. This work was supported by the Thailand rch Fund (TRF) via the Royal Golden Jubilee Ph.D. m grant no. PHD/0099/2543, and the SUT Research Grant T7-706-44-12-19. S.S. and A.E.F. also thank the Division emical Engineering, the University of Queensland, for use laboratory space and equipment.

Nomenclature

total glucose concentration, g of glucose/100 g of solution
solubility concentration, g of glucose/100 g of solution
coefficient of variation of the growth rate distribution, dimensionless
mean crystal growth rate, μm/min
growth rate of crystals at 2.5% of the cumulative undersize distribution, μm/min
growth rate of crystals at 97.5% of the cumulative undersize distribution, μm/min
growth rate constant, μm/min
particle size, μm
mean size, μm
growth rate order
relative superaturation $(C - C^*)/C^*$, dimensionless
geometric standard deviation, μm
absolute temperature, K, or °C where specified
time, hr
number mean particle size, μm
volume median particle size, μm

References

Goldberg, R. N.; Tewari, Y. B. *J. Phys. Chem. Ref. Data* **1989**, *18*, 809−880.
Lloyd, N. E.; Nelson, W. J. In *Starch: Chemistry and Technology*. 2nd Ed.; Whistler, R. L., BeMiller, J. N., Paschall, E. F., Eds.; Academic Press: San Diego, CA, 1984; pp 611−660.
(3) Kraus, J.; Nyvlt, J. *Zuckerindustrie (Berlin)* **1994**, *119*, 24−29.
(4) Mulvihill, P. J. In *Starch Hydrolysis Products: Worldwide Technology Production and Applications*; Schenck, F. W., Hebeda, R. E., Eds.; VCH Publishers: New York, 1992; pp 121−176.
(5) Johns, M. R.; Judge, R. A.; White, E. T.: In *Crystallization as a Separation Process*; Myerson, A. S., Toyokura, K., Eds.; ACS Symposium Series 438; American Chemical Society: Washington, DC 1990; pp 198−209.
(6) Nyvlt, J.; Kraus, J. *Zuckerindustrie (Berlin)* **1994**, *119*, 219−222.
(7) Srisa-nga, S.; Flood, A. E. Proceedings of the 10th Asian Pacific Confederation of Chemical Engineering (APCChE) Congress, Kitakyushu, Japan, October 17−20, 2004; Paper 3C-10, 2004.
(8) Flood, A. E.; Johns, M. R.; White, E. T. *Carbohydr. Res.* **1996**, *288*, 45−56.
(9) Beckmann, W.; Boje, G.; Rössling, G.; Arlt, W. Proceedings of the 13th Symposium on Industrial Crystallization, LGC-CNRS; PROGEP: Toulouse, France. September 16−19. 1996: Biscans, B., Garside, J., Eds.
(10) Boje, G.; Beckmann, W.; Arlt, W.; Rössling, G. Proceedings of the Fourth International Workshop on Crystal Growth of Organic Materials; Ulrich, J., Ed.; Shaker Verlag: Aachen, 1997.
(11) Dincer, T. D.; Parkinson, G. M.; Rohl, A. L.; Ogden, M. I. *J. Cryst. Growth* **1999**, *205*, 368−374.
(12) Butler, B. Ph.D. Thesis, The University of Queensland, Brisbane, QLD, Australia, 1998.
(13) Garnier, S.; Petit, S.; Coquerel, G. *J. Cryst. Growth* **2002**, *234*, 207−219.
(14) Mueller, H. U.S. Patent 3,547,696, 1970.
(15) Butler, B. K.; Zhang, H.; Johns, M. R.; Mackintosh, D. L.; White E. T. Proceedings of the Conference on Separation Science and Technology; Los Angeles, CA, Nov 16−21, 1997; Ho, W. S. W., Luo, R. G., Eds.; AIChE: New York, 1997; pp 289−294.
(16) Myerson, A. S.; Ginde, R. In *Handbook of Industrial Crystallization*. 2nd ed.; Myerson, A. S. Ed.; Butterworth-Heinemann: Boston, MA, 2002; pp 121−176.
(17) Young, F. E. *J. Phys. Chem.* **1957**, *61*, 616−619.
(18) Allen, T. *Particle Size Measurement: Volume 1 Powder Sampling and Particle Size Measurement*. 5th ed.; Kluwer Academic Publishers: Dordrecht, 1997.
(19) Addai-Mensah, J. Ph.D. Thesis, The University of Queensland, Brisbane, QLD, Australia, 1992.
(20) Flood, A. E.; Johns, M. R.; White, E. T. *AIChE J.* **2000**, *46*, 239−246.
(21) Pantaraks, P.; Flood, A. E. *Cryst. Growth Des.* **2005**, *5*, 365−371.
(22) Liang, B.; Hartel, R. W.; Berglund, K. A. *AIChE J.* **1989**, *35*, 2053−2057.

CG050432R

Proc. 10th APCChE Congress (2004) (10 pages)

Mutarotation Rates and Equilibrium of Simple Carbohydrates

On-line Number 133

Sukanya Srisa-nga and Adrian E. Flood
School of Chemical Engineering, Suranaree University of Technology, 111 University Avenue, Muang, Nakhon Ratchasima, 30000, Thailand, E-mail: adrianfl@ccs.sut.ac.th

ABSTRACT

Crystalline sugars are significant commodities in the world market, however the crystallization behaviour of many sugars is still not well known. Recently it has been shown that the mutarotation reaction of reducing sugars plays a significant role in determining the crystallization rate of these sugars, and thus it is beneficial to be able to model and predict mutarotation rates for common sugars. The mutarotation rate and equilibrium of simple carbohydrates; D-glucose, D-galactose, D-cellobiose, D-maltose, and D-turanose, in aqueous solutions were measured between 7 and 35°C, using ^{13}C-NMR. The effects of sugar concentration and temperature on the rate of mutarotation and mutarotation equilibrium were observed. It has been found that the rate of mutarotation slightly decreases as the sugar concentration increases. The rate constant of the studied sugars follows an Arrhenius relationship with respect to temperature, and activation energies for the reactions were found from an Arrhenius plot. There are no clear correlations between the equilibrium constant and the sugar concentration or the temperature. Finally, it is quite clear that the mutarotation rate of ketose sugars is higher than the mutarotation rate of aldose sugars, and the number of rings in the structure (i.e. monosaccharide and disaccharide) does not have a significant effect on the rate of mutarotation.

KEYWORDS

Mutarotation, D-glucose, ^{13}C-NMR, equilibrium composition

INTRODUCTION

Carbohydrates occur in all plants and animals and are the main source of energy supply in most cells. Simple carbohydrates, for example, monosaccharides: D-xylose, D-glucose, D-fructose, D-galactose, L-sorbose, and D-mannose, and disaccharides: D-cellobiose, D-maltose, and D-turanose, undergo interconversion between the anomeric or tautomeric forms (pyranose, furanose, aldehyde or keto, and hydrated forms) in solution. The interconversion is particularly important in aqueous solution, because the sugars appear in aqueous solutions in biological systems, and most processing of the sugar is also performed in aqueous solution. This reaction causes changes in the optical rotation of the solutions, and thus it is called the mutarotation reaction. The interconversion between the different ring forms of the sugars must pass through the straight chain (aldehyde or keto) form of the sugar via ring opening and ring closing reactions. These reactions are acid/base catalyzed, and at approximately pH 4 the reaction rate is minimized; the reactions are faster at extremes of pH (Nelson and Beegle, 1919). This apparent first order reaction is catalyzed by substances which can act simultaneously as proton donors and acceptors e.g. polar solvent, and also follows an Arrhenius relationship with respect to temperature (Kraus and Nyvlt, 1994 and Flood et al., 1996).

Crystallization is one of the main separation and recovery operations. It is used in many industries to remove a valuable substance from an impure mixture, glucose monohydrate from honey, for example. The crystal form can be anhydrous or hydrated depending on the operating conditions. However, only one crystal form is stable at a particular condition. D-Glucose, for example, can be crystallized from

Proc. 1st Int. Conference on Modeling in Chemical & Biological Engineering Sciences (2 (29 pages)

An Improved Model of the Seeded Batch Crystallization of Glucose Monohydrate from Aqueous Solutions

Adrian E. Flood[1*], Sukanya Srisa-nga[2]

[1] School of Chemical Engineering, Institute of Engineering, Suranaree University of Technology, Nakhon Ratchasima 30000, Thailand

[2] Department of Chemical Engineering, Faculty of Engineering, Ubon Rajathanee University, Muang Sriki, Ubon Ratchathani 34190, Thailand

*Corresponding author: Tel. 66-44-22-4497, Fax 66-44-22-4220, E-mail: adrianfl@sut.ac.th

Running head: Improved model of glucose crystallization

Keywords: Glucose monohydrate; Batch crystallization; Process modeling; Mutarotation.

ABSTRACT

The current research has produced an accurate model of the seeded batch crystallization of glucose monohydrate which is able to determine the population density of crystals in the batch system as a function of particle size and batch time, $n = n(L,t)$. The current study has addressed limitations of previous models by allowing non monosize seed crystals, and models growth rate dispersion. Because of the nature of the 'common history' crystals that are produced by the growth of glucose monohydrate, the modifications required to the model to account for these additions to the model are remarkably simple. By predicting the full population density the model produces an accurate mass balance for the crystallization process,

Analysis of the Effect of the Mutarotation Reaction on the Crystallization of α-Glucose Monohydrate

(9 pages)

Sukanya Srisa-nga[1], Adrian E. Flood[1], and Edward T. White[2]

[1]Suranaree University of Technology, School of Chemical Engineering, Nakhon Ratchasima, 30000, Thailand.

[2]The University of Queensland, Division of Chemical Engineering, Brisbane, QLD, 4072, Australia.

adrianfl@sut.ac.th

This study presents a model of the crystallization of α-glucose monohydrate crystallized from aqueous solutions over its range of stability (~ -4 to 50 °C). The crystallization process is complicated by the mutarotation reaction which interconverts α- and β-glucopyranose, which are the major components of glucose in the solution. Only the α-form of the sugar is formed in the crystallization process under the conditions studied, and thus as crystallization occurs some of the β- form of the sugar is converted back to the α- form in order to maintain the mutarotational equilibrium. Analysis of the process via measurement of crystallization kinetics and equilibrium, mutarotational kinetics and equilibrium, and modeling of process kinetics, show that the mutarotation reaction is significant if the seed addition rate is greater than about 5 mass percent of the initial suspension. The mutarotation reaction is likely to be significant in industrial crystallization of α-glucose monohydrate which often uses seeding rates up to 15 mass percent.

1. Introduction

Glucose is a commodity chemical that is used in a wide variety of food and pharmaceutical applications, as well as being a common feedstock for the chemical industry to produce citric acid, gluconic acid, and other specialty chemicals. The product is produced in large quantities both as aqueous solutions, and as anhydrous or monohydrate crystal forms.

Industrial crystallizations of glucose are usually carried out in batch crystallizers due to difficulties of crystal size control in continuous crystallization of the sugar. Typical patented processes can be found in the records of the patent office (Newkirk 1925, Edwards 1982). Despite the importance of the processes to industrially crystallize glucose monohydrate and anhydrous glucose, there is still a limited amount of data on important kinetic data required to properly design the crystallization equipment.

anhydrous α-glucose, and anhydrous β-glucose) in water are already well known (Young 1957). The current group has already performed measurements of the secondary nucleation threshold and crystal growth kinetics in solutions where the proportion of α-glucose is maintained at a constant level (Srisanga *et al.* 2005) and mutarotation reaction rates and equilibria (Srisanga and Flood 2004). In the current study a model of the batch crystallization of glucose monohydrate in its range of crystallization (~ -4 to 50 °C) has been developed using the previously acquired data. The model predicts the crystal growth rates, crystal deposition rates, compositions of both α-glucose and β-glucose, and other key operating parameters.

2. Materials and Methods

Experiments performed to collect data on the kinetic parameters used in the model have been described elsewhere (Srisanga *et al.* 2005, Srisanga and Flood 2004). The secondary nucleation threshold and the composition dependence of the crystal growth rates (under surface integration controlling conditions) was measured at 10, 25, and 40 °C to obtain models of the temperature and composition dependence of these variables in pure aqueous solutions over the approximate range of temperatures for α-glucose monohydrate crystallization. The temperature and composition dependence of the mutarotation kinetics and equilibria were measured in aqueous solutions in the same range of temperatures to model the temperature and composition dependence of these variables. There is also a slight effect of pH on the mutarotation rates, but this is not significant in the narrow range of pH used for the industrial crystallizations.

The solubility in terms of the crystallization temperature (in °C) has been modeled by fitting a cubic equation through the data of Young, giving

$$C^* \text{ (kg glucose/kg sol}^{n}\text{)} = 0.01\left(33.82 + 0.6484T + 0.001357T^2\right)$$

The mutarotation reaction is modeled as a first order reversible reaction of α- to β-glucopyranose (a simplification which is well justified from the experimental work). The simplified kinetics are represented by

$$\alpha - \text{glucose} \leftrightarrow \beta - \text{glucose}$$

with the forward reaction having a rate k_1 (s^{-1}) and the backward reaction having a rate k_2 (s^{-1}). The overall rate of reaction (which is the apparent rate as fitted in a first order decay curve) is

$$k = k_1 + k_2$$

Proc. 11th Int. Workshop on Industrial Crystallization (2004)

Secondary Nucleation Threshold and Crystallization of α-Glucose Monohydrate in Aqueous Solutions

Sukanya Srisa-nga[1], *Adrian E. Flood*[1], *and Edward T. White*[2]

[1]School of Chemical Engineering, Suranaree University of Technology, Nakhon Ratchasima, 30000, Thailand.

[2]Department of Chemical Engineering, The University of Queensland, Brisbane, QLD, 4072, Australia.

adrianfl@ccs.sut.ac.th

Investigations of the secondary nucleation threshold (SNT) and the crystal growth of α-glucose monohydrate were conducted in aqueous solutions in an agitated batch system at 10, 25, and 40°C. The SNT decreases as the induction time increases and is temperature independent. Seeded batch crystallizations of this sugar were carried out isothermally within the SNT region to avoid undesired nucleation. Growth rates were found to be linearly dependant on the relative supersaturation of total glucose when the mutarotation reaction is not rate limiting. The growth rate constant follows an Arrhenius relationship with an activation energy of 42.5 kJ/mole.

1. Introduction

Crystallization is a major separation and recovery processes. It is used in many industries to remove a valuable substance from impure mixtures; removal of glucose monohydrate from hydrolysed starches is an example. Crystallization must be well understood to ensure that the separation process is well controlled.

The major objective of this study was to determine the crystal growth rate of glucose monohydrate in aqueous solution. The secondary nucleation threshold (SNT) of this system was analysed to ensure the batch crystallizations would progress without significant nucleation. The effects of temperature and supersaturation on the surface integration controlled crystal growth of α-glucose monohydrate were observed. The crystal growth rate data together with the

mutarotation reaction rate and equilibrium data, which we have measured previously, will be used to generate a model to predict if the mutarotation reaction has a significant effect on the overall crystallization of simple sugars, especially for α-glucose monohydrate.

2. Experimental procedure

2-1. Materials

All glucose solutions were prepared from AR grade **D**-glucose anhydrous supplied by Chem-Supply Pty. Ltd., Australia, and water treated by reverse osmosis (RO). **D**-Glucose anhydrous was confirmed less than 2% moisture using the dry substance method. Seed crystals were prepared from **D**-glucose monohydrate supplied by Asia Pacific Specialty Chemical Limited (APS), Australia. The 63-90 μm dry-sieved fraction of these commercial α-glucose monohydrate crystals was wet sieved in denatured ethanol using a 63 μm test sieve in order to remove fine particles or dust from the bulk particles. This wet-sieved product was washed in 50% (by weight) glucose solution to remove dust and surface nuclei from the surface of the particles. Two samples of this slurry were taken to measure the particle size distribution (PSD) using the Malvern MasterSizer/E.

The dispersant used in particle size measurement was prepared from anhydrous ethanol (CSR Ltd., Sydney), RO water, and **D**-glucose anhydrous. 10% (by weight) of water was added to ethanol, and glucose crystals. The mixture was agitated using a magnetic stirrer bar at 40°C overnight. This solution was kept under stagnant conditions until the solution temperature was decreased, to room temperature and only the clear solution was used as a dispersant. Glucose monohydrate crystals did not dissolve in this solution; this was proved by measuring the particle size distribution of glucose monohydrate crystals using the Malvern MasterSizer/E at many time intervals. There was found to be no significant change in the distribution over time, indicating no growth or dissolution was occurring.